Secret arsenal of a cereal killer - cryptic activation of secondary metabolite biosynthesis in *Fusarium graminearum.*

by

Kristina Shostak

A thesis submitted to the Faculty of Graduate and Postdoctoral Affairs

in a partial fulfillment of the requirements for the degree of

Doctor of Philosophy

In

Biology

Carleton University
Ottawa, Ontario

Abstract

Fusarium graminearum is a fungal pathogen and is a major causal agent of diseases in several agriculturally important crop species. In addition to the disease that diminishes grain yield, this pathogen produces secondary metabolites that are harmful to both plants and animals. Secondary metabolites are not essential for survival, instead, they enable the pathogen to successfully infect its host. In fungi, genes necessary to produce secondary metabolites are often arranged together in the genome, forming secondary metabolic clusters (SMCs). The *F. graminearum* genome contains 76 such clusters with a potential to produce a diverse array of secondary metabolites (SMs). However, given high functional specificity and energetic cost, most of these clusters remain silent, or "cryptic," unless the organism is subjected to an environment conductive to SM production. Alternatively, SMCs can be activated by genetically manipulating their activators or repressors. The goal of this dissertation is to establish the transcriptional factor TRI6 and the MAP kinase MGV1 as regulators of secondary metabolism by genetically altering their expression and thus activating cryptic SMCs in *F. graminearum.* TRI6 is a transcriptional factor that regulates the trichothecene group of mycotoxins and other non-trichothecene genes. MGV1 is a MAP kinase, implicated in regulation of diverse cellular responses, including secondary metabolite biosynthesis. We used transcriptomic and metabolomic analyses to identify SMCs regulated by *TRI6* and *MGV1.* We discovered that at the transcriptional level, *MGV1* and *TRI6* co-regulate biosynthesis of four SMs; however, *MGV1* also exerts its control of three SMCs at the

post-transcriptional level. Finally, at the mechanistic level, we demonstrate that TRI6 regulates the trichothecene genes by directly binding to the promoters of the genes of the cluster. However, the regulation of other SMCs such as gramillin is achieved indirectly, through physical binding of TRI6 to the cluster-specific protein GRA2.

Acknowledgements

First and foremost, I would like to express my gratitude to my amazing supervisor, Dr. Gopal Subramaniam for his patient mentorship and unceasing enthusiasm. I also would like to thank the current and past members of my lab whose technical assistance and friendship have been invaluable. Sean Walkowiak, Li Wang, Chris Bonner, Nimrat Manes, Mary Miltenburg, Elizabeth Brauer, I was happy to work with you. Furthermore, I am grateful to my committee members Dr. John Vierula, Dr. Therese Ouellet, and Dr. Nicolas Rodrigue for their help in advancing my project.

This work is a product of collaboration with several researchers and technicians, whose contribution and support are greatly appreciated. I would like to express special gratitude to Dr. David Overy, who guided my exploration of the metabolomics field, and Amanda Sproule and Tom Witte for their additional help and advice in this area. I also would like to thank Dr. Barbara Blackwell and Indira Thapa for their assistance with the NMR studies, and Dr. Nora Foroud and Dianevys Gonzalez-Peña for inspiration and help with the MGV1 project.

Finally, I would like to thank my family and friends for their ongoing support through this journey.

Preface

This work is comprised of two chapters adapted from the research manuscript that has been submitted (Chapter 2) and a work that is in preparation for submission (Chapter 3), of which K.S. is the primary co-author. The author contributions for each chapter are as follows.

Chapter 2

This chapter is a full manuscript and a collaborative work of K. S., C. Bonner, A. Sproule, I. Thapa, S.W.J. Shields, B. Blackwell, J. Vierula, D. Overy and R. Subramaniam. (Submitted to Molecular Microbiology). "Cryptic activation of secondary metabolic clusters by the global transcriptional regulator TRI6 in *Fusarium graminearum*." K.S. is the main contributor to this manuscript, having performed all experiments with the exception of UPLC-HRMS and NMR experiments, which were conducted by A. S., I. T., S.W.J. S., B. B., and D. O. C.B. sequenced, assembled, and annotated the *F. graminearum* genome used for the analysis of transcriptomic data. J. V., D. O., and R. S. contributed to manuscript writing and editing.

Chapter 3

This chapter is a manuscript in preparation with contributions from K. Shostak, D. Gonzalez-Peña, C. Bonner, A. Sproule, T. Witte, J. Vierula, D. Overy, N. Foroud, and R. Subramaniam. K.S. is the main contributor to all analyses presented here and performed all experiments with the exception of *F. graminearum* strain construction, which was accomplished by D. G. -P. and N. F., and UPLC-HRMS, which was done by

A. S. and D. O. T. W. wrote the R script for correlation analysis of metabolomics dataset. C.B. sequenced, assembled, and annotated the *F. graminearum* genome used for the analysis of transcriptomic data. J. V., N. F. and R. S. contributed to manuscript writing and editing.

Contents

Abstract 1
Acknowledgements 3
Preface 4
Chapter 2 4
Chapter 3 4
List of Tables. 9
List of Figures 10
Supporting information. 10
List of Abbreviations 11
Chapter 1. Introduction 14
1.1 Overview of *Fusarium graminearum* 14
1.1.1 Economic importance 14
1.1.2 *F. graminearum* life cycle 14
1.2 Overview of secondary metabolites in filamentous fungi 16
1.2.1 Genetics of secondary metabolism 19
1.2.2 Functions of fungal secondary metabolites 20
1.2.2.1 Nutrient acquisition – a role for siderophores 20
1.2.2.2 Secondary metabolites in inter-species interactions 21
1.2.2.3 Secondary metabolites as host-specific virulence factors 22
1.3 Regulation of secondary metabolite production in filamentous fungi 26
1.3.1 Signal transduction pathways involved in secondary metabolite biosynthesis 26
1.3.3.1 The GPCR signaling pathway 26
1.3.1.2 The TOR signaling pathway 28
1.3.1.3 The cAMP-PKA signalling pathway 31
1.3.1.4 The MAP kinase signalling pathways 32
1.3.2 Control of secondary metabolism by global transcriptional regulators 35
1.3.2.1 Carbon catabolite repression and activation of secondary metabolite clusters 36

1.3.2.2 Nitrogen catabolite repression and activation of secondary metabolite clusters 37
1.3.2.3 The role of light in secondary metabolite production 40
1.3.2.4 Regulation of secondary metabolite biosynthesis by the environmental pH 42
1.3.3 Transcriptional activation of secondary metabolite clusters by pathway-specific regulators 44
1.4 Thesis outline 45
Chapter 2. Cryptic activation of secondary metabolic clusters by the global transcriptional regulator *TRI6* in *Fusarium graminearum* 47
2.1 Abstract 47
2.2 Introduction 47
2.3 Results 51
2.3.1 *TRI6* regulates both primary and secondary metabolism in *F. graminearum* 51
2.3.2 *TRI6* regulates both global and pathway-specific transcription factors 55
2.3.3 *TRI6* influences a broad spectrum of secondary metabolite clusters 58
2.3.4 *TRI6* regulates production of trichothecenes, fusaoctaxins, and gramillins 60
2.3.5 TRI6 binds to promoters of trichothecene genes 67
2.3.6 Interaction of TRI6 with pathway-specific transcription factors in the gramillin and fusaoctaxin SMC 69
2.4 Discussion 71
2.5 Conclusion 75
2.6 Experimental procedures 76
2.6.1 *F. graminearum* strains and culture conditions 76
2.6.2 Gene expression analysis by RNAseq and RT-qPCR 77
2.6.3 Metabolomic analysis 78
2.6.4 NMR spectroscopy analysis 80
2.6.5 Chromatin Immunoprecipitation and qPCR 81
2.6.6 Yeast strain construction and yeast-two-hybrid screen 82
Chapter 3. Regulation of secondary metabolite production by MAP kinase *MGV1*. 84

3.1 Abstract 84
3.2 Introduction 84
3.3 Results 88
3.3.1 *MGV1* transcriptionally regulates primary and secondary metabolic pathways. 88
3.3.2 *TRI6* and *MGV1* regulate different aspects of cellular metabolism 91
3.3.3 *MGV1* regulates biosynthesis and accumulation of secondary metabolites 95
3.4 Discussion 103
3.5 Conclusion 108
3.6 Materials and Methods 108
3.6.1 *F. graminearum* strain construction 108
3.6.2 Culturing conditions 109
3.6.3 Gene expression analysis (RNAseq, RT-qPCR) 109
3.6.4 Metabolomic analysis 109
Chapter 4. Perspectives and future directions 111
4.1 Cryptic activation of secondary metabolism in *Fusarium graminearum* 111
4.2 Beyond regulation of secondary metabolism – construction of a global regulatory network in *F. graminearum* 113
Bibliography 116
Appendix A: Supplementary figures. 143

List of Tables.

Table 2.1. *TRI6* regulates expression of transcription factors……..…….….56

Table 2.2. *TRI6* regulates five distinct SM gene clusters……59

Table 2.3. *TRI6* regulates production of distinct secondary metabolites……64

Table 2.4. TRI6 binding motifs in the promoters of trichothecene, gramillin and fusaoctaxin gene clusters…….....68

Table 3.1. *MGV1* and *TRI6* both regulate aurofusarin, trichothecene, and fusaoctaxin SMCs……..……..……...93

Table 3.2. *MGV1* regulates several known secondary metabolites. ……...98

List of Figures.

Fig. 1.1. The life cycle of *F. graminearum* ……...……15

Fig. 1.2. Schematic diagram of a wheat floret morphology ……..……16

Fig. 1.3. Most prevalent SM classes biosynthesized by *F. graminearum* ……..……...17

Fig. 1.4. Putative biosynthetic pathways leading to production of 3-ADON, 15-ADON, and 3ANX by *F. graminearum* ……..……24

Fig. 2.1. *TRI6* regulates genes of primary and secondary metabolism ……..……....53

Fig. 2.2. Principal component analysis of metabolites regulated by *TRI6* ……..……....62

Fig. 2.3. *TRI6* differentially regulates the production of secondary metabolites ……65

Fig. 2.4. TRI6 interacts with GRA2, but not with FGM4. ……..……...70

Fig. 3.1. HOG1 and CWI MAPK pathway modules in *F. graminearum* ……....87

Fig 3.2. MGV1 regulates genes in non-preferred nutrient conditions ……...90

Fig. 3.3. Principal component analysis of metabolites regulated by *MGV1* ……97

Fig. 3.4. Kinetics of secondary metabolite production ……..……...98

Fig 3.5. MGV1 regulates production of secondary metabolites ……...…….101

Supporting information.

Supplementary tables S2.1 to S2.10 and S3.1 to S3.7, and the R script (S_file_1_Polished_correlation_script.R) are electronic files not included in the main text of the dissertation.

Supplementary figures S2.1 to S2.14 and S3.1 to S3.3 are included as Appendix A on pages 143-160.

List of Abbreviations

15-ADON	15-acetyldeoxynivalenol
3-ADON	3-acetyldeoxynivalenol
3ANX	7-α hydroxy,15-deacetylcalonectrin
ABC transporter	ATP-binding cassette transporter
AC	adenylyl cyclase
AD	activating domain
AMP	adenosine monophosphate
ATF1	activating transcription factor 1
ATP	adenosine triphosphate
BCAA	branched-chain amino acid
BCK1	bypass of C kinase
BD	DNA binding domain
bHLH	basic helix-loop-helix
BMH1	brain modulosignaling homolog 1
BMH2	brain modulosignaling homolog 2
bZIP	basic leucine zipper
C2H2	2 cysteine, 2 histidine
cAMP	cyclic adenosine monophosphate
CCR	carbon catabolite repression
CWI	cell wall integrity
DAPG	2,4-diacetylphloroglucinol
DEG	differentially expressed genes
DON	deoxynivalenol
EPT	epoxytrichothec-9-ene
FA	fusaric acid
FCA4	*F. graminearum* catalase 4
FHB	Fusarium head blight
FPP	farnesyl pyrophosphate
FPPI	*Fusarium* protein-protein interaction
FunTAP	*Fusarium* network of trichothecene associated proteins
GABA	gamma-aminobutyric acid
GAP	GTPase-activating protein
GDP	guanosine diphosphate
GEF	guanine exchange factor
GIV1-5	GPCR important for virulence 1-5
GPA1	G-protein α protein 1
GPA2	G-protein α protein 2
GPB	G-protein β protein
GPCR	G-protein coupled receptor

GPMK1	*Gibberella* pathogenicity MAP kinase 1
GTP	guanosine triphosphate
GTR1	GTP binding protein resemblance 1
GTR2	GTP binding protein resemblance 2
H3K27me3	histone 3 lysine 27 trimethylation
H3K9ac	histone 3 lysine 9 acetylation
HAT	histone acetyltransferase
HOG1	high osmolarity glycerol 1
HPT1	histidine phosphotransferase 1
HRMS	high resolution mass spectrometry
KMT6	lysine methyltransferase 6
LeuRS	leucyl-tRNA synthetase
LST8	lethal with sec thirteen 8
MAP	mitogen activated protein
MAPK	mitogen activated protein kinase
MAPKK	mitogen activated protein kinase kinase
MAPKKK	mitogen activated protein kinase kinase kinase
MEP2	methylammonium/ammonium permease
MGV1	MAPK for growth and virulence
MIH1	mitotic inducer homolog 1
MKK1	mitogen activated protein kinase kinase
MS/MS	tandem mass spectrometry
MSG5	multicopy suppressor of GPA1
NP	non-ribosomal peptide
NPN	non-preferred nutrient
NPS	non-ribosomal peptide synthetase
OS1	osmolarity sensor 1
OSMAC	one strain - many compounds
PCA	principal component analysis
PCN	phenazine-1-carboxamide
PK	Polyketide
PKA	protein kinase A
PKS	polyketide synthetase
PN	preferred nutrient
PP2A	protein phosphatase 2A
PPI	protein-protein interaction
PTC	peptidyl transferase center
PTC3	phosphatase two C 3
RAS1	homologous to RAS proto-oncogene 1
RGS	regulator of G protein signaling
ROS	reactive oxygen species

RRG1	response regulator protein 1
SM	secondary metabolite
SMC	secondary metabolite cluster
SSK2	suppressor of sensor kinase
TAP42	two A phosphatase associated protein
TF	transcriptional factor
TOR	target of rapamycin
TORC	target of rapamycin complex
TPS	terpene synthetase
UPLC	ultra-high-performance liquid chromatography
WSC1,2,3	cell wall integrity and cell response component 1,2,3
Y2H	yeast-2-hybrid

Chapter 1. Introduction

1.1 Overview of *Fusarium graminearum*

1.1.1 Economic importance

F. graminearum is a fungal pathogen and a causative agent of Fusarium head blight (FHB), a devastating disease affecting economically important crop species such as wheat (*Triticum aestivum*), barley (*Hordeum vulgare*), oat (*Avena sativa*), and maize (*Zea mays*) [1]. Diseased crops produce shrivelled, undersized grain kernels that are unfit for consumption due to contamination with toxic compounds synthesized by the fungus. FHB is a serious concern in many parts of the world, including Canada and its trading partners. A recent survey analysis of FHB prevalence in Canada between 2001 and 2017 reported 11 of those as FHB epidemic years, when the disease was observed in >90% of the surveyed 486 spring wheat fields across Canada with the average disease index of 5.3%-27% (compared to 0.02%-3.7% in non-disease years) [2].

1.1.2 *F. graminearum* life cycle

F. graminearum infection strategy is closely linked to the life cycle of the host (Fig. 1.1). The fungus overwinters on previous year's stalk debris in the form of mycelia and sexual structures called perithecia (Fig. 1.1). During the following spring, as wheat grows to the flowering stage, perithecia mature and forcibly release the sexual ascospores, which get deposited on the inflorescence tissues of wheat [1,3]. *F. graminearum* also produces asexual spores (conidia) from conidiophores (Fig. 1.1) [1]. Upon landing on the host's flowering spikelets, conidia and ascospores differentiate into mycelia and

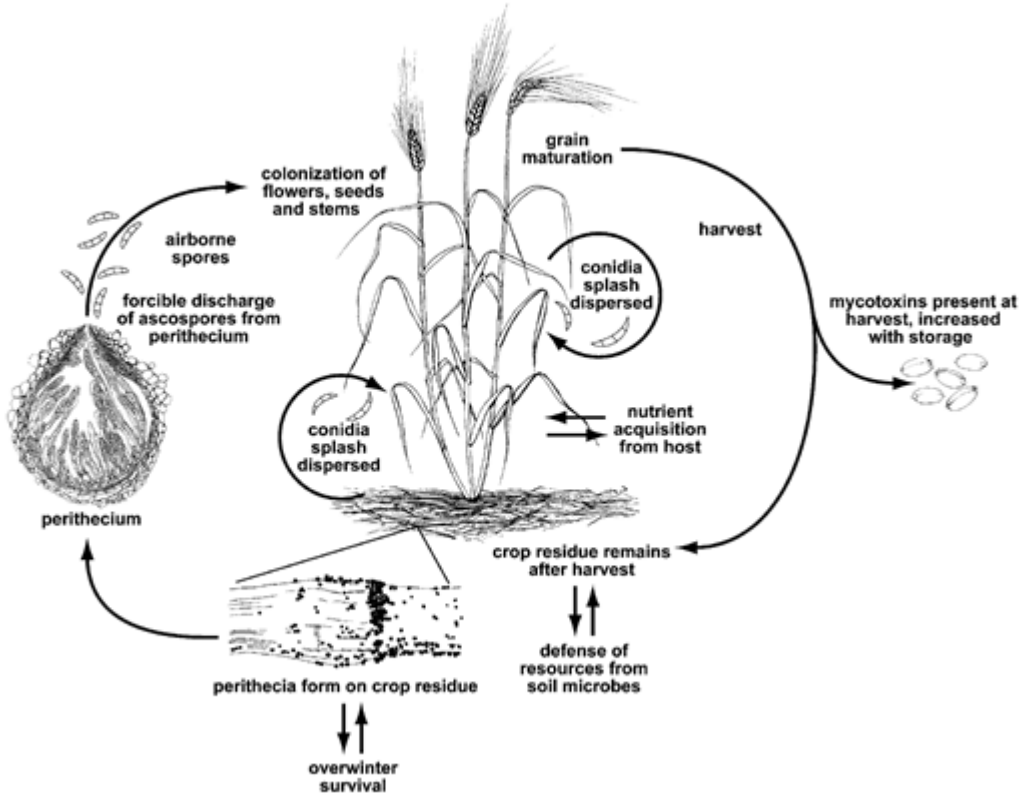

Fig. 1.1. The life cycle of *F. graminearum,* causal agent of *Fusarium* head blight on wheat (Trail, 2009).

colonize the surface of the plant before penetrating through susceptible tissues (Fig. 1.2) [1]. This is a biotrophic stage of infection, when the host does not display disease symptoms [1,3]. As mycelia grows intracellularly, necrosis of the plant tissue ensues resulting in shrunken kernels referred to as "tombstone kernels" [1,3]. Tissues susceptible to colonization include the adaxial surfaces of lemma and palea of the florets, exposed anthers, as well as stomata and base of the wheat glumes, where epidermis and parenchyma are thin-walled (Fig. 1.2) [3]. The spread of the fungus between spikelets advances through the vascular bundles via the rachis node [3].

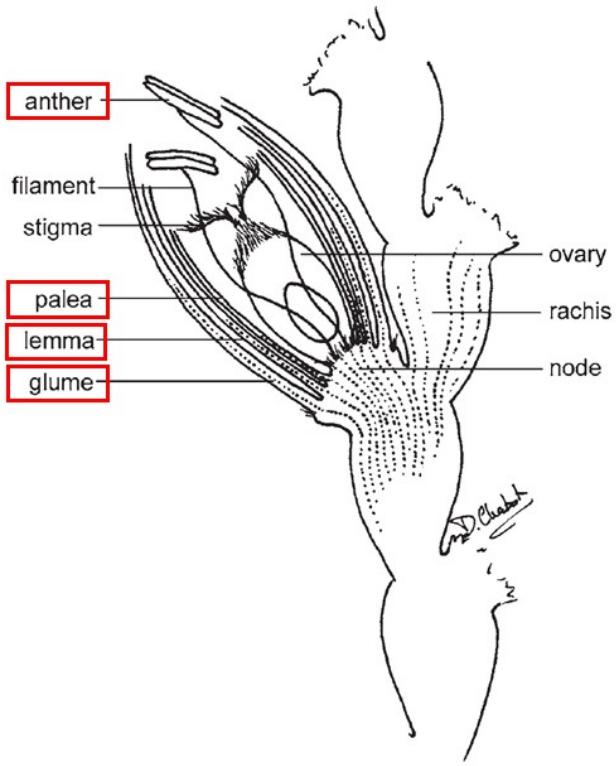

Fig. 1.2. Schematic diagram of a wheat floret morphology. Tissues most susceptible to *F. graminearum* invasion are outlined in red. Adapted from Miller *et al.*, 2004.

1.2 Overview of secondary metabolites in filamentous fungi

F. graminearum produces several classes of secondary metabolites (SMs), some of which have roles in host infection. SMs are low molecular weight compounds produced by the microorganisms, but are not essential for the survival of the organism [4–7]. They are biosynthesized as an adaptation strategy to deal with specialized environmental conditions and establish its niche in the ecosystem [7–10]. In the filamentous fungi three groups of SMs are most abundant: non-ribosomal peptides (NPs), polyketides (PKs), and terpenes (Fig. 1.3).

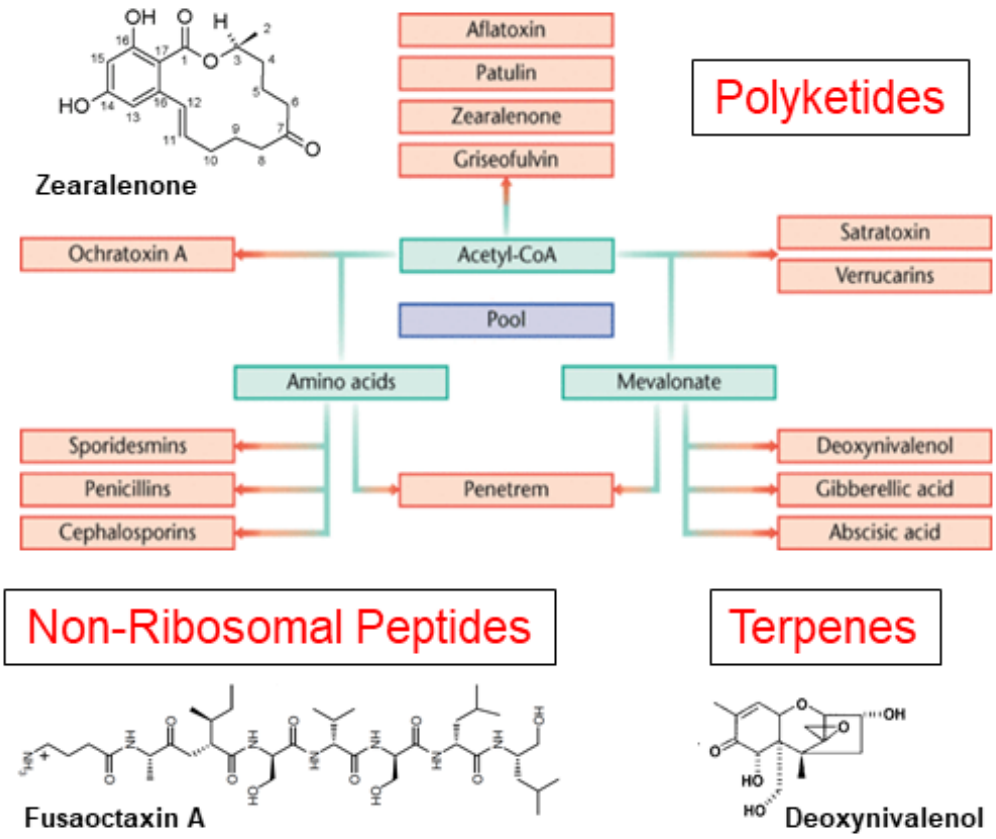

Fig. 1.3. Fungal organisms are capable of producing a multitude of secondary metabolites. Most prevalent SM classes biosynthesized by *F. graminearum* include NPs, polyketides, and terpenes. The precursors to these molecules originate from acetyl CoA, amino acids, and the mevalonate pathway.

NPs are synthesized by the large multi-modular non-ribosomal peptide synthases (NPSs) linking amino acids into polypeptide chains (Fig. 1.3) [11,12]. NPSs contain a minimum of three domains. An adenylation domain carries out ATP-dependent adenylation of the starter amino acid. A peptidyl carrier domain transfers each successive amino acid from an adenylation domain to a condensation domain. The condensation domain is a catalytic unit, forming the peptide bonds between the successive amino acids in a chain [11,13]. Some of the *F. graminearum* NPS products include

the virulence factors gramillins and fusaoctaxin A, and the siderophores ferricrocin and malonichrome [13–15].

Polyketides are the ketide chains biosynthesized from acetyl-CoA and malonyl-CoA units that participate in protein, carbohydrate, and fatty acid metabolism (Fig. 1.3). These units are connected by the multi-modular polyketide synthase enzymes (PKSs) [11,13]. A minimal PKS consists of an acyl transferase module responsible for recruitment of the correct building block, a ketoacyl synthase module, which catalyzes the formation of the ketide chain, and an acyl carrier domain, which facilitates the assembly of the growing polyketides [13]. Well-studied examples of polyketides in filamentous fungi include aflatoxins produced by the *Aspergillus* spp., the pigment aurofusarin and the estrogenic mimic zearalenone, both of which are synthesized by the *Fusarium* spp. [13]. A combined action of NPS-PKS hybrids offers additional diversity to this class of SMs. These enzymes are typically PKSs fused to the NPS modules [11]. To date, a single product of a NPS-PKS hybrid has been described in *F. graminearum,* called fusarin C [13].

The final group of compounds are terpenes that are synthesized from the isoprene by-products farnesyl pyrophosphate (FPP) of the mevalonate pathway (Fig. 1.3) [16]. Terpene synthases (TPSs) carry out the cyclization of FPPs to obtain the basic terpene structure, which is then modified by a variety of tailoring enzymes [11]. Examples of terpenes include culmorin and a deoxynivalenol (DON)-related group of compounds (Fig. 1.3) [11].

1.2.1 Genetics of secondary metabolism

The *NPSs*, *PKSs*, and *TPSs* are located within secondary metabolic clusters (SMCs) in the fungal genome together with the other genes involved in its regulation [17–19]. These clusters also encode tailoring enzymes like transferases and cytochrome P450 monooxygenases, as well as transport proteins for chaperoning precursors between cellular compartments or shuttling final products out of the fungal cell. Many SMCs also include cluster-specific transcription factors (TFs) coordinating expression of the SMC genes [11,20]. In the fungal genomes, many SMCs are located in the sub-telomeric regions and are associated with the heterochromatin DNA [21–23]. Clustered organization and presence of epigenetic regulation allow for efficient spatial and temporal control of the SMC gene expression [9,17–19].

F. graminearum is predicted to contain 76 SMCs; 67 of these were identified by a comprehensive approach involving a combination of SMC prediction algorithms and co-expression analyses in the predicted gene regions [20]. An additional nine SMCs (C68-C76) were identified through manipulation of histone methylation. Specifically, targeted deletion of the lysine methyltransferase KMT6 led to de-repression of ~20% of all genes, including many of the genes in the SMCs [24]. The presence of relatively high number of SMCs in the genome envisages the potential of *F. graminearum* to produce a diverse array of natural products. To date, only a few compounds have been identified in this species, limited by the highly specialized conditions required to activate SM gene clusters.

1.2.2 Functions of fungal secondary metabolites

The roles of fungal natural products are diverse, they aid the organism in establishing its niche in the ecosystem. SMs can function in nutrient acquisition, be used as chemical warfare in cross-kingdom interactions, or as virulence factors for host colonization [9,10,25,26].

1.2.2.1 Nutrient acquisition – a role for siderophores

Iron is an essential component in aerobic metabolism of filamentous fungi [26]. However, free iron molecules have low bio-availability due to low solubility, and in the presence of the reactive oxygen species, such as H_2O_2, can produce highly toxic hydroxyl radicals [26]. Siderophores are SM molecules possessing strong iron-chelating properties. They are produced by microorganisms to circumvent low availability of iron in the environment [26,27]. In plant-pathogenic fungi, siderophores have a proposed role in efficient iron uptake by the fungi from their host [26]. In *F. graminearum* three siderophores have been characterized. The SM triacetyl fusarinine C is a product of the biosynthetic gene *NPS6*. *F. graminearum* Δ*nps6* strain is highly sensitive to iron starvation and oxidative stress and has diminished virulence in the wheat host [28]. The product of NPS2, ferricrocin, was shown to be important for sexual development, as the *F. graminearum* strain missing *NPS2* produces only immature sexual spores [27]. A strain lacking both *NPS2* and *NPS6* showed an enhanced phenotype – a complete failure to produce ascospores, an increased sensitivity to iron depletion and oxidative stress, and a decrease in virulence as compared with either *Δnps2* or *Δnps6* strains [27]. The role of the third siderophore malonichrome is not known, as there is no severe phenotype

associated with the deletion of its biosynthetic gene *NPS1* [27]. However, triple *Fusarium* mutant *Δnps2Δnps6Δnps1* has an enhanced phenotype, when compared with *Δnps2Δnps6*, which suggests overlapping functions of the three siderophores [27].

1.2.2.2 Secondary metabolites in inter-species interactions

Filamentous fungi co-exist and compete with a multitude of other microbial species in their environment. It is not surprising, therefore, that some of the SMs they produce are used in competition against bacteria and other fungi [29–33].

In *Fusarium* spp., fusaric acid (FA) plays a significant role in competition against both bacteria and the other fungi. *F. oxysporum* uses FA to suppress production of antimicrobial agents 2,4-diacetylphloroglucinol (DAPG) and phenazine -1-carboxamide (PCN) by the biocontrol bacteria *Pseudomonas fluorescens* and *Pseudomonas chlororaphis*, respectively [29–31]. Additionally, FA represses the quorum-sensing signal in *P. chlororaphis* through inhibition of quorum-sensing regulatory genes [30]. FA is also used by an endophyte of maize *F. verticilloides* to decrease *Ustilago maydis* infection [32,33]. Co-inoculation of these two species induced FA gene expression and toxin production in *F. verticilloides* [33]. Further, *U. maydis* exhibited a decreased growth in presence of FA at concentrations comparable to those produced by *F. veticilloides* [33].

Fusarium fujikuroi relies on a combination of natural products to counteract the fungal pathogenic bacterium *Ralstonia solanacearum,* which infects chlamydospores of several *Fusarium* spp. Ralsolamycin A, a compound produced by *R. solanacarum,*

induces production of SMs bikaverin and beauvericin in *F. fujikuroi,* which together provide a degree of resistance against the bacterial infection [25].

Finally, it was discovered that DON, primarily used by *F. graminearum* as a virulence factor on wheat can also function as a defense against another fungus. *Trichoderma atroviridae* has been used as a biocontrol agent to manage FHB. However, the presence of DON results in decreased expression of *T. atroviridae NAG1,* a chitinase-encoding gene partially responsible for the efficiency of *T. atroviridae* as a biocontrol agent [34].

1.2.2.3 Secondary metabolites as host-specific virulence factors

Fusarium spp. are pathogens in several agricultural crop species, in part due to their arsenal of natural products. In *F. graminearum,* the role of trichothecenes in pathogenicity on wheat has been well-characterized. Recent efforts have also identified gramillins A and B and fusaoctaxin A compounds as host-specific SM virulence factors in maize and wheat, respectively [14,15].

Trichothecenes are sesquiterpene molecules synthesized from the FPP precursors by terpene synthases [16,35]. In *F. graminearum*, the genes responsible for trichothecene biosynthesis are distributed across three chromosomes [36]. Twelve of the genes are located on chromosome 2 that include the terpene synthase *TRI5*, the transcriptional regulators *TRI6* and *TRI10*, the transporter *TRI12*, and several tailoring enzymes [3,20,36]. Additional modifying enzymes cytochrome P450 monooxygenase TRI1 and trichothecene 3-O-acetyl transferase TRI101 are encoded on chromosomes 1 and 4,

respectively [3,36,37]. Modifications catalyzed by the tailoring enzymes determine the final structures of the trichothecene molecules. A recent survey identified the three most prevalent trichothecenes produced by *F. graminearum* isolates in Canadian wheat and maize as 15-acetyldeoxynivalenol (15-ADON), 3-acetyldeoxynivalenol (3-ADON), and 7-α hydroxy, 15-deacetylcalonectrin (3ANX) toxin (Fig. 1.4) [38]. The 3- and 15- ADON molecules are the acetyl ester derivatives of the deoxynivalenol (DON) structure, modified by the esterase encoded by the different *TRI8* alleles in the 3-ADON and 15-ADON producers [39]. Meanwhile, 3ANX results from TRI1 hydroxylating C7 of the DON precursor calonectrin, as opposed to both C7 and C8 in ADON producers [40].

During the infection process, the presence of DON at the rachis node of the wheat spikelet allows *F. graminearum* mycelia to spread between the kernels in the wheat head [41]. *F. graminearum* strains with abolished DON production are capable of infecting the inoculated kernel, but cannot spread to the rest of the wheat head [41]. The toxicity of DON and the other trichothecenes is targeted towards the large ribosomal subunit of the eukaryotes. Structural analysis demonstrated that DON interferes with the peptidyl transferase center (PTC) of the *Saccharomyces cerevisiae* 60S ribosomal subunit [42]. Further investigations implicated the epoxide ring on C12 of the DON molecule in stabilizing its conformation during the interaction with PTC [43]. However, more work is required to elucidate the complete mechanism behind trichothecene toxicity.

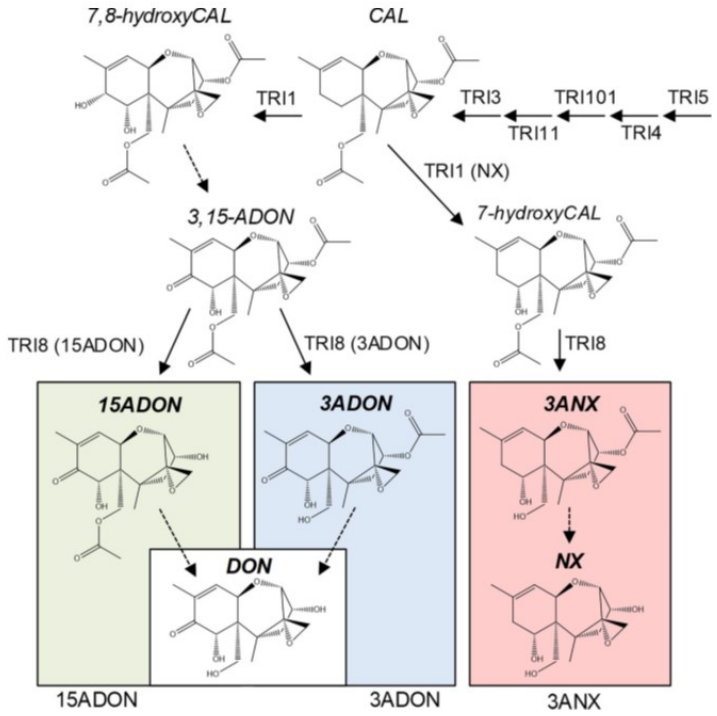

Fig. 1.4. Putative biosynthetic pathways leading to production of 3-ADON, 15-ADON, and 3ANX by *F. graminearum*. Calonectrin (CAL); 7,8-dihydroxycalonectrin (7,8-hydroxyCAL); 7-hydroxycalonectrin (7-hydroxyCAL); 3,15-diacetyldeoxynivalenol (3,15-ADON); 15-acetyldeoxynivalenol (15ADON); 3-acetyldeoxynivalenol(3ADON); deoxynivalenol (DON); 3ANX (NX-2 toxin); NX (NX-3 toxin). Adapted from Crippin *et al.,* 2019.

The ability of *F. graminearum* to invade the intracellular space in the wheat host is also attributed to a SM [15,44]. During the infection process, plant tissues prevent progression of the invading fungal hyphae by closing the plasmodesmata openings between neighbouring cells [15]. To counter this defense, *F. graminearum* produces a linear octapeptide fusaoctaxin A, which blocks plasmodesmata closure and allows the hyphae to progress [15]. Fusaoctaxin A is a product of the SMC designated C64 and depends on two NPSs, NPS9 and NPS5 for its biosynthesis [15,20]. NPS9 recruits the gamma-

aminobutyric acid (GABA) starter unit, and the NPS5 attaches the remaining seven amino acids to make the final product [15]. The action of fusaoctaxin A appears to be host-specific. An *F. graminearum* strain with abolished fusaoctaxin A production was able to infect maize stalks but not wheat heads [15]. Further, it was demonstrated that supplementing the non-wheat pathogens *Fusarium oxysporum* f. sp. *cubense* and *Fusarium poae* with fusaoctaxin A conferred upon these strains the ability to infect wheat, further demonstrating the necessity of this compound for virulence in wheat [15].

As an infection strategy in maize, *F. graminearum* produces a distinct set of bicyclic non-ribosomal peptides, gramillins A and B [14]. These are products of the NPS8 encoded in the SMC designated C02 [20]. The structure of gramillins is unusual due to their cyclization, which is facilitated through an anhydride bond and the presence of a lipid side group [14]. Infection studies with *F. graminearum* strains devoid of the main biosynthetic gene *NPS8* and the endogenous transcription factor *GRA2* revealed that gramillins are essential for the fungal spread in maize silks [14]. However, the same strains were not defective in virulence on wheat heads [14]. In agreement with these findings, a purified mixture of gramillins A and B was highly phytotoxic to young maize leaves, while having no effect in wheat leaves [14].

Thus, *F. graminearum* produces several SMs as a host invasion strategy. Given the diversity of SMs used to colonise different plant hosts and the resources associated with producing them, a complex regulatory mechanism is required to control their biosynthesis.

1.3 Regulation of secondary metabolite production in filamentous fungi

SMs are both specialized and energetically costly to produce; therefore, their production is tightly controlled through a hierarchy of cellular regulators [17,45,46]. When environmental changes are sensed, a signal is transduced into the cell where it is integrated by transcriptional regulators. These transcriptional regulators can be subdivided into global and pathway- or cluster-specific TFs. The global TFs activate or repress the pathway-specific TFs either transcriptionally or through formation of protein complexes [45,47,48].

1.3.1 Signal transduction pathways involved in secondary metabolite biosynthesis

Since SM production is a strategy for survival under specific environmental conditions, elements of the environmental sensing pathways frequently act as upstream regulators of secondary metabolism [45,49]. Several conserved pathways have been characterized in filamentous fungi for both environmental signal sensing and for signal transduction processes leading to SM biosynthesis. These include G-protein coupled receptors (GPCRs), target of rapamycin (TOR), cyclic adenosine monophosphate-protein kinase A (cAMP-PKA), and mitogen activated protein kinase (MAPK) pathways [45].

1.3.3.1 The GPCR signaling pathway

Heterotrimeric G-proteins are conserved signaling components in all eukaryotes. The GPCR system consists of a seven-domain receptor embedded into the plasma membrane and tethered to a heterotrimeric G-protein composed of the α, β, and γ

subunits in their inactive form [50]. The α subunit is attached to the guanosine diphosphate (GDP) molecule [50,51]. When a ligand binds to the receptor, it induces guanine nucleotide exchange and results in the detachment of the guanosine triphosphate (GTP)-bound Gα and the Gβγ heterodimer, both of which activate downstream signalling pathways [50]. To return the GPCR system to its inactive state, the Gα-bound GTP is hydrolyzed into GDP by the regulator of G protein signaling (RGS), facilitating the GDP-Gα complex re-association with the Gβγ and the receptor [50].

The *F. graminearum* genome encodes for 123 putative GPCRs, some with non-canonical domain organisation, three genes encoding the putative Gα components, and two genes encoding the Gβ and the Gγ subunits [52,53]. The GPCR system in *F. graminearum* is involved in sensing nutrients, light, and pheromones, and transduces the information to the MAPK cascades and the cAMP-PKA pathway [50,54–56].

Characterization of GPCR signaling components in *F. graminearum* confirmed the importance of the heterotrimeric complex for development, reproduction, and secondary metabolism. Targeted deletion of the *GPA2* gene that encodes the Gα subunit resulted in reduced pathogenicity on wheat, accompanied by chitin accumulation in the cell wall of the *Δgpa2* strain [53]. This result led to a hypothesis that the reduction in virulence could be due to increased levels of chitin eliciting plant defense responses [53]. Another gene that encodes the Gα component, GPA1, was implicated in sexual development and mycotoxin production. The *Δgpa1* strains were deficient in perithecia production, and showed enhanced biosynthesis of DON and zearalenone compared

with the wild-type strain [53]. Of interest is that the strain with deletion of the Gβ subunit-encoding *GPB1* also showed increased DON and zearalenone accumulation but was deficient in virulence compared with the wild-type strain. It should be noted, however, that the *Δgpb1* growth rate *in vitro* was also diminished by 25% compared to the wild-type [53]. Detailed characterization of Gγ subunit in *F. graminearum* has not been carried out so far.

A recent effort to characterize the 105 GPCR genes in *F. graminearum* identified five genes, *GIV1-GIV5*, that were upregulated during the infection process. Targeted deletion of these genes resulted in reduction of virulence by 25-73% compared with the wild-type [57]. Moreover, authors were able to identify specific functions for *GIV1*, *GIV2*, and *GIV3* genes. *GIV1* was implicated in infection cushion formation during the early stages of infection, while *GIV2* and *GIV3* were involved in growth after penetration - neither *Δgiv2* nor *Δgiv3* strains could spread past the rachis node [57]. The role of these five GPCRs in mycotoxin production was not evaluated.

1.3.1.2 The TOR signaling pathway

The TOR pathway is present in all eukaryotes and is essential for sensing nutrient availability and promoting growth [58]. Studies in *S. cerevisiae* have identified two TOR complexes, both involved in promoting cell growth- TORC1 in anabolic processes, and TORC2 in the reorganization of actin cytoskeleton. Only TORC1 is sensitive to rapamycin and is present in filamentous fungi [59]. TORC1 is a heterotrimeric complex composed of components LST8, KOG1, and the TOR1 kinase. The complex is

activated by the GTPase heterodimer, GTR1-GTR2, which is regulated by a system of GTPase activating proteins (GAPs) and guanine exchange factors (GEFs) [60].

The activity of TORC1 is influenced by nutrient availability and is best characterized in *S. cerevisiae*. Amino acids directly modulate activity of the TOR signaling pathway. For example, methionine regulates the TORC1 complex by inducing methylation of the PP2A phosphatase. PP2A dephosphorylates the GTR1-inhibiting GAP, which leads to the TORC activation [60,61]. Leucine also activates TORC through GTR1. Leucyl-tRNA synthetase (LeuRS) is an enzyme responsible for attaching the leucine to tRNA. The leucine-bound LeuRS also interacts with GTR1 to activate the TOR1 complex [62]. In contrast, glutamine regulates TORC1 independently of GTR1/GTR2 [63]. In addition to regulation by specific amino acids, TORC1 also responds to general amino acid starvation, through a mechanism that has not been studied in detail [60].

TORC1 is also regulated by glucose availability through interaction with an AMP-activated protein kinase SNF1, which is activated due to high cellular AMP/ATP ratios resulting from glucose starvation [60]. SNF1 phosphorylates the KOG1 component of the TORC1 complex, causing it to disassociate and abolish TORC1 activity [64].

In plant-pathogenic fungi, TOR complex mediates pathways contributing to virulence and SM production. In *F. oxysporum*, TOR controls virulence pathways such as invasive growth and root adhesion in response to nutrient starvation [65]. In *F. fujikuroi*,

rapamycin treatment results in downregulation of the SM genes involved in bikaverin and gibberellin biosynthesis [66].

In *F. graminearum*, TOR signalling affects DON production through three circuitries, two of which depend on a major target of TORC1, the phosphatase complex TAP42 [67]. The first pathway involves a type 2A protein phosphatase PPG1 in the TAP42 complex. It was proposed that PPG1 regulates *TRI* gene expression by de-phosphorylating AreA, a known transcriptional regulator of DON production [67,68]. In addition, a recent study showed that TOR also regulates biogenesis of lipid droplets through the TAP42–PPG1 cascade [69]. A part of DON biosynthesis is carried out in lipid vesicles called the "toxisomes", and since TOR regulates lipid droplet formation, it was suggested that TOR influences DON production through lipid droplet biogenesis [68,69]. Finally, TOR regulates *TRI* gene expression and DON production through its downstream effector kinase SCH9 [67]. Targeted deletion of *SCH9* in *F. graminearum* led to reduced DON production and virulence on wheat [70]. The strain lacking the SCH9-interacting kinase MAF1 exhibited the same phenotype, resulting in a hypothesized TORC-SCH9-MAF1 kinase cascade model controlling *Fusarium* virulence and DON production [67,70].

As mentioned previously, the TOR complex can be activated by glutamine, which is a preferred nitrogen source in *F. graminearum* [71]. Recent work identified two adaptor 14-3-3- proteins, BMH1 and BMH2, which inhibit DON production in the presence of glutamine [72]. It was found that the glutamine sensitivity and the TOR

pathway influence each other, but the mechanism of interactions and their coordinated influence on DON production is not known.

1.3.1.3 The cAMP-PKA signalling pathway

Another important branch of environmental signaling is the cAMP-PKA pathway. In filamentous fungi, the cAMP-PKA system responds to environmental signals and is important for both vegetative growth and pathogenicity [47,58,73–75]. For example, abolishing key components of the PKA pathway in *F. graminearum* results in significant reduction in vegetative growth and infection on wheat [73,75,76].

The activation of the PKA pathway results in the production of the cAMP messenger molecules through the action of adenylyl cyclase (AC). cAMP binds the regulatory subunits of PKA leading to release of the catalytic subunits, which phosphorylate the downstream targets [77]. Mutations of AC in *F. graminearum* or double deletion of both catalytic and regulatory subunits of PKA resulted in defects in conidia and perithecia formation, demonstrating the importance of PKA in both sexual and asexual development [73,75,76]. Mutations in AC and catalytic PKA subunits resulted in diminished DON biosynthesis, whereas mutation in regulatory PKA resulted in increased DON production on wheat heads, rice grain, and in the trichothecene induction medium [73,75,76]. Mutation of the regulatory PKA subunit also resulted in decreased expression of genes from the aurofusarin metabolic cluster, suggesting a regulatory crosstalk between these SMCs [76].

A targeted deletion of the catalytic subunit of PKA in *F. graminearum* resulted in altered expression of the *TRI* cluster and genes from the isoprenoid pathway, origin of the DON precursor FPP [77]. Similar studies in *F. verticillioides* showed that PKA is involved in regulation of the polyketide bikaverin and the peroxisomal proteins necessary for production of the polyketide precursors acetyl-CoA and malonyl-CoA [77].

Studies of DON regulation by the cAMP-PKA pathway in *F. graminearum* revealed a complex pattern implicating both trichothecene regulatory genes *TRI6* and *TRI10* [78]. TRI6 has been shown to auto regulate its expression by binding its own promoter. Recent evidence implies that PKA relieves this self-inhibition, though the mechanism by which PKA performs this function is not known [78]. In addition, a model has been proposed where the global regulator AreA is phosphorylated by PKA, inducing its interaction with TRI10 to regulate DON production [47,78].

1.3.1.4 The MAP kinase signalling pathways

In eukaryotes, the MAP kinase pathway is characterized by the three-tiered phosphorylation cascade. First, MAP kinase kinase kinases (MAPKKKs) are activated by the upstream signals originating from active GPCRs perceiving environmental signals. The cascade ensues with the MAPKKK phosphorylation of the MAP kinase kinases (MAPKKs) [79]. These, in turn, phosphorylate the MAPKs, which translocate into the nucleus to phosphorylate transcription factors and other signalling proteins to regulate gene expression [67,79]. Originally characterized in *S. cerevisiae*, there are three MAPK modules that are conserved in *F. graminearum* and are implicated in diverse

physiological functions. These modules include the high osmolarity glycerol HOG1, the *Gibberella* pathogenicity map kinase GPMK1 (*S. cerevisiae* FUS3), and the map kinase for growth and virulence MGV1 (*S. cerevisiae* SLT2) [80–82].

The HOG1 pathway in *S. cerevisiae* is involved in osmolarity sensing. However, in *Schizosaccharomyces pombe*, the same pathway also mediates responses to other environmental stimuli such as heat, oxidation, and nutrient limitation [83–85]. Similar to *S. pombe*, the HOG1 homolog in *F. graminearum* is implicated in response to various stresses. The *F. graminearum Δhog1* strains exhibited hypersensitivity to high osmolarity and hydrogen peroxide treatments, as well as to cell membrane and cell wall stresses [86]. Further research has demonstrated that the *Δhog1* mutants exhibit slow hyphal growth, defects in perithecia formation, and diminished virulence in wheat heads [86,87]. The HOG1 pathway in *F. graminearum* also has a role in SM regulation. Targeted deletion of the transcription factor *ATF1*, whose expression is regulated by HOG1, resulted in a decreased DON and zearalenone production *in planta* [88]. However, in axenic cultures, Δ*atf1* produced more DON and aurofusarin than the wild-type, while levels of zearalenone were unchanged [88].

The second MAPK module in *S. cerevisiae,* FUS3 is involved in the pheromone-sensing pathway. It mediates a variety of cellular changes associated with mating, including cell cycle arrest, polarized growth, cell adhesion and fusion, and nuclear fusion [83]. The *F. graminearum* FUS3 homologue GPMK1 also has a role in sexual reproduction, as the *Δgmpk1* strain is defective in perithecia formation [82]. In addition,

this kinase regulates filamentous growth, conidiation, virulence, and DON biosynthesis [82]. Targeted deletion of the components of the GPMK1 module, such as the transmembrane receptor SHO1, STE11 (MAPKKK) and STE7 (MAPKK) resulted in defects in DON biosynthesis [89].

Unlike HOG1 and FUS3, the SLT2 kinase has a wider role in the physiology of *S. cerevisiae*. SLT2 regulates the cell wall integrity (CWI) pathway, mediating responses to temperature differences, osmotic shock and treatments with cell wall biogenesis inhibitors [90,91]. SLT2 is involved in recycling cellular components; it controls induction of the mitochondrial and peroxisome recycling as well as expression of chaperones required for proteasome abundance [92,93]. Additionally, SLT2 is also involved in several aspects of cell cycle regulation, such as G1/S stage progression, and the growth of mating projections [83].

In *Fusarium* spp., the SLT2 homolog is encoded by the *MGV1* gene. Like HOG1 and GPMK1 pathways, the MGV1 circuitry has an important role in the development and pathogenicity of *F. graminearum*. Although hyphal growth of the Δ*mgv1* mutant in liquid culture was comparable to wild-type, mycelia grew at a decreased rate on solid medium and had defective cell walls, associating MGV1 with the CWI pathway [80]. Additionally, the Δ*mgv1* strain was incapable of producing perithecia and ascospores, implicating MGV1 in sexual development. In pathology studies, targeted deletion of the *MGV1* gene abolished the spread of *F. graminearum* from the site of inoculation to the neighbouring spikelets on wheat heads [80]. It was concluded that the mutant is unable to

produce necessary virulence factors. Consistently, DON biosynthesis was reduced in *Δmgv1* strains compared with the wild-type *in planta* [80]. *In vitro* experiments demonstrated that the Δ*mgv1* mutant produced both butenolide and 15ADON in the nutrient-rich medium [94]. In the nutrient-deficient medium, Δ*mgv1* produced lower quantities of DON, while butenolide production remained unchanged [94]. Meanwhile, gene expression of neither metabolic cluster differed from the wild-type levels in nutrient-deficient medium, suggesting that MGV1 does not exert transcriptional control, but rather regulates these two SMCs at either post-transcriptional or at translational levels [94]. Unlike in *S. cerevisiae*, no role for MGV1 in cell cycle regulation or recycling of cellular components has been established in *F. graminearum*.

1.3.2 Control of secondary metabolism by global transcriptional regulators

In the hierarchy of responses to the environmental changes, the GPCR, TOR, cAMP-PKA, and MAPK pathways relay environmental signals by reversibly phosphorylating global transcriptional factors [17,45,67]. These, in turn, modulate pathway-specific TFs to alter expression levels of the SMC genes [45,47,48].

The global regulators of transcription are characterized by their ability to regulate the functions of signaling components in many pathways in response to the environmental stimuli. They also have structural similarities, as most global TFs contain a number of Cys_2His_2 DNA-binding domains and tend to form homodimers to control gene expression [46,95,96]. Many of the global regulators mediating environmental changes are highly conserved across filamentous fungi. Disruption of these regulators results in

severe defects in vegetative growth, production of either ascospores or conidiophores or both [97–100]. Thus, global regulators play a significant role in fungal pathogenesis.

1.3.2.1 Carbon catabolite repression and activation of secondary metabolite clusters

Carbon catabolite repression (CCR) is a regulatory mechanism where the expression of genes required for the utilization of secondary sources of carbon is suppressed by the presence of a preferred substrate such as glucose [101,102]. This system is essential to plant-pathogenic fungi due to their reliance on complex carbon sources such as cellulose and lignin present in plant hosts [56].

Carbon sensing is mediated through the GPCR signaling and is relayed to the regulator of carbon metabolism, CreA, a transcription factor containing a Cys_2His_2 zinc finger DNA binding domain [56,103]. Cellular localization and activity of CreA are regulated by both phosphorylation and ubiquitination, though the details of how CreA is regulated by these modifications have not been elucidated [56].

Though glucose is the preferred carbon source, *Fusarium* spp. can assimilate other sugars, and SMs biosynthesized in the presence of different carbon sources vary widely. For example, three strains of *F. avenaceum* demonstrated robust growth on six monosaccharides (arabinose, xylose, fructose, sorbose, galactose, mannose), five disaccharides (cellobiose, lactose, maltose, sucrose and trehalose), and three polysaccharides (dextrin, inulin, and xylan) [104]. Influence of these carbon sources on SM production underscores the specificity of environmental conditions for SM biosynthesis. For instance, high levels of the SM aurofusarin were produced by all three strains in

cultures supplemented with inulin, maltose, and arabinose. The fusarin C cluster genes were most upregulated when strains were grown on mannose and cellobiose; moniliformin accumulated the most when strains were grown in sucrose and xylose [104]. Similarly, evaluation of ten non-glucose carbon sources (sucrose, 1-kestose, nystose, amylose, amylopectin, cellobiose, fructose, maltose, xylose and galactose) supported mycelial growth of different *F. graminearum* chemotypes [102]. The expression of *TRI* genes and production of trichothecenes were highest in presence of sucrose, 1-kestose, and nystose [102].

Another study in *F. graminearum* demonstrated that targeted deletion of the regulator of carbon source availability *CreA* results in 90% reduction of vegetative growth with significant conidiation defects, and complete absence of virulence on wheat heads [67,99]. The same study identified CreA binding motifs in 10 of the 13 *TRI* genes. However, neither DON production assays in the Δ*creA* strain or CreA binding studies were carried out [67,99].

1.3.2.2 Nitrogen catabolite repression and activation of secondary metabolite clusters

Assimilation of nitrogen sources is similar to carbon utilization in that low availability of the preferred nitrogen source such as glutamate or aspartate results in upregulation of genes that assimilate non-preferred sources of nitrogen [47,71,105]. The key transcriptional regulator involved in this process is the transcription factor AreA [106]. When the preferred source of nitrogen is limited, *AreA* is highly expressed; it is also regulated at the post-transcriptional level through stabilization of the mRNA [4]. AreA

activates other regulators of nitrogen assimilation such as the *NMR1* and *AreB* genes [4,107]. AreB is a co-regulator of AreA, while NMR1 acts as a negative regulator of AreA [4,107].

Targeted deletion of the *F. oxysporum AreA* homolog, *FNR1,* results in growth on glutamine comparable to the wild-type, but the mutant strain has reduced ability to assimilate non-preferred nitrogen sources such as hypoxanthine, uric acid, asparagine, histidine, and proline [71]. In addition, the infection rate of the mutant strain on tomato seedlings is significantly slower compared with the wild-type [71]. Similarly, *F. graminearum ΔareA* is unable to assimilate non-preferred amino acids and is defective in conidiation and virulence [47,108].

Interestingly, *F. graminearum* strains lacking *AreA* exhibit reduced GPMK1 phosphorylation and PKA activity compared with the wild-type, though the mechanism by which AreA regulates these two pathways is not clear [47]. In *Candida albicans*, nitrogen permease MEP2 interacts with the RAS1 protein, which acts upstream of both cAMP and MAPK pathways [109]. AreA has been confirmed as a positive regulator of *MEP2* transcription, thus it is proposed that AreA affects PKA and MAPK pathways through transcriptional control of *MEP2* [47].

Both AreA and AreB have well-established roles in regulating production of SM compounds in *Fusarium* spp. A study in *F. fujikuroi* determined that AreA acts as a positive regulator of nine SMCs and a negative regulator of seven SMCs under nitrogen-limiting conditions [110]. In the same study, analysis of the *F. fujikuroi ΔareB*

mutant revealed that AreB positively regulates six SMCs and negatively regulates seven SMCs [110]. Interestingly, only nine clusters were controlled by both regulators, including gibberellic acid and fumonisin SMCs [110,111]. Finally, the product of the uncharacterized NPS11 was positively regulated by AreA while being negatively regulated by AreB. Together, these findings suggest independent roles for AreA and AreB in the secondary metabolism of *F. fujikuroi* [110].

In *F. verticillioides*, AreA exerts temporal control over fumonisin B biosynthesis during the maize kernel infection. Fumonisin B is produced during infection of late, mature maize kernels, but not during infection of the early blister-stage maize. The *F. verticillioides* strain disrupted in *AreA* lacks fumonisin B production and is diminished in the infection rate on mature maize kernels [97]. In contrast, *ΔareA* infects blister-stage maize at the same rate as the wild-type [97].

In *F. graminearum*, biosynthesis of trichothecenes is induced by the non-preferable nitrogen sources and is also regulated by AreA .[47,108] In the presence of preferred nitrogen source ammonium, the *ΔareA F. graminearum* strain exhibits a significant increase in DON production, as compared to the growth without ammonium [47]. Further, DON induction by non-preferable arginine was reduced 14-fold in *ΔareA* compared with the wild-type. This suggested that AreA acts as a negative regulator of DON in the presence of preferred nitrogen source, but a positive regulator in the presence of non-preferred nitrogen [47]. A co-immunoprecipitation study identified physical interaction between AreA and the trichothecene regulator TRI10 [47]. The same

work found evidence that AreA is phosphorylated by PKA, which led to the current model of DON regulation, where PKA-phosphorylated AreA binds TRI10 and together this complex modulates *TRI* gene expression [47,78].

In addition to the action of AreA and AreB as transcription factors, research in *F. fujikuroi* found evidence for these regulators in epigenetics [110]. The histone 3 lysine 9 acetylation (H3K9ac) mediated by histone acetyltransferases (HATs) results in an open chromatin conformation conducive to transcription. The *F. fujikuroi areB* mutant exhibited significantly reduced acetylation levels in the fusaric acid and gibberellin SMCs [110]. The *areA* mutant also showed a decrease in acetylation of the gibberellic acid cluster, but the fusaric acid genes were only moderately affected [110]. These results were consistent with a microarray screen study, which showed a decrease in transcription of both SMCs in absence of *AreA* and *AreB*. In contrast, fumonisin SMC gene expression was significantly downregulated in *ΔareA* and *ΔareB*, while the acetylation levels were unchanged. Together, these results implicate AreA and AreB in epigenetics through recruitment of HAT proteins to initiate transcription of some SMCs [110].

1.3.2.3 The role of light in secondary metabolite production

In fungi, dark conditions favour the developmental processes of sexual and asexual reproduction and SM biosynthesis, while light has an inhibitory effect [55]. Response to light is regulated by the trimeric complex consisting of the LaeA, VelB, and VeA proteins, termed the velvet complex. LaeA is the mediator of transcriptional changes through structural modulation of chromatin (LaeA possesses a

methyltransferase domain) [67,112]. The first step of heterotrimer formation occurs in the cytoplasm, where VeA interacts with VelB [55,113]. The VeA-VelB complex is localized into the nucleus in the dark, where VeA bridges the VelB and LaeA proteins, leading to LaeA methylation activity [22,55,113].

Abolishing the function of the velvet complex in plant-pathogenic fungi results in defects of vegetative growth, conidiation, virulence, and SM biosynthesis [114,115]. Furthermore, studies in *Aspergillus nidulans* have revealed that *laeA* mutation results in repression of the sterigmatocystin and penicillin SMCs through H3K9 methylation and a decrease in biosynthesis of both metabolites [22,112] . In line with this, constitutive expression of *VeA* in *A. nidulans* resulted in increased levels of the trimeric VeA-VelB-LaeA complex in the nucleus and increased production of sterigmatocystin [116].

In *F. fujikuroi,* targeted deletion of *VeA* and *LaeA* abolishes production of the gibberellins, fumonisins and fusarins, indicating positive regulation of these clusters. The same mutations result in upregulation of the bikaverin production, indicating that the velvet complex can act both as a positive and a negative regulator [115]. Interestingly, a link between LaeA and acetylation was suggested in this organism. Constitutive expression of a histone acetylase, *HAT1*, in the *F. fujikuroi laeA* mutant background led to the restoration of gibberellin biosynthesis [117].

In *F. graminearum,* deletion of the *VeA* component of the velvet complex results in the reduction of DON and aurofusarin biosynthesis [114,118]. Studies showed that LaeA regulates production of trichothecenes and zearalenone by modulating transcriptional

levels of the TF genes, *TRI6* and *ZEB2*, from trichothecene and zearalenone SMCs, respectively [119]. Overall, transcriptional changes linked to LaeA have been found in genes belonging to 47 of 77 predicted SMCs [119].

1.3.2.4 Regulation of secondary metabolite biosynthesis by the environmental pH

An alteration of pH in culture has a significant impact on fungal metabolism with changes to SM production. For example, in *Aspergillus parasiticus*, high extracellular pH induces the biosynthesis of penicillin, while repressing the production of aflatoxin [120]. In *F. graminearum*, an acidic environment is required for initiation of 15-ADON biosynthesis [121]. The key regulator responsive to pH change in filamentous fungi is the transcription factor PacC. Similar to AreA and CreA, PacC also possesses the Cys_2His_2 zinc fingers [122]. Like *TRI6*, the *F. graminearum PacC* homolog *Pac1* auto-regulates itself through promoter binding [100].

PacC is an example of a cleavage-mediated protein maturation mechanism. In an acidic environment, the inactive PacC precursor is held in a closed conformation not accessible to the proteases [123]. In the alkaline conditions, conformation changes occur that permit the endosomal membrane complex proteases, PalA and PalB to cleave the inactive PacC precursor and produce a truncated PacC enzyme (PacC-53). This intermediate is further cleaved by the proteasome to produce a transcriptionally active form of PacC (PacC-27) [123,124].

Targeted deletions studies with the *PacC* in various *Fusarium* spp. have demonstrated various vegetative growth defects [100,125–127]. These studies also revealed a

variety of species-specific phenotypes, consistent with the large number of pathways that are regulated by PacC. For example, the *F. verticillioides* lacking *PacC* homolog, *Pac1,* displayed impaired growth at high pH and conidiation defects at acidic and neutral pH [125]. The *F. oxysporum ΔpacC* was sensitive to hydrogen peroxide and under alkaline conditions exhibited the stress-induced accumulation of vacuoles in the hyphae [127].

In *Fusarium* spp., PacC is a negative regulator of SM biosynthesis. *F. verticillioides* lacking a functional Pac1 produced more fumonisin compared with the wild-type at both acidic and alkaline pH [125]. Similarly, the PacC in *F. fujikuroi* acts as a repressor of bikaverin biosynthesis. Exposure of a *F. fujikuroi* Δ*pacC* strain to low pH (pH 4) led to an increased expression of bikaverin SMC genes as well as higher bikaverin biosynthesis compared to the wild-type strain [126]. In an alkaline environment, expression of *BIK1,* a gene encoding the bikaverin-synthesizing PKS, was absent in the wild-type but present in the *pacC* mutant. These results place PacC as a bikaverin repressor under both pH conditions [126]. Further, a promoter analysis of the bikaverin gene cluster revealed three PacC binding sites in the *BIK1* promoter. Accordingly, mutation of PacC binding motifs resulted in higher PKS gene expression [126].

Over time, *F. graminearum* axenic cultures result in acidification of the medium, suitable for trichothecene production achieved through upregulation of the trichothecene regulatory and biosynthetic genes, and downregulation of *Pac1* [128]. A buffered culture at pH 6.5 did not produce 15-ADON [128]. Targeted deletion of *Pac1*

caused an increase in DON production at pH 3, an effect which was rescued by constitutive expression of the gene in the mutant strain [100]. Interestingly, deletion of *Pac1* was not sufficient to induce higher toxin production at neutral pH, consistent with the notion that other factors influence *TRI* gene expression [100]. Promoter analysis of the main *TRI* cluster uncovered 14 Pac1 binding sites (between one and three sites upstream of each *TRI* gene), suggesting potential direct regulation of the trichothecene genes by Pac1 [100].

1.3.3 Transcriptional activation of secondary metabolite clusters by pathway-specific regulators

The last level of the regulatory hierarchy of mycotoxin production involves transcription factors dedicated to regulation of a single SM biosynthesis pathway. It is common for the SMCs to encode pathway- or cluster- specific transcriptional factors to control expression of most or all genes necessary for SMC product biosynthesis [45,50]. In *F. graminearum,* 35 SMCs have pathway- specific transcriptional regulators [20,129]. Structurally, most of these pathway-specific TFs contain a limited set of domain types, which include $Zn(II)_2CYS_6$, bZIP, and bHLH domains.

$Zn(II)_2CYS_6$ DNA binding domains are specific to the fungal phyla; they constitute the largest group of pathway-specific TFs. These proteins can bind DNA as monomers, homodimers, or heterodimers [11,45]. In *F. graminearum,* 25 SMCs contain a $Zn(II)_2CYS_6$ TF, including aurofusarin, ferricrocin, butenolide, and fusarielin-producing clusters [20,129]. In *F. fujikuroi,* the bikaverin SMC is regulated by two cluster- specific TFs,

one of which, BIK5, has a $Zn(II)_2CYS_6$ organization. Bikaverin production was not absent in the mutant lacking both TFs, suggesting that regulation of this SMC is complex [126].

The bZIP domains in TFs are characterized by a basic DNA binding region, a leucine zipper dimerization domain, and recognition of the palindromic consensus sequences [11,17]. In *F. graminearum,* the fusaoctaxin A SMC encodes a pathway-specific transcriptional regulator harbouring a bZIP DNA binding domain with ankyrin repeats [15]. Other SMCs regulated by cluster-specific TFs possess structural features that are unique. For example, the SMC designated C12 in *F. graminearum* is responsible for production of an uncharacterized polyketide and is regulated by a cluster-specific transcriptional regulator with an unusual structure. This TF (FGSG_02288) contains a C3H1 domain typical of a zinc finger that has not been characterized [130].

1.4 Thesis outline

F. graminearum is a main causative agent of FHB epidemics throughout the world. Along with diseased kernels, the fungus also produces toxic compounds in asymptomatic tissues that reduces value of the grains. The genome of the organism encodes ~76 SMCs with a potential to biosynthesize many novel metabolites. Our knowledge of the few characterized SMs indicates that most of these compounds have specialized roles in an ecological niche occupied by the fungi. The biosynthesis of SMs is a very energy-intensive process; therefore, most of these SMCs are silent under

standard laboratory conditions and are only activated under a defined set of environmental conditions.

In this thesis, I aimed to cryptically activate silent SMCs through genetic manipulation of two key signalling components of the regulatory hierarchy – the global transcriptional regulator, TRI6, and the MAP kinase, MGV1. TRI6 is a known regulator of trichothecene biosynthesis; however, recent evidence indicates that it is a global regulator. I hypothesized that in addition to regulating the trichothecene cluster, TRI6 also regulates other SMCs. In chapter 2, I demonstrate that cryptic activation of *TRI6* results in the activation of several non-trichothecene SMCs. Using metabolic profiling, novel compounds were identified and assigned to the appropriate SM gene clusters.

MGV1 is a component of a MAPK cascade involved in many diverse physiological and developmental pathways in *F. graminearum*. Prior work implicated MGV1 in control of trichothecene and butenolide production, though the extent of its role in the regulation of secondary metabolism has not been extensively studied. My thesis hypothesized that as a signalling component, MGV1 might be involved in the regulation of myriad secondary metabolism biosynthesis. In chapter 3, I used transcriptomic and metabolomic screens to identify SMs regulated by the MAPK MGV1. A comparative analysis between the genes regulated by *TRI6* and *MGV1* uncovered both common and differential regulation of SMCs by these two regulators at transcriptional and post-transcriptional levels.

Chapter 2. Cryptic activation of secondary metabolic clusters by the global transcriptional regulator *TRI6* in *Fusarium graminearum*

2.1 Abstract

In *Fusarium graminearum*, the transcription factor *TRI6* positively regulates the trichothecene biosynthetic gene cluster leading to the production of the secondary metabolite 15-ADON. However, recent studies have shown that *TRI6* also regulates genes outside of the trichothecene gene cluster. In this study, a combination of transcriptomic and metabolomic analyses with a deletion mutant and overexpressor strains of *TRI6* was used to establish the role of TRI6 in the regulation of several secondary metabolite gene clusters (SMCs) in *F. graminearum.* Evidence for a direct and an indirect regulation of gene clusters by TRI6 were obtained by chromatin immunoprecipitation and yeast two hybrid experiments. The results showed that the trichothecene genes are under direct control, while the gramillin gene cluster is indirectly controlled by TRI6 through its interaction with the transcription factor GRA2.

2.2 Introduction

The biosynthesis of secondary metabolites (SMs) by fungi is a physiological response to both the environment and the ecological niche that it occupies. Thus, the number and the functional diversity of SMs produced by a given fungus is a reflection of the range of circumstances for which that fungus has endured. These include defense against competitors, inter and intra-species interactions, nutrient acquisition, and symbiotic and pathogenic interactions [45,131].

The pathogenic interaction between *Fusarium graminearum* and its host wheat results in the expression and activation of many SM biosynthetic gene clusters that enables the fungus to infect and spread in the wheat spikelets and subsequently inside the whole plant. A group of trichothecene compounds related to deoxynivalenol (DON) play a role in the dissemination of the fungus between kernels via the rachis in the wheat spikelets, resulting in damaged and undersized kernels associated with Fusarium head blight (FHB) disease [132,133]. Recently, SMs with a host-specific role in virulence have been identified in *F. graminearum* [14,15]. Both gramillins A and B, lipopeptide products of the non-ribosomal peptides synthase 8 (*NPS8*) gene cluster were demonstrated to act as virulence factors in maize silk infection, but not in wheat [14]. Another SM, fusaoctaxin A, a product of *NPS5-NPS9* SMC was shown to inhibit callose deposition, enabling cell-to-cell progression of the fungal mycelia in wheat coleoptiles and leaf tissues [15,44].

Given the high energy cost involved in the production of SMs, fungi have evolved a mechanism to regulate the expression of SMCs through a transcription factor hierarchy. In this regulatory hierarchy, global transcription factors (TFs) sense environmental cues and redirect primary metabolites to SM pathways; and through the activation of pathway-specific TFs, a myriad of SMs are produced [50,105]. Shared structural features such as cysteine/histidine (C_2H_2) zinc finger DNA binding domains are a notable hallmark of global TFs [134,135]. Transcription factors such as AreA and AreB, CreA, and PacC are found in many filamentous fungi and possess zinc finger domains

to facilitate promoter binding to genes responsive to a multitude of environmental conditions, regulating both growth and development [106,134–136]. For instance, the global regulator AreA is involved in a nitrogen catabolite repression signalling pathway where repression occurs in preferred nitrogen sources (such as glutamine or asparagine), and activation occurs in response to the utilization of non-preferable nitrogen compounds [4]. In *F. graminearum*, AreA is necessary for assimilation of nitrate, and non-preferred amino acids and is linked to the regulation of DON production through interaction with the transcription regulator TRI10 [108]. In *Fusarium fujikuroi*, AreA/B are involved in the regulation of gibberellin and fumonisin biosynthesis [111,137]. Similar to AreA/B, the global regulator CreA is expressed in several fungal species during carbon catabolite repression, as a response to the absence of a preferred carbon source such as glucose [101,102]. The deletion of *CreA* in *F. graminearum* has significant consequences including reduced growth, conidiation, and virulence; however, a molecular mechanism by which *CreA* functions is yet to be elucidated [67]. One well characterized global regulator is the pH sensing PacC, which plays a role in the differential regulation of SMC expression. For example, in the human pathogen *A. parasiticus*, high extracellular pH induces the biosynthesis of penicillin, while repressing the production of aflatoxin [120]. In the plant pathogen *Fusarium verticillioides,* PacC acts as a negative regulator of fumonisin biosynthesis under alkaline pH and similarly, in *F. graminearum* downregulation of Pac1 in acidic environment contributes to the expression of the trichothecene (*TRI*) gene cluster, leading to the synthesis of DON [100,125].

In *F. graminearum*, the TF TRI6 exhibits many characteristics of a global regulator. Similar to other environment-sensing regulators, *TRI6* expression is regulated by environmental conditions including pH and light, as well as carbon and nitrogen limitation [47,100,102,138]. Recently, ChIP-Seq and microarray expression profiling studies identified multiple genes and potential targets influenced by TRI6 that are not part of the trichothecene SMC, strongly suggesting that TRI6 extends its control beyond the regulation of DON biosynthesis [35,139]. The affected genes included those of the mevalonate pathway synthesizing isoprenoid "building blocks" for terpene biosynthesis, as well as the metabolism of the branched chain amino acid pathway, defense, protein transport and secondary metabolism [35,140]. Similar to other global regulators, *TRI6* is also subject to self-regulation [139]. In nutrient-preferred (non-limiting nitrogen) conditions, the TRI6 protein binds to its own promoter, repressing its expression in this environment [139].

Here we present evidence that entrenches the role of TRI6 as a global TF, mediating transition from primary to secondary metabolism in accordance with nutrient availability. Prior studies used a Δ*tri6* mutant strain to identify differentially expressed genes (DEGs) in preferred nutrient (PN) and non-preferred nutrient (NPN), where the nitrogen source is limiting and identified direct targets of TRI6 by chromatin immunoprecipitation – sequencing analysis in PN conditions [35,139]. This study extends these observations by comparing the effect of *TRI6* deletion to constitutive expression of *TRI6* when strains were grown in preferred and non-preferred nutrient conditions. In

addition to gene expression, we also used metabolomic profiling and identified five non-trichothecene producing SMCs that included clusters involved in the biosynthesis of gramillins and fusaoctaxin A, regulated by *TRI6*. Finally, ChIP-qPCR confirmed prior findings that TRI6 binds to its own promoter and revealed direct regulation of several other genes of the trichothecene gene cluster. We also demonstrate that TRI6 does not regulate the fusaoctaxin SMC through promoter binding or through interaction with its pathway-specific TF FGM4. However, TRI6 demonstrated a weak interaction with the gramillin TF GRA2, suggesting it is indirectly involved in the regulation of gramillin biosynthesis pathway.

2.3 Results

2.3.1 *TRI6* regulates both primary and secondary metabolism in *F. graminearum*

To identify SM genes regulated by *TRI6*, we performed a global expression profile of the wild-type *F. graminearum* and the two mutant strains - a strain deleted for *TRI6* (Δ*tri6*) and the Δ*tri6* strain complemented with constitutive expression of *TRI6* (Δ*tri6*/*TRI6*) grown in both PN and NPN media conditions. The PN condition is nutrient-rich, while the non-preferred conditions are conducive for the production of an array of secondary metabolites [141]. Since previous studies were successful in inducing trichothecene production at 24 hr timepoint in the NPN growth medium, we used this condition to measure gene expression [139]. We identified 743 DEGs in the F. graminearum wild-type relative to the Δtri6 strain in the PN medium, representing ~5% of the genome (Fig. 2.1A). To verify the number of genes regulated by *TRI6*, we

compared 750 genes differentially expressed between Δ*tri6* and Δ*tri6*/*TRI6* strains to the 743 DEGs. A comparison between the two datasets revealed 372 genes that are specifically regulated by *TRI6* in the PN condition (Fig. 2.1A). Among the 372 genes, 275 were positively influenced by *TRI6*, while 97 genes were negatively regulated (Table S2.1). Functional analysis of these 372 genes revealed an enrichment of genes associated with primary and secondary metabolism, as well as energy, transport, and detoxification (Table S2.2). We also identified enrichment of genes involved in leucine catabolism consistent with a prior work that suggested a complex regulatory feedback mechanism between *TRI6* and the branched-chain amino acid (BCAA) pathway (Table S2.2) [140,142]. These results were also consistent with our prior study that identified TRI6 targets with associated functions in primary metabolism, cell rescue, defense and virulence [139].

In the NPN condition, 1,199 genes representing ~8% of the genome were significantly differentially expressed in the Δ*tri6* strain relative the wild-type (Fig. 2.1A). Similar to analysis with PN expression data, we also compared the 1,199 DEGs to the 1,220 genes differentially expressed between Δ*tri6* and Δ*tri6*/*TRI6* strains (Fig. 2.1A). We observed 687 genes that were complemented by *TRI6* suggesting specific regulation of these genes in NPN conditions by *TRI6* (Fig. 2.1A). Of the 687 genes, 318 genes were positively regulated by *TRI6* and 369 were negatively regulated (Table S2.3). Functional analysis of the 687 DEGs revealed an increase in proportion of genes related to primary

and secondary metabolism, transport and virulence categories as compared to the PN conditions (Table S2.2) [142].

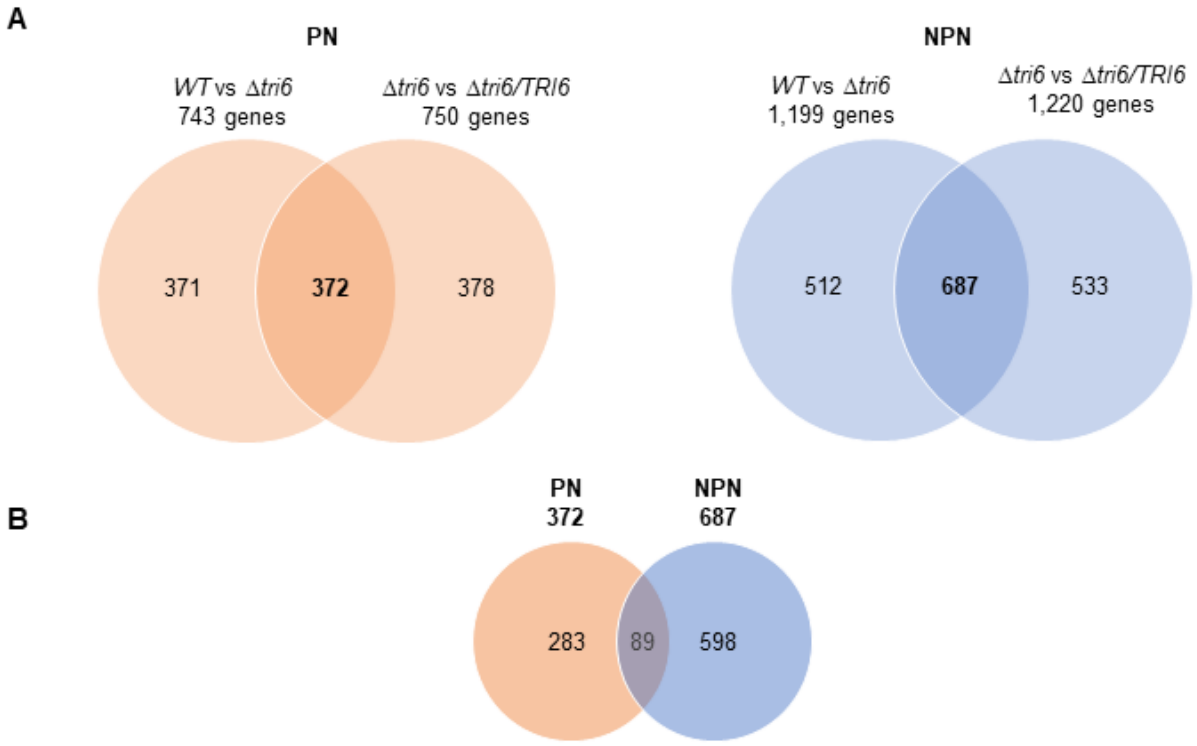

Fig. 2.1. *TRI6* regulates genes of primary and secondary metabolism in preferred nutrient (PN) and non-preferred nutrient conditions (NPN). (**A**) The Venn diagrams represent 743 genes differentially expressed in Δ*tri6* strain relative to the wild-type and 750 DEGs in the Δ*tri6/TRI6* strain relative to the Δ*tri6* wen grown in PN conditions for 24 hours. In the NPN condition, 1,199 DEGs in the Δ*tri6* strain relative to the wild-type and 1,220 DEGs in the Δ*tri6/TRI6* strain relative to the Δ*tri6* strain. (**B**) The Venn diagram represents the 970 genes that are regulated by *TRI6* in both culture conditions.

In addition to the genes expressed exclusively in either PN (372) or NPN (687) conditions, our analysis also uncovered 89 genes that are differentially regulated by *TRI6* in both environmental conditions, constituting 24% and 13% of PN and NPN

specific genes, respectively (Fig. 2.1B, Table S2.4). Among the 89 genes, twenty-eight genes are linked to SM production (Table S2.4). These included nine genes that belong to the gramillin SMC, as well as 19 genes distributed among the aurofusarin, orcinol, trichothecenes, fusarins, fusaristatin, fusaoctaxin, and other SM biosynthetic gene clusters (Table S2.4). The remaining 61 genes that are regulated by *TRI6* in both PN and NPN conditions are not linked to SM production but encode proteins with diverse functions (Table S2.4). These include transporters, oxidases, and other modifying enzymes. Functional analysis of the 89 genes revealed an enrichment of genes involved in secondary metabolism, defense related proteins, and metabolism of peptide antibiotics (Table S2.2) [142]. The clear association of the genes regulated by *TRI6* with several aspects of secondary metabolism in both nutrient environments underscore the complex mechanisms by which *TRI6* regulates SM gene clusters and reinforces the view of TRI6 as a global TF.

To validate the gene expression trends, we selected six genes for RT-qPCR analysis and relative expression of all these genes was consistent with the RNA-seq data (Fig. S2.1). Under NPN conditions, *NPS8* and FGSG_00046 from the gramillin SMC showed a significant increase in expression in the Δ*tri6* strain relative to both the wild-type and Δ*tri6/TRI6* strains (Fig. S2.1 A, B). In contrast, decreased expression of fusaoctaxin A SMC genes *NPS5* and *NPS9* were observed in Δ*tri6* in NPN conditions (Fig. S2.1 C, D). Similarly, expression of *PKS29* and FGSG_04592 encoding a short-chain dehydrogenase from the SMC designated C16 [20] were downregulated in the Δ*tri6* strain

(Fig. S2.1 E, F). As expected, *TRI6* itself showed complete absence of expression in the Δ*tri6* strain (Fig. S2.1 G). Overall, the global gene expression indicated that *TRI6* is involved in both positive and a negative regulation of SMCs.

2.3.2 *TRI6* regulates both global and pathway-specific transcription factors

As a global regulator, we expect *TRI6* to exert its influence on the expression of pathway-specific transcription factors. A study by Son *et al*. reported 709 genes encoding transcription factors in the *F. graminearum* genome [129]. Analysis of our data showed that *TRI6* regulated 34 transcription factors in both nutrient conditions, with seven and twenty-six exclusively in PN and NPN, respectively, and one in both conditions (Table 2.1). A majority of the TFs regulated by *TRI6* contain Zn_2Cys_6, ankyrin, bZIP, homeodomain-like, and bHLH domains characteristic of pathway-specific regulators in fungi (Table 2.1) [46]. Among the Zn_2Cys_6 TFs, five of them are regulated in PN and 18 are regulated in NPN conditions.

Of the seven TFs regulated in PN condition, four have function ascribed, including *SUC1* involved in sucrose utilization, *TRI10* and *GRA2*, regulators of trichothecene and gramillin biosynthesis, respectively, and FGSG_02825, an activator of an uncharacterized secondary metabolic cluster C30 (Table 2.1) [37]. The TF FGSG_04209 has no known function but contains a FMN-binding domain with homology to a transcriptional repressor of glucose assimilation in *Bacillus subtilis* (Table 2.1) [37,143]. These results indicate that under nutrient-rich conditions, at least two TFs regulated by *TRI6* may be involved in nutrient assimilation.

Table 2.1. *TRI6* regulates expression of transcription factors.

Conditions	Gene	Known function	Domain structure†	SMCs regulated (product)
NPN	FGSG_01795	SMC regulator	Zn_2Cys_6	C08 (PKS - unknown)
	FGSG_02288	SMC regulator	C_3H_1 zinc finger	C12 (PKS - unknown)
	FGSG_02320	SMC regulator	Zn_2Cys_6	C13 (pigment - aurofusarin)
	FGSG_02323	SMC regulator	Zn_2Cys_6	C13 (pigment - aurofusarin)
	FGSG_03881 (*TRI15*)	SMC regulator	C_2H_2 zinc finger	C23 (terpene - trichothecene)
	FGSG_12597 (*UGA3*)	SMC regulator	Zn_2Cys_6	C32 (unknown)
	FGSG_08080	SMC regulator	Zn_2Cys_6	C49 (butenolide)
	FGSG_10994 (*FGM4*)	SMC regulator	Ankyrin repeat	C64 (NPS - fusaoctaxin A)
	FGSG_00342		C_2H_2 zinc finger	
	FGSG_05682	arginine metabolism	Zn_2Cys_6	
	FGSG_04932		C_2H_2 zinc finger	
	FGSG_02718		Homeodomain-like	
	FGSG_07076		NF-X1 type zinc finger	
	FGSG_02368		Zn_2Cys_6	
	FGSG_08831		Zn_2Cys_6	
	FGSG_11186		Zn_2Cys_6	
	FGSG_12134		Zn_2Cys_6	
	FGSG_12094 (*LYS14*)	lysine biosynthesis	Zn_2Cys_6	
	FGSG_13613	lysine-specific demethylase	Jumonji	
	FGSG_04803 (*MAL33*)	maltose fermentation	Zn_2Cys_6	
	FGSG_04901		Zn_2Cys_6	
	FGSG_01760		Zn_2Cys_6	
	FGSG_03292		Zn_2Cys_6	
	FGSG_04581		Zn_2Cys_6	
	FGSG_13098		Zn_2Cys_6	
	FGSG_09111		Zn_2Cys_6	
PN & NPN	FGSG_11658 (*GRA2*)	SMC regulator	bHLH	C02 (NPS - gramillin)
PN	FGSG_04209		FMN-binding domain	
	FGSG_03538 (*TRI10*)	SMC regulator	Fungal specific TF domain	C23 (terpene - trichothecene)
	FGSG_02825	SMC regulator	Zn_2Cys_6	C30 (unknown)
	FGSG_03246		Zn_2Cys_6	
	FGSG_03683		Zn_2Cys_6	
	FGSG_10891		Zn_2Cys_6	
	FGSG_13386 (*SUC1*)	sucrose utilization	Zn_2Cys_6	

† Pfam annotation

Under the NPN condition, *TRI6* regulated 27 TFs (Table 2.1). Of these, three contained a C_2H_2 zinc finger domain, reminiscent of global regulators, though only TRI15 (FGSG_03881) has been characterized as a putative regulator of the trichothecene SMC [17,144]. TFs with other domains were also identified including FGSG_13613 that possess a jumonji (jmjC)-type DNA-binding domain, present in proteins that regulate production of secondary metabolic compounds sterigmatocystin and orcellinic acid [145].

The TF FGSG_07076 contained an NF-X1 type zinc finger domain predicted to occur in fungi but is poorly characterized [146].

Nine of the 27 TFs regulated by *TRI6* in NPN conditions are assigned to eight SMCs (Table 2.1). These included the aurofusarin SMC (FGSG_02320 and FGSG_02323), the butenolide SMC (FGSG_08080), the gramillin cluster (*GRA2,* FGSG_11658), and the recently characterized SMC C64 responsible for fusaoctaxin A production (*FGM4,* FGSG_10994) [15 14]. Other SMCs designated C08, C12, and C32 have not been characterized [20]. However, SMCs C08 and C12 are responsible for the production of unknown polyketides and are regulated by FGSG_01795 and FGSG_02288, respectively. The putative TF FGSG_02288 contains C_3H_1 zinc finger domain, found mainly in mRNA-binding proteins across the eukaryotic kingdom, but not associated with a specific regulatory function in fungi [130].

The remaining 18 transcriptional factors regulated by *TRI6* in NPN have no assigned role in secondary metabolite production; only three have been linked to specific functions. The regulators FGSG_05682 and FGSG_12094 are involved in arginine and lysine metabolism, respectively, while FGSG_04803 is involved in maltose assimilation (Table 2.1) [37].

Thus, *TRI6* affects putative global regulators containing C_2H_2 zinc finger domains. Moreover, it also regulates pathway-specific TFs involved in nutrient assimilation, as well as regulation of specific SMCs in both PN and NPN environments.

These results reaffirm our notion that TRI6 is a global, rather than pathway-specific transcriptional regulator.

2.3.3 *TRI6* influences a broad spectrum of secondary metabolite clusters

Bioinformatics analysis predicted 67 SMCs comprised of 689 genes in *F. graminearum*, including genes encoding biosynthetic, transporter, modifying enzymes, and transcriptional factors [20]. Analysis of global expression profiling in this study revealed 52 of the 689 secondary metabolic genes, representing 26 of 67 SMCs to be differentially regulated by *TRI6* in PN conditions (Table S2.5). Of these, 47 genes were significantly upregulated in the Δ*tri6* strain relative to the wild-type strain, and five were downregulated (Table S2.5). Similarly, in the NPN conditions 108 genes, representing 39 SMCs were differentially expressed in the Δ*tri6* strain. Of the 108 genes, 54 were upregulated, and the remaining 54 were downregulated (Table S2.6).

It should be emphasized that expression of a subset of genes in a SMC does not necessarily imply the activation of the respective SMC responsible for metabolite synthesis. Thus, we established more stringent criteria to denote the activation of a SMC. Along with expression of the cluster-specific transcription factor and key biosynthetic genes, other criteria included co-expression of genes responsible for the transport of toxic intermediates and their conversion into non-toxic compounds by activity of putative detoxification enzymes. Based on these new criteria, our analysis revealed five SMCs under the control of *TRI6*. This included the trichothecene, aurofusarin, gramillin, butenolide, and fusaoctaxin A gene clusters (Table 2.2).

Table 2.2. *TRI6* regulates five distinct SM gene clusters.

Growing Conditions	Cluster ID (known product)	MIPS ID	Product Description	Role keyword	Regulation by TRI6†
PN	C02 (gramillin)	FGSG_00046	hypothetical protein	transporter	+
		FGSG_11658	Myc-type basic helix-loop-helix bHLH domain (*GRA2*)	TF	
		FGSG_15673	nonribosomal peptide synthetase	NPS8	
		FGSG_15680	Cytochrome E- group I	potential detoxifying	
NPN	C02 (gramillin)	FGSG_00046	hypothetical protein	transporter	-
		FGSG_11658	Myc-type basic helix-loop-helix bHLH domain (*GRA2*)	TF	
		FGSG_15673	nonribosomal peptide synthetase (*NPS8*)	NPS	
		FGSG_15680	Cytochrome E- group I	potential detoxifying	
	C13 (aurofusarin)	FGSG_02320	transcription factor	TF	-
		FGSG_02322	major facilitator superfamily transporter	transporter	
		FGSG_02323	fungal specific transcription factor domain-containing	TF	
		FGSG_02324	polyketide synthase (*PKS26*)	PKS	
		FGSG_02325	conidial pigment polyketide synthase partial	PKS	
		FGSG_02327	dimethylaniline monooxygenase 3	potential detoxifying	
	C23 (trichothecene)	FGSG_03537	trichodiene synthase (*TRI5*)	TPS	+
		FGSG_03541	trichothecene efflux pump (*TRI12*)	transporter	
		FGSG_03535	trichodiene oxygenase (*TRI4*)	potential detoxifying	
		FGSG_16251	regulatory (*TRI6*)	TF	
	C49 (butenolide)	FGSG_08077	nadh-dependent flavin oxidoreductase	biosynthetic	+
		FGSG_08078	hypothetical protein	biosynthetic	
		FGSG_08079	benzoate 4-monooxygenase	biosynthetic	
		FGSG_08080	transcription factor	TF	
		FGSG_08081	2og-fe oxygenase family	biosynthetic	
		FGSG_08083	glutamate decarboxylase	biosynthetic	
		FGSG_08084	major facilitator superfamily transporter	transporter	
	C64 (fusaoctaxin A)	FGSG_10990	non-ribosomal peptide synthetase (*NPS9*)	NPS	+
		FGSG_10991	cytochrome p450 family	potential detoxifying	
		FGSG_10994	A Chain Structure Of Ankyrin Repeat (*FGM4*)	TF	
		FGSG_10995	hypothetical protein	transporter	
		FGSG_17487	nonribosomal peptide synthetase (*NPS5*)	NPS	

†refers to positive (+) or negative (-) regulation by *TRI6*

Consistent with previous findings, genes of the *TRI* gene cluster regulated by *TRI6* included a trichodiene synthase (*TRI5*), an efflux pump (*TRI12*), and a trichodiene oxygenase (*TRI4*) (Table 2.2, NPN). The aurofusarin SMC is a large gene cluster, encoding two transcription factors (FGSG_02320, FGSG_02323) and two polyketide synthases (*PKS26* and FGSG_02325); all of which were negatively regulated by *TRI6* along with the transporter (FGSG_02322) and a potential detoxifying enzyme dimethylaniline monooxygenase (FGSG_02327) (Table 2.2, NPN). The gramillin SMC contains all four gene classes defined by the new criteria - a nonribosomal peptide synthase (*NPS8*), a cluster-specific transcription factor (*GRA2*), a transporter

(FGSG_00046) and a potential detoxifying enzyme (FGSG_15680). All four of these were positively regulated by *TRI6* in PN and negatively regulated in NPN conditions (Table 2.2). The butenolide producing SMC contains several biosynthetic genes (FGSG_08077, FGSG_08078, FGSG_08079, FGSG_08081, FGSG_08083), an endogenous transcription factor (FGSG_08080), and a transporter (FGSG_08084). All of these were positively regulated by *TRI6* in the NPN culture condition (Table 2.2, NPN). Similar to the gramillin SMC, the fusaoctaxin SMC also contains all four of the evaluated gene classes – nonribosomal peptide synthases (*NPS5, NPS9*), a potential detoxifying gene (cytochrome P450, FGSG_10991), an endogenous transcription factor (*FGM4*), and a transporter (FGSG_10995), all of which were positively regulated by *TRI6* in NPN conditions (Table 2.2, NPN). Thus, by applying the new criteria to determine the activation of SMCs, we predicted that all five SMCs regulated by *TRI6* will produce the respective metabolites.

2.3.4 *TRI6* regulates production of trichothecenes, fusaoctaxins, and gramillins

In order to link transcriptional activation of the SMCs with the biosynthesis of their respective compounds, we generated SM profiles from culture extracts of the *F. graminearum* wild-type, Δ*tri6,* and Δ*tri6/TRI6* strains by ultra performance liquid chromatography - high resolution mass spectrometry (UPLC-HRMS). To obtain a quantity of mycelia sufficient for metabolite extraction, we grew *F. graminearum* in PN cultures over the course of 9 days. The time course experiment was undertaken to identify the day when the nutrient became limited leading to the production of

secondary metabolites (Fig. S2.2). As shown, 15-ADON, gramillin, fusaoctaxin, and some analogues begin to accumulate at day 4 and peak between day 7 and 8 (Fig. S2.2). For all subsequent analysis, each UPLC-HRMS profile from day 8 was deconvoluted (broken down into individual parts) into a series of "mass features" (denoted by retention time and pseudomolecular ion - where multiple "mass features" represent individual SMs detected, as well as SM fragments and adducts), and compiled into a data matrix of mass feature intensity values for univariate and multivariate statistical analyses. Principal component analysis (PCA) performed on the mass feature data matrix revealed variations in metabolite production over the time course. As observed in the score plot (Fig. 2.2), the Δ*tri6* strain separates from the wild-type and the Δ*tri6/TRI6* strains along the principal component 1, explaining the majority of variation in the model (71%). It is apparent that trends in SM production of the wild-type strain were more similar to the Δ*tri6/TRI6* than to the Δ*tri6* strains (Fig. 2.2). Biologically, this may imply that constitutive expression of *TRI6* compensated for the production of SMs influenced by the Δ*tri6* deletion. There is also a slight separation of the samples along PC2 (explaining 11.4% of variation in the model), reflecting minor variance in SM production between biological and technical replicates of each strain (Fig. 2.2). Differential production of 103 mass features between the wild-type and Δ*tri6* strains, as well as between Δ*tri6* and Δ*tri6/TRI6* strains, were found to be significant in pairwise comparisons (p-value < 0.05), underscoring the diversity of SMs that are regulated by *TRI6* (Table S2.7). The majority of the mass features detected (91 features) were

positively regulated by *TRI6*, while only 12 mass features were negatively regulated (Table S2.7).

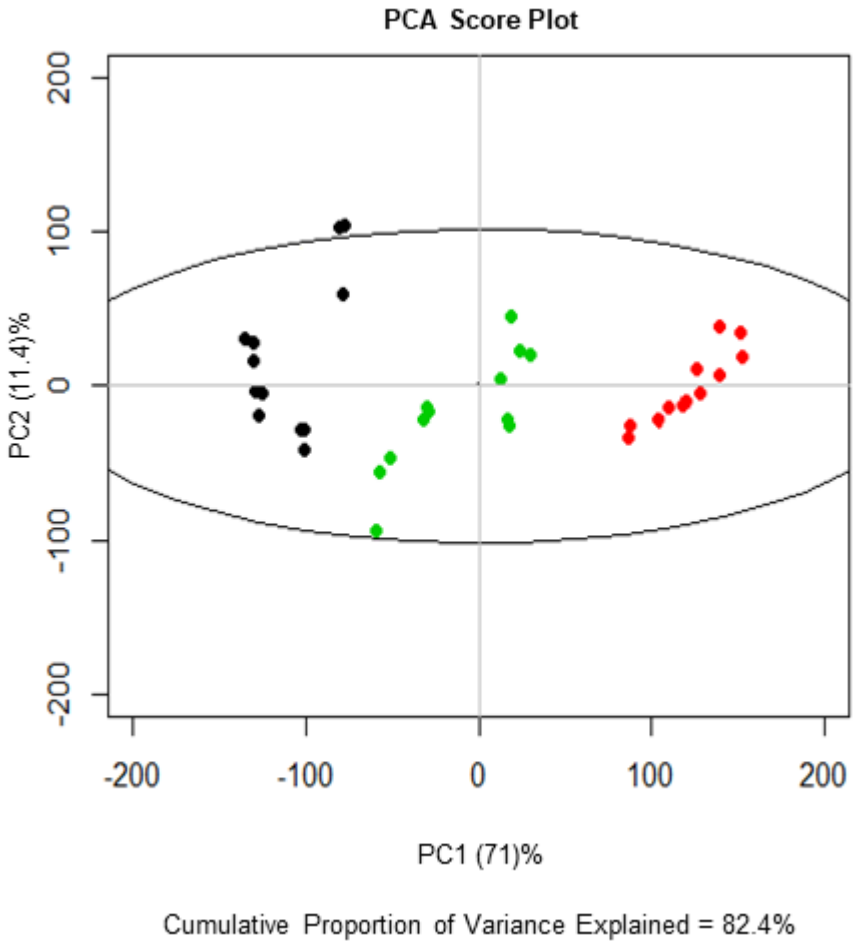

Fig. 2.2. Principal component analysis of metabolites regulated by *TRI6*. *TRI6* is responsible for majority of the variations in metabolomics profiles of *F. graminearum* wild-type, Δ*tri6*, and Δ*tri6/TRI6* strains grown in PN medium for 9 days. PC1 vs. PC2 shown. Black dots = wild-type sample replicates; red = Δ*tri6*; green = Δ*tri6/TRI6*.

Biosynthesis of 15-ADON, gramillins A & B, fusaoctaxin A, and other SMs exhibited similar kinetic profiles (Fig. S2.2). The metabolites began to accumulate at day 4 and continued to accumulate until day 8 in both the wild-type and the Δ*tri6* strains,

except for 15-ADON, which was entirely absent in the Δ*tri6* strain (Fig. S2.2A). Metabolic profiling also showed that multiple mass features exhibited similar kinetic profiles to 15-ADON, that corresponded to three separate metabolites (Fig. S2.2B-D; Table 2.3). MS/MS experiments of the $[M+H]^+$ ion for each metabolite yielded similar patterns in neutral losses confirming that all three metabolites were trichothecene analogs. The first metabolite, designated as isotrichodiol analog **1**, had a predicted molecular formula of $C_{20}H_{32}NO_5S$. Following scaled up fermentation and subsequent metabolite purification, MS/MS and NMR experiments (Figs. S2.3 – S2.10) demonstrated that the isolated metabolite was a unique derivative of isotrichodiol, a precursor in the trichothecene biosynthetic pathway, where the epoxide function at C-13 underwent nucleophilic attack by the thiol of N-acetylcysteine and cyclized through the acidic function of N-acetylcysteine to release a molecule of water and form a 7-membered ring at C-12 – identified here as 12,13- N-acetylcystidyl- isotrichodiol (Fig. S2.10). Molecular formulae were also predicted for the two remaining trichothecene analogs: $C_{20}H_{33}N_2O_5S$ (isotrichodiol analog **2**) and $C_{20}H_{32}NO_6S$ (isotrichotriol analog **3**). MS/MS experiments comparing isotrichodiol analogs confirmed that analog **2** differed from isotrichodiol analog **1** with the presence of an extra amino group in the N-acetylated cysteine moiety, while the isotrichotriol analog **3** contained an additional hydroxyl function on the isotrichodiol moiety and could be N-acetylcystidyl-isotrichotriol. Lack of sufficient quantity from scaled up isolation efforts prevented purification and further characterization of **2** and **3** by NMR. Similar to 15-ADON, biosynthesis of all three analogs (**1**-**3**) were positively regulated by *TRI6* (Figs. 2.3,

S2.11). Unlike 15-ADON, these three compounds were present in trace amounts in Δ*tri6* strain grown in PN for 4-9 days (Fig. S2.2A-D).

Table 2.3. *TRI6* regulates production of distinct secondary metabolites.

Mass Feature (RT_*m/z*)	Pseudomolecular Ion Annotation	Protonated Molecular Forumula	Observed Monoisotopic Mass	Δppm	Spectral Accuracy	Regulation by *TRI6* †	SMC ID‡
RT3.62_339.1422	15-ADON $[M+H]^+$	$C_{17}H_{23}O_7$	339.1433	-1.56	98.23	+	C23
RT4.41_398.1983	Isotrichodiol analog (1) $[M+H]^+$	$C_{20}H_{32}NO_5S$	398.1988	-1.93	98.52	+	
RT3.86_413.2103	Isotrichodiol analog (2) $[M+H]^+$	$C_{20}H_{33}N_2O_5S$	413.2093	-2.83	97.90	+	
RT4.02_414.1926	Isotrichotriol analog (3) $[M+H]^+$	$C_{20}H_{32}NO_6S$	414.1939	-1.41	98.01	+	
RT3.9_773.511	Fusaoctaxin A $[M+H]^+$	$C_{36}H_{69}N_8O_{10}$	773.5127	-0.54	98.65	+	C64
RT3.91_787.5018	Fusaoctaxin analog (1) $[M+H]^+$	$C_{35}H_{67}N_{10}O_{10}$	787.5020	-2.05	99.26	+	
RT3.94_757.516	Fusaoctaxin analog (2) $[M+H]^+$	$C_{36}H_{69}N_8O_9$	757.5181	-0.14	98.83	+	
RT3.96_771.5062	Fusaoctaxin analog (3) $[M+H]^+$	$C_{35}H_{67}N_{10}O_9$	771.5080	0.13	97.73	+	
RT4_801.5155	Fusaoctaxin analog (4) $[M+H]^+$	$C_{36}H_{69}N_{10}O_{10}$	801.5193	-1.83	94.69	+	
RT4.19_847.3668	Gramillin A $[M+H]^+$	$C_{35}H_{59}N_8O_{12}S_2$	847.3688	-0.63	97.53	-	C02
RT4.2_861.3817	Gramillin B $[M+H]^+$	$C_{36}H_{61}N_8O_{12}S_2$	861.3823	-2.54	94.21	-	

†refers to positive (+) or negative (-) regulation by *TRI6*

‡according to Sieber *et al.* 2014

In a similar manner, the octapeptide fusaoctaxin A ($[M+H]^+$ 773.511±0.02) and four other related analogs originating from the same *NPS5-NPS9* gene clusters exhibited kinetic profiles similar to that of 15-ADON (Fig. S2.2G-K, Table 2.3) [15]. Fusaoctaxin A was upregulated five-fold in the wild-type and four-fold in the Δ*tri6/TRI6* strains (*p*-value≤0.05) compared to the Δ*tri6* strain on day 8, when nutrients were limited (Fig. 2.3). The MS/MS experiments were performed using the $[M+H]^+$ ion of each of the four fusaoctaxin analogs, which yielded fragmentation patterns containing similar mass fragments and neutral losses confirming a level of structural similarity between the analogs and fusaoctaxin A. The HRMS spectral accuracy algorithms (MassWorks™, Cerno Bioscience, USA) were used to predict protonated molecular formula for each analog (Table 2.3). We confirmed the origin of the

fusaoctaxin analogs from the *NPS5-NPS9* gene cluster by deletion of the biosynthetic gene *NPS9* (FGSG_10990) (Fig. S2.12). The UPLC-HRMS metabolite profiling of culture extracts of the Δ*nps9* strain unequivocally indicated that fusaoctaxin A and the additional four analogs originate from the SMC *NPS5-NPS9* (Table S2.8). Due to the formation of an insoluble precipitate upon purification, insufficient quantities of the fusaoctaxin analogs were obtained during scaled up isolation efforts for full structural elucidation

Transcription profiling indicated that *TRI6* negatively regulated the expression of the gramillin SMC in NPN conditions (Table 2.2). UPLC-HRMS metabolite profiling validated the expression data findings, with significant upregulation (p-value≤0.05) of metabolite features representing both gramillins A and B in pairwise comparisons of WT and Δ*tri6/TRI6* with the Δ*tri6* strain (Table 2.3, Fig. 2.3). The NPN culture conditions also showed differential expression of genes associated with butenolide and the aurofusarin SMCs (Table 2.2). However, mass features associated with both butenolide and aurofusarin were absent from the metabolomics dataset.

Fig. 2.3. (pg. 66) *TRI6* differentially regulates the production of secondary metabolites. *F. graminearum* strains Δ*tri6,* Δ*tri6/TRI6*, and the wild-type were grown in the PN condition for 8 days. (**A**) *TRI6* positively regulates the expression of 15-ADON and an uncharacterized analog of isotrichodiol (**1**) as their production was abolished in the Δ*tri6* strain (p≤0.05). (**B**) *TRI6* also positively regulates the production of fusaoctaxin A and two additional compounds originating from the same gene cluster (Fusaoctaxin analogs **1,2**) (**C**). *TRI6* negatively regulates the biosynthesis of both gramillins A and B as the production increased in the Δ*tri6* when compared to the wild-type strains and the constitutive expressor. Box plots are representative of three biological each with four technical replicates. Signal intensity was measured in counts per second (cps) and normalized to total ion current.

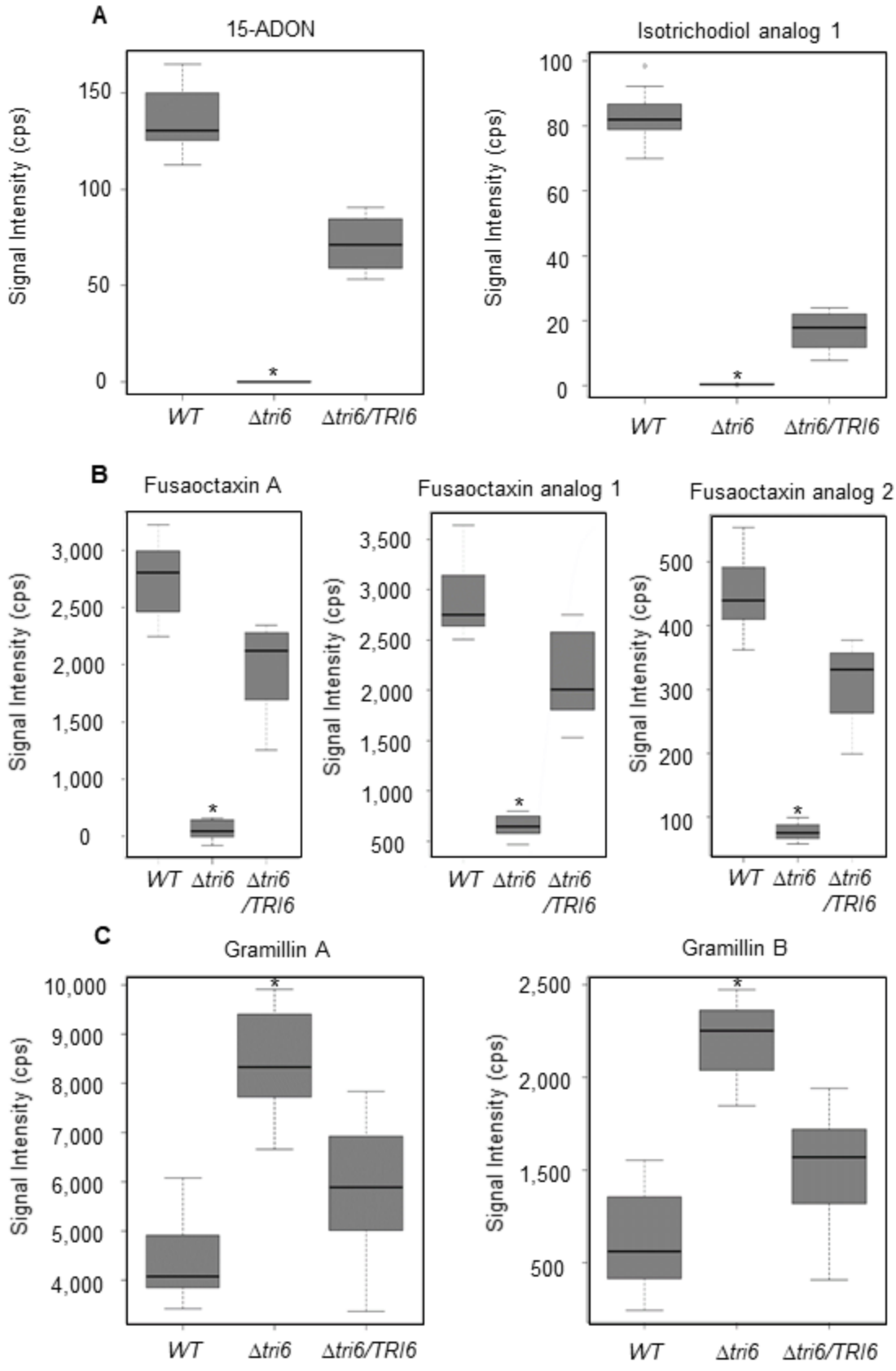
A
15-ADON
Signal Intensity (cps)
150
100
50
0
*
WT
Δtri6
Δtri6/TRI6
Isotrichodiol analog 1
Signal Intensity (cps)
100
80
60
40
20
0
*
WT
Δtri6
Δtri6/TRI6
B
Fusaoctaxin A
Signal Intensity (cps)
3,000
2,500
2,000
1,500
1,000
0
*
WT
Δtri6
Δtri6 /TRI6
Fusaoctaxin analog 1
Signal Intensity (cps)
3,500
3,000
2,500
2,000
1,500
1,000
500
*
WT
Δtri6
Δtri6 /TRI6
Fusaoctaxin analog 2
Signal Intensity (cps)
500
400
300
200
100
*
WT
Δtri6
Δtri6 /TRI6
C
Gramillin A
Signal Intensity (cps)
10,000
9,000
8,000
7,000
6,000
5,000
4,000
*
WT
Δtri6
Δtri6/TRI6
Gramillin B
Signal Intensity (cps)
2,500
2,000
1,500
500
*
WT
Δtri6
Δtri6/TRI6

2.3.5 TRI6 binds to promoters of trichothecene genes

Having shown that *TRI6* regulates production of SMs when grown in both PN and NPN conditions, we next set out to establish the mechanism by which *TRI6* exerts its control. Our prior work showed that the TRI6 protein binds to a palindromic GTGA/TCAC sequence in the promoter of *TRI6* and likely represses its expression in PN conditions [139]. We were interested to know if TRI6 similarly binds to the promoters of other genes in the trichothecene, gramillin, and fusaoctaxin SMCs and regulates expression in PN and NPN nutrient conditions. The binding to the promoters of the SMC genes was evaluated by chromatin immunoprecipitation and quantitative PCR analysis.

As mentioned, we previously identified a palindromic GTGA/TCAC sequence separated by a variable number of nucleotides as a TRI6 binding motif [139]. In this study, we limited the search to GTGA/TCAC repeats separated by 12 nucleotides or less in the promoters, 1000 base pairs upstream of the open reading frame of every gene in the trichothecene, gramillin, and fusaoctaxin A SMCs. We identified six genes (*TRI1, TRI3, TRI4, TRI6, TRI8, TRI101*) with these motifs in the promoters of the trichothecene SMC, six genes (*GRA2,* FGSG_00036, FGSG_00045, FGSG_00046, FGSG_00048, FGSG_11656) with motifs in the gramillin SMC, and two genes (*FGM4,* FGSG_10991) in the fusaoctaxin A SMC (Table 2.4).

Our results showed that in the PN culture conditions, except for *TRI6*, all of the promoters containing the GTGA/TCAC motif originating from the trichothecene,

gramillin and fusaoctaxin A SMCs failed to bind TRI6 (Table 2.4, Fig. S2.14 A). However, under the NPN culture condition, TRI6 bound to all of the trichothecene SMC promoters tested (Table 2.4, Fig. S2.14 B); but, did not bind to the promoters of any genes of either the gramillin or the fusaoctaxin clusters (Table 2.4). As a negative control, we used a sequence lacking the TRI6 binding motif, which showed no binding to TRI6 in either PN or NPN conditions (Table 2.4, Fig. S2.14 B). These results support our previous observations suggesting that *TRI6* is subject to autoregulation and that TRI6 acts as a positive regulator of *TRI* genes in NPN conditions. Since the promoters of gramillin and fusaoctaxin gene clusters did not bind TRI6, we hypothesized that the regulation of these clusters is indirect, likely through interaction with pathway-specific regulators present within each of the clusters.

Table 2.4. TRI6 binding motifs in the promoters of trichothecene, gramillin and fusaoctaxin gene clusters.

Secondary Metabolic	Gene	Binding Motif Pairs	Location in Promoter		TRI6 Binding	
			Start	End	PN	NPN
Trichothecene	TRI8	TCACTCAC	-13	-6	-	yes
	TRI3	GTGAgctttGTGA-37nt-TCACcagtgggGTGA	-899	-836	-	yes
	TRI4	GTGAgggcagagtccGTGA	-171	-153	-	yes
		TCACattttaTCAC	-395	-382	-	yes
	TRI6	GTGAtaaaatGTGA	-788	-775	yes	yes
	TRI1	GTGAggcaagccatgTCAC	-128	-110	-	yes
	TRI101	GTGAtgatttgtgGTGA	-506	-490	-	yes
Gramillin	FGSG_00048	GTGAagatcgcaTCAC	-157	-142	-	-
	FGSG_00045/FGSG_00046†	GTGActtaaaGTGA	-787	-773	-	-
		GTGAtGTGA	-80	-72	-	-
	GRA2	GTGAacaagcgaaagTCACgacagcagcaaaGTGA	-393	-359	-	-
	FGSG_00036/FGSG_11656†	TCACaaaacTCAC	-704	-692	-	-
Fusaoctaxin A	FGSG_10991	TCACagGTGA	-246	-237	-	-
	FGM4	GTGActttgactTCAC	-275	-260	-	-
n/a	intergenic space	no TRI6 binding motif (negative control)	ACCTCAATAGACGGTC		-	-

† Two genes sharing a promoter sequence

2.3.6 Interaction of TRI6 with pathway-specific transcription factors in the gramillin and fusaoctaxin SMC

To investigate the possibility of TRI6 interaction with pathway-specific regulators, we used a yeast two-hybrid assay (Y2H) to show interaction between TRI6 and the transcription factors GRA2 and FGM4 present in the gramillin and fusaoctaxin gene clusters, respectively. β-galactosidase activity of yeast strains co-transformed with the FGM4 fused to the DNA-binding domain (FGM4(BD)) and TRI6 fused to the activation domain (TRI6(AD)) demonstrated no interaction compared to the control co-transformants containing empty vectors (EV(AD) and EV(BD), respectively (data not shown). Since GRA2 exhibits high auto-activation activity when fused with the DNA-binding domain, we used TRI6 as a binding domain to measure TRI6-GRA2 interaction. β-galactosidase activity showed a modest (1.2- fold) increase with the GRA2(AD)-TRI6(BD) interaction compared to the EV(AD)-TRI6(BD) control (*p* value =0.07) (Fig. 2.4 A). It should be noted that this interaction was reproducibly detected with multiple clones in three independent experiments. Western blotting was used to confirm the expression of both TRI6(BD) and GRA2(AD) proteins (Fig. 2.4 C). We used previously confirmed positive interactors FGSG_05281(AD) and FGSG_09800(BD) as a positive control (Fig. 2.4 B) [147]. These results indicate that TRI6 interacts with the pathway specific transcription factor GRA2, but not with FGM4.

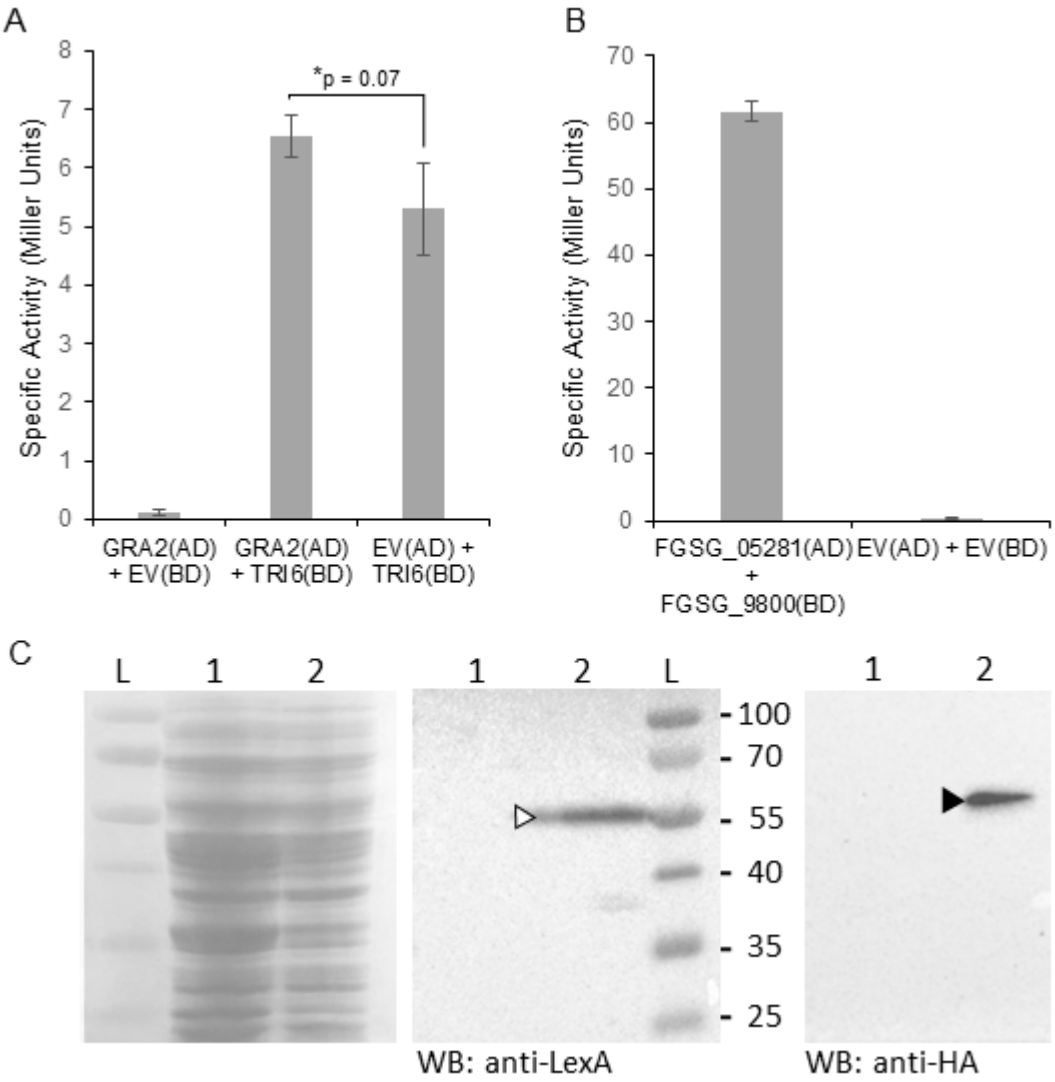

Fig. 2.4. TRI6 interacts with GRA2, but not with FGM4. (**A**) TRI6-GRA2 shown weak interaction quantified by β-galactosidase assay (*p* value = 0.07). (**B**) An interaction between FGSG_05281 and FGSG_9800 proteins were used as a positive control. β-galactosidase activity in Miller units was measured by ONPG assay using three technical replicates. Bars represent a mean of three biological replicates with error bars representing standard deviation. Significance was determined by Student's *t*-test at p≤ 0.05 unless otherwise stated. GRA2 = gramillin cluster TF (FGSG_11658), FGM= fusaoctaxin cluster TF (FGSG_10994), EV= empty vector; (AD)= activation domain, (BD) = DNA binding domain. (**C**) Expression of TRI6 (47kDa) and GRA2 (48kDa) partners was confirmed by Western blot analyses using anti-LexA antibodies for TRI6 and anti-HA antibodies for GRA2 (separate blots). A 50 µg aliquot of protein from uninduced (lanes #1) and induced (lanes #2) yeast cultures and was separated by SDS-PAGE and stained with Coomassie Blue stain and probed with antibodies.

2.4 Discussion

Regulation of secondary metabolism in fungi has been proposed to follow a multi-level organization with global regulators sensing environmental conditions to coordinate pathway specific regulators [50,148]. Previous studies alluded that TRI6 in *F. graminearum* belongs to the family of global regulators and with the evidence provided in this study, this notion is entrenched. We used a Δ*tri6* strain and its complement to identify 970 genes that are regulated by *TRI6* (Fig. 2.1). Our findings indicated that 8% and 16% of the genes in the 67 SMCs identified in *F. graminearum* [20] are regulated by *TRI6* in PN and NPN conditions, respectively (Tables S2.5, S2.6). A combination of expression profiling and metabolomic profiling revealed three SMCs that are regulated by *TRI6*. In addition to 15-ADON biosynthesis, we were able to establish a regulatory role for *TRI6* in the biosynthesis of two additional SMCs - fusaoctaxin A (& analogs) and gramillins A/B.

Several new analogs produced from trichothecene intermediates were identified as modified forms of isotrichodiol (**1**,**2**) and isotrichotriol (**3**) (Table 2.3). The production of the N-acetylcysteine conjugates of isotrichodiol and isotrichotriol were linked with TRI6 expression and its regulation of 15-ADON production. Both isotrichodiol and isotrichotriol are reactive intermediates involved in the early stages of trichothecene biosynthesis. During trichothecene biosynthesis, TRI5 converts farnesyl pyrophosphate precursor into trichodiene, and TRI4 (a cytochrome P450 monooxygenase) catalyzes oxygenation of trichodiene at three or four positions to yield the epoxides isotrichodiol

or isotrichotriol; these substrates in turn cyclize non-enzymatically to form EPT (12,13-epoxytrichothec-9-ene) or 3-hydroxy EPT (isotrichodermol) – precursors in the biosynthesis of non-*Fusarium* and *Fusarium* trichothecenes [149]. The observed N-acetylcysteine isotrichodiol and isotrichotriol conjugates in *F. graminearum* are likely by-products formed during the non-enzymatic cyclization of isotrichotriol to prevent excessive accumulation of highly reactive isotrichotriol and isotrichodiol intermediates. Presence of these molecules early in the biosynthesis pathway explains their appearance in trace amounts in the Δ*tri6* strain, in contrast to the complete absence of the 15-ADON final product, which requires additional biosynthetic steps (Fig. S2.2 A-D) [149].

It is not clear why the various isotrichodiol and isotrichotriol analogs were observed; however, conjugation of the cysteine thiol with the epoxide function at C-13 (observed from isotrichodiol analog **1**) is reminiscent of an endogenous mechanism for detoxification [150]. The epoxide moiety of trichothecenes (and their biosynthetic intermediates) is highly reactive and responsible for the biological activity of this class of molecules [150]. Glutathione-S-transferases are ubiquitous enzymes, present in all organisms; in *F. graminearum*, they play a role in the phase II detoxification mechanism to cope with endogenous toxins and xenobiotics [151]. For example, trichothecene (DON) detoxification in plants occurs through several mechanisms, one of which involves glutathione conjugation (at C-10 of the α,β-unsaturated ketone and at the C-13 of the epoxy group) via a glutathione-S-transferase [150]. Resulting DON-glutathione and associated breakdown products (DON-cysteinylglycine and DON-cysteine) have been

associated with DON detoxification in DON-treated wheat lines [152,153]; and an N-acetylcysteine derivative of DON at the C-13 position has also been observed in naturally contaminated grain [154].

The new products associated with the fusaoctaxin cluster included four analogs, but not the previously identified cleavage products fusapentaxin A and fusatrixin A (Table 2.3, Analogs **1-4**) [15,155]. Targeted deletion of the biosynthetic gene *NPS9* resulted in an absence of all five identified fusaoctaxins, substantiating their association with this cluster (Table S2.8). In the fusaoctaxin A biosynthesis pathway, NPS9 is responsible for recruiting the GABA starting unit, while the multi-modular NPS5 facilitates incorporation of the remaining 7 amino acids [15]. Therefore, it can be suggested that the novel compounds identified contain a GABA unit and rely on the presence of a functional NPS9. Overall, the changes in biosynthesis of gramillins and fusaoctaxin-related compounds posits TRI6 at the top of hierarchy in the signalling pathway regulating SMCs.

The position of TRI6 in the hierarchical regulation of SM is supported by the observations that 34 transcription factors, eleven of which are located within the secondary metabolic clusters are regulated by TRI6 (Table 2.1). Our results also confirmed a previous study that showed that *TRI10*, a transcriptional regulator in the trichothecene gene cluster was downregulated by *TRI6* [35]. TRI10 contains an uncharacterized fungal-specific transcription factor domain and likely functions as a transcriptional co-regulator [35]. In support, *TRI10* has been demonstrated to influence

genes involved in isoprenoid biosynthesis and several genes of unknown function, likely through interaction with another global regulator AreA [47,156]. Additionally, *TRI6* also affected the expression of five transcriptional regulators with the $Zn(II)_2Cys_6$ domain, a characteristic feature of many pathway-specific transcription factors in fungi [46].

Although a substantial number of genes associated with SMCs is differentially regulated by *TRI6*, a synergistic expression of pathway specific transcription factors, along with structural genes, modification/detoxification enzymes, and transporters is a more inclusive definition of SM activation. Of the SMCs affected by *TRI6*, the trichothecene, gramillin, fusaoctaxin, aurofusarin and butenolide gene clusters met all these criteria. We were able to substantiate metabolite production associated with three of these clusters by UPLC-HRMS metabolite profiling. In the case of aurofusarin, associated metabolite features were excluded from metabolomics analyses as signal intensities fell below minimal thresholds used in the data preprocessing of the metabolite profiles; however, production was confirmed from direct evaluation of UPLC-HRMS .RAW data files. Butenolide is an extremely polar metabolite and elutes early with the solvent front in the chromatographic conditions used and thus could not be resolved.

Since the biosynthesis of SMs is energy intensive, it is tightly regulated through a complex interaction of global regulators and, if necessary, engage pathway-specific transcription factors. In some cases global transcriptional regulators directly bind

promoters of structural genes as with the case of AreA that regulates the gibberellin cluster genes in *F. fujikuroi* under nitrogen limiting conditions [137]. In other instances, transcription regulation relies on interaction of multiple regulators. For example, in *Aspergillus* species AreA was shown to bind the promoters of pathway specific transcriptional co-activators AflR and AflJ for aflatoxin biosynthesis [106]. Similarly, studies in *A. parasiticus* showed evidence of an inhibitor that competes with AflJ to block AflR to the cognate promoters [157]. In our attempts to clarify the mechanism of fusaoctaxin and gramillin regulation, we evaluated TRI6 as a potential binding partner of pathway specific transcription factors. We found no interactions between TRI6 and FGM4, but detected a weak interaction with GRA2, responsible for gramillin cluster activation [14]. GRA2 belongs to the helix-loop-helix family of proteins with an ability to form homodimers [158]. Therefore, it is conceivable that homodimerization of GRA2 (data not shown) leaves a smaller pool to interact with TRI6. A similar idea has been proposed in the cAMP-PKA regulation of 15-ADON biosynthesis pathway, where the transcriptional regulator TRI10 interacts with the global regulator AreA to regulate *TRI* genes [47,78]. Future work will be aimed at isolating protein complexes associated with TRI6 in various environmental conditions.

2.5 Conclusion

In conclusion, we have collected evidence to show that *TRI6* plays a significant role in the regulation of multiple SMCs shown to contribute to *F. graminearum* pathogenesis including trichothecenes, fusaoctaxins, and gramillins. We combined gene

expression with metabolic profiles to link the expression of SMCs to associated products. In the process, we identified novel products whose structure and functions remain to be elucidated. We provide criteria such as co-activation of transcription factors, structural genes and transporters within a SMC that will enable us to determine the activation and ultimately the production of specific metabolites and their intermediates.

2.6 Experimental procedures

2.6.1 *F. graminearum* strains and culture conditions

F. graminearum NRRL29169 is the wild-type strain and was used as the parental strain for the construction of the transgenic strains in this study. The construction of Δ*tri6* and Δ*tri6/TRI6* strains have been previously described (schematic diagram in Figure S2.12) [139]. Macroconidia were produced in carboxymethylcellulose media and used as the inoculum for all cultures at concentration of $5x10^3$ spores mL^{-1} [159]. All strains in the study were cultured in the preferred nutrient (PN) conditions (56 mM NH_4Cl, 8.1 mM $MgSO_4$ $7H_2O$, 0.23 mM $FeSO_4 \cdot 7H_2O$, 14.7 mM KH_2PO_4, 2 g L^{-1} Peptone, 2 g L^{-1} Yeast extract, 2 g L^{-1} malt extract and 111 mM glucose) in the dark, at 28°C, with shaking at 160 rpm for 24 hours. For non-preferred nutrient (NPN) conditions (6.2 mM Putrescine di-hydrochloride, 22 mM KH_2PO_4, 0.8 mM $MgSO_4 \cdot 7H_2O$, 85.6 mM NaCl, 116.8 mM sucrose, 108.6 mM glycerol v/v, pH 4.0), the strains were first cultured in PN for 24 hours as described, followed by washing and growth in NPN.

Deletion of the *NPS9* (FGSG_10990) gene was accomplished by adaptation of the system developed by Frandsen *et al.* [160]. Briefly, 1kb 5′ flanking gene sequence was amplified by PCR using primer pair O1/2, while 1kb 3′ gene sequence was amplified using primer pair A3/4 (Table S2.9, Fig. S2.13). Amplified sequence fragments were cloned into vector pRF-HU2 on either side of the hygromycin resistance gene and the resultant vector was introduced into *F. graminearum* by *Agrobacterium*-mediated transformation [160]. The flanking regions facilitated homologous recombination of the hygromycin resistance gene in place of *NPS9.* The deletion was confirmed by the NovaSeq6000 genome sequencing at the Genome Quebec Innovation Centre for sequencing at McGill University (Montreal, Canada) (Fig. S2.13).

2.6.2 Gene expression analysis by RNAseq and RT-qPCR

F. graminearum wild-type, Δ*tri6* and Δ*tri6/TRI6* strains were grown in 4 mL of PN for 24 hours and 4 mL of NPN for 24 hours and total RNA was extracted from three biological replicates per strain using Trizol reagent as described previously [139]. Total RNA was sequenced using Illumina NextSeq 500 platform at the Center for the Analysis of Genome Evolution and Function at the University of Toronto. Raw sequencing reads were deposited to NCBI GEO (Accession #GSE141331). The raw reads were trimmed and aligned to the *F. graminearum* gene coding sequences predicted in NRRL29169 assembly (GWAS Accession# SPRZ00000000) using RNA-Seq Analysis feature in CLC Genomics Workbench version 12 with the following parameters: mismatch cost 2, indel cost 3, length fraction 0.9, similarity fraction 0.8, maximum number of hits for a read 10.

Read trimming and mapping statistics are presented in Table S2.10. Unique gene read counts were manually curated for genes with a minimum of 50 unique gene reads. Filtered counts were then imported into R environment and normalized using default parameters in DESeq2, which uses negative binomial models to represent the number of reads assigned to a gene in a sample [161]. Differential expression analysis was also carried out using DESeq2, with the threshold fold change ≥ 2 and the FDR-adjusted p-value ≤ 0.05.

Gene expression from RNA-Seq data was confirmed by reverse-transcriptase quantitative PCR (RT-qPCR). One µg of total RNA was reverse-transcribed using high-capacity cDNA reverse transcription kit with random hexamer primers (Applied Biosystems, USA). The qPCR was performed using the Applied Biosystems PowerUp SYBR Green reaction mix and QuantStudio 3 Real-Time PCR system (Thermo Fisher). Relative expression was calculated using Pfaffl method [162]. *EF1a* (FGSG_08811) and *β-tubulin* (FGSG_09530) were independently used as reference genes. Significance was determined by Student's *t*-test at p ≤ 0.05. Primers used for the amplification are listed in Table S2.9.

2.6.3 Metabolomic analysis

For each time point, spores from *F. graminearum* wild-type, Δ*tri6* and Δ*tri6/TRI6* were inoculated in 65 mL of PN culture and incubated in the dark at 28° C for 24 hours with constant shaking at 170 rpm. Following 24 hours growth, cultures were vortexed to obtain homogeneous suspension and aliquoted into four 15 mL cultures and were

incubated while stationary on a ~10° incline in the dark at 28° C. The cultures were grown in stationary phase for 3, 4, 5, 6, 7, 8, and 9 days to obtain adequate biomass for metabolite extraction. The metabolites were extracted by shaking the mycelial mats in 25 mL of acetonitrile at 150 rpm for 1 hour. A 15 mL aliquot of supernatant was evaporated using GeneVac (Thermo Fisher). Extracts were reconstituted in acetonitrile to 500 µg mL^{-1} and a 2 µl aliquot was analyzed by the Thermo Scientific Dionex Ultimate 3000 UHPLC system using a Kinetex 100 Å C18 column (Phenomenex, 2.1 x 50 mm, 1.7 µm) with a flow rate of 0.35 mL min^{-1}. Solvent A was water with 0.1% formic acid; solvent B was acetonitrile containing 0.1% formic acid. The gradient programme started with 5% solvent B for 0.5 min, increased to 95% over the following 4 min, then held at 95% solvent B for 3.5 min. Finally, gradient returned to 5% solvent B over the course of 1 minute and remained at this concentration for 3 min to equilibrate between samplings.

The HRMS was performed using Thermo LTQ Orbitrap XL high resolution mass spectrometer in ESI+ mode, monitoring *m/z* 100-2000 range with the following parameters: capillary temperature (320 ˚C), sheath gas flow (40), auxiliary gas flow (5), sweep gas flow (2), source voltage (4.2 kV), capillary voltage (35 V, tube lens 100 V, maximum injection time (500 ms), microscans (1). For MS/MS experiments, the HRMS was operated in ESI^+ mode monitoring *m/z* 100-2000 using the following parameters: sheath gas (40), auxiliary gas (5), sweep gas (2), spray voltage (4.2 kV), capillary temperature (320 ˚C), capillary voltage (35 V), tube lens (100 V), maximum injection

time (500 ms) and microscans (1). Selected ions were isolated using a 1 m/z window and fragmented using CID at 35 eV with activation Q at 0.25 and activation time 30 ms.

MassWorks™ software (v5.0.0, Cerno Bioscience) was used to improve spectral accuracy and confirm the molecular formulas of the daughter ions. The sCLIPS searches were performed in dynamic analysis mode with elements C, H, N and O allowances set at minimum 1 and maximum 100. Charge was specified as 1, mass tolerance was set to 5 ppm and the profile mass range was -1.00 to 3.50 Da.

Raw data processing was carried out using mzMine2 as previously described, with the exceptions of the noise level threshold of 2 $x10^5$ cps selected based on UHPLC-HRMS raw data files and RT tolerance of 0.1 min used throughout the analysis [163,164]. Data matrix was then manually curated in MS Excel- duplicated values, medium and acetonitrile "blank" controls were removed. Further processing was performed in the R environment [165]. Data was scaled using pareto scaling (where scaling factor is the square root of the standard deviation). Principal component analysis and univariate statistical analysis were done using the *muma* package as previously described to calculate fold change difference between variables at $p \leq 0.05$ [163,165].

2.6.4 NMR spectroscopy analysis

NMR 1D, 2D experiments: 1D (^1H), (^{13}C), 2D NMR (^1H – ^1H COSY, ^1H – ^1H TOCSY, ^1H – ^{13}C HSQC, ^1H – ^{13}C HMBC, ^1H – ^{13}C HSQC-TOCSY, ^1H – ^1H NOESY) spectra were recorded using standard Bruker pulse sequences on a Bruker Avance II 500 MHz NMR spectrometer equipped with 5 mm triple resonance inverse (TXI) probe

with Z-gradient coils . The NMR sample was prepared by dissolving 2 mg of the compound in 600 µL of $CDCl_3$. Data were recorded and processed using Bruker Topspin 1.3. COSY and TOCSY NMR spectra were used to identify neighboring protons and spin systems. HSQC and HSQC-TOCSY NMR spectra identified the corresponding ^{1}H-^{13}C resonances and HMBC NMR spectra were used to connect the spin systems (2/3 bond correlations) and identify quaternary carbons. Stereochemistry at C-2 and C-11 was confirmed with NOESY NMR spectra. All the NMR supplementary information is included in supplementary figures S2.3-S2.10.

2.6.5 Chromatin Immunoprecipitation and qPCR

F. graminearum wild-type, Δ*tri6* and Δ*tri6/TRI6* strains were grown in 50 mL of liquid media under PN and NPN conditions as described. Cross-linked DNA-protein complex was prepared as previously described in Nasmith *et al.* (2011). 750 µg of DNA cross-linked protein was incubated on ice with 50 µL HA-magnetic beads (Miltenyi Biotech) and 5 µg salmon sperm DNA (ssDNA) for one hour, then mixed with 1% blocking solution and loaded onto the magnetic column pre-washed with 400 µL Lysis buffer with 2 µg ssDNA. The column was then washed with 1 mL low salt wash buffer (0.1% SDS, 1% Triton X-100, 2 mM EDTA, 20 mM Tris-HCl (pH 8.1), 150 mM NaCl), followed by 1 mL high salt wash buffer (0.1% SDS, 1% Triton X-100, 2 mM EDTA, 20 mM Tris-HCl (pH 8.1), 500 mM NaCl), 1 mL lithium chloride wash buffer (0.25 M LiCl, 1% IGEPAL-CA630 or NP-40, 1% sodium deoxycholate, 1 mM EDTA, 10 mM Tris-HCl (pH 8.1)), and 1 mL TE buffer (pH8). Immunoprecipitates were eluted with 200 µL

freshly prepared hot (~95˚C) elution buffer (0.5% SDS and 0.1 M NaHCO3). To reverse cross-linking samples were treated as previously described in Nasmith *et al.* [139].

Quantitative PCR was performed as described using the total DNA precipitated from 750µg of protein. *EF1a* (FGSG_08811) and *TRI10* (FGSG_03538) were independently used as endogenous control sequences. Enrichment was calculated using Pfaffl method as a quantity of DNA precipitated from *HATRI6* strain relative the DNA from Δ*tri6* strain. Statistical significance was calculated by the Student's *t*-test at $p \leq 0.05$.

2.6.6 Yeast strain construction and yeast-two-hybrid screen

Coding sequences of *TRI6 (*FGSG_16251*), GRA2 (*FGSG_11658*)*, and *FGM4 (*FGSG_10994*)* were amplified from the total RNA extracts of *F. graminearum* prepared as previously described. Fragments were cloned into the Gateway pENTR vector using pENTR directional TOPO cloning kit (Thermo Fisher Scientific), followed by Gateway cloning into pEZY45 (activation domain B42) and pEZY202 (DNA binding domain LexA) by Gateway LR Clonase II reaction (Thermo Fisher Scientific). Yeast two-hybrid vectors were co-transformed into *S. cerevisiae* strain RFY206 using standard lithium acetate method as previously described [166]. The interaction was quantified by a β-galactosidase activity with ONPG substrate as previously described [167]. Empty vectors pJG4-5 (activation domain) and pEG202 (DNA-binding domain) were co-transformed as a negative control. *S. cerevisiae* strain with FGSG_05281(AD) and FGSG_9800(BD) was used as a positive control [147]. Significant difference in interaction was assesses by the Student's *t*-test. To ensure protein expression under tested conditions, proteins from

both non-induced and induced cultures were subjected to a Western blot analysis. Cultures were induced overnight and total protein was extracted as previously described [147]. Protein concentration was determined by Bradford assay and duplicate 50µg protein aliquots were separated on a 12% SDS-PAGE gel before transferring to two PVDF membranes (one for each antibody) using a semi-dry transfer method. Membranes was blocked using Membrane Blocking Agent (GE Healthcare, RPN2125V) and probed with HA antibodies to detect GRA2(AD) (Roche, Germany), and with LexA antibodies to detect TRI6(BD) (Millipore Sigma, USA). Antibody signal was detected using the chemiluminescence substrate (SuperSignal™ West Femto Maximum Sensitivity Substrate, Thermo Scientific, USA).

Chapter 3. Regulation of secondary metabolite production by MAP kinase *MGV1*.

3.1 Abstract

In *Fusarium graminearum,* MAP kinase MGV1 is well-characterized as a regulator of the cell wall integrity pathway. Prior studies have also implicated MGV1 in the regulation of production of several secondary metabolites. In this work, we combined transcriptomic and metabolomic approaches to identify secondary metabolic clusters (SMCs) and associated compounds regulated by MGV1. Our analysis indicated that *MGV1* controls transcription of the trichothecene, aurofusarin, fusaoctaxin, and butenolide SMCs. *MGV1* regulated *TRI6* expression, suggesting that transcriptional control of the SMCs by *MGV1* occurs through *TRI6*. Moreover, our analyses revealed that *MGV1* exerts its control of the fusarin, gramillin, and ferricrocin SMCs at the post-transcriptional level.

3.2 Introduction

In the previous chapter, we explored the role of a global regulator TRI6. We established its role in both the direct regulation of trichothecene genes that produce the mycotoxin 15-ADON, and the indirect regulation of SMCs involved in the biosynthesis of gramillin and fusaoctaxin A. In this chapter, we will explore the role of a signaling component MAPK that amplifies input signals to modulate the expression of SMCs. The MAPK signalling cascades are universal amplifiers of signals in all eukaryotes. They are

essential for transducing signals from the cell surface receptors to the regulators of primary and secondary metabolism, which induce many cellular responses [58,79].

A MAPK cascade consist of three kinase proteins phosphorylating each other in a sequential manner. Thus, upon perceiving a signal from the cell surface receptor, MAPKKK phosphorylates its downstream target MAPKK, which, in turn, phosphorylates the MAPK [58,79,83]. As discussed in Chapter 1, there are three distinct MAPK pathways present in *Fusarium graminearum*. The MAPK pathway HOG1 is responsible for sensing and responding to the osmotic stress [81]. The MAP kinase module MGV1 is linked to both monitoring and maintenance of the CWI pathway [80]. Finally, the GPMK1 is responsible for filamentous growth and sexual reproduction [67]. All three of these pathways are important for vegetative growth, reproduction, and pathogenicity in *F. graminearum* [87]. My thesis will only focus on the first two modules, HOG1 and MGV1, as they are major contributors to the regulation of SMCs in *F. graminearum*. The key components that are part of these two MAPK pathways are outlined in Figure 3.1A.

In *F. graminearum,* several proteins transduce the osmotic stress signal to the HOG1 cascade. First, histidine kinase OS1 activates the histidine phosphotransferase HPT1, which dephosphorylates the response regulator protein RRG1 [67,168]. The activated RRG1 transduces the signal downstream to the SSK2-PBS2-HOG1 MAPK cascade [67,169]. One of the well-characterized downstream targets of HOG1, ATF1 is a repressor of four catalase genes, which are activated during oxidative stress [88]. Targeted

deletion of *ATF1* and the members of the HOG1 cascade results in defects in perithecia formation, sensitivity to both osmotic shock and oxidative stress, and reduction of virulence in wheat heads [81,86–88,169]. The diminished pathogenicity has been attributed to the inability of HOG1 pathway-deficient stains to produce sufficient DON *in planta* [81,86–88,169]. In line with this, the pathogenicity assays have demonstrated that neither *hog1* nor *atf1* mutants were able to progress past the rachis node in the infected wheat heads [81,88]. However, both the *Δhog1* and *Δatf1* strains have been enhanced in their ability to produce DON *in vitro* [81,88]. Additionally, both *atf1* and *hog1* mutants showed an increase in aurofusarin production *in vitro* and a decrease in zearalenone production *in planta*, implicating HOG1 pathway in regulation of secondary metabolism [81,88].

In the MGV1-mediated CWI pathway, environmental perturbations are sensed by the wall integrity and stress response component (WSC) receptors, which are well-studied in yeast but remain unconfirmed in *F. graminearum* [67]. These receptors transduce the signal to the upstream member of the MAPK cascade BCK1. BCK1 phosphorylates the MAPKK MKK1, which in turn phosphorylates MGV1 [67,90]. Targeted deletion of *MKK1* results in decreased phosphorylation of both MGV1 and HOG1, revealing a cross-talk between the CWI and high osmolarity pathways [170].

The signal received by the CWI pathway in *F. graminearum* is modulated through both MKK1 and MGV1 activities. Activity of MGV1 is repressed through dephosphorylation by the phosphatase MSG5, while the activity of MKK1 can be downregulated by a protein phosphatase PTC3 [68,171,172]. Of interest, PTC3 was also

shown to negatively regulate the HOG1 pathway, demonstrating another point of crosstalk between the CWI and the osmolarity sensing MAPK circuitries [172].

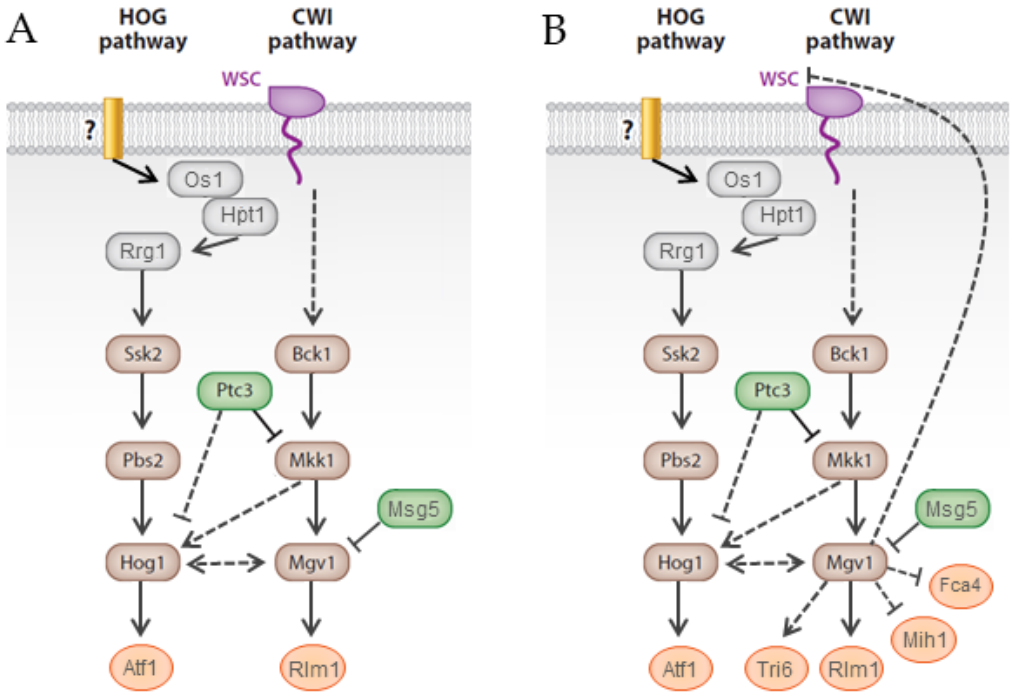

Fig. 3.1. HOG1 and CWI MAPK pathway modules in *F. graminearum*. (**A**) Transmembrane proteins CWI and uncharacterised receptor complexes recognize environmental stimuli and transduce the signals to the MAPK cascades. (**B**) *MGV1* regulation of components discovered in this study. Brown modules = kinases, green= phosphatases, orange = downstream effectors. Grey modules = regulatory components. Solid arrows indicate direct regulation, dashed – interactions that are indirect or poorly characterized in *F. graminearum*. Diagram is adapted from Chen, Kistler, & Ma, 2019.

Upon activation of the CWI pathway, *F. graminearum* MGV1 phosphorylates the transcription factor RLM1, which is essential for mitigating responses to cell wall damaging agents and osmotic stress [170]. RLM1 is a known mediator of the MGV1 regulation of virulence and 15-ADON production in *F. graminearum*. Research has shown that the *Δrlm1* strains are both non-pathogenic and produce less DON compared

to the wild-type [80,94,170]. Further, MGV1 has been implicated in regulation of aurofusarin and butenolide production [94,170].

MAP kinases amplify and transduce signals from the environment to downstream regulators, which include broad-range and pathway-specific TFs that control expression of secondary metabolic genes. Since *MGV1* influences 15-ADON biosynthesis, we hypothesized that the global regulator of secondary metabolism *TRI6,* encoded in the trichothecene SMC, is regulated by *MGV1*. We conducted both transcriptomic and metabolomic studies to establish secondary metabolic clusters regulated by *MGV1*. Our studies determined that *MGV1* regulates trichothecene, aurofusarin, and fusaoctaxin A production transcriptionally through *TRI6*, while also controlling biosynthesis of fusarins, gramillins, and ferricrocin post-transcriptionally. Our findings also increased our understanding of the roles of the *MGV1* and *TRI6* with respect to their position in the regulatory hierarchy. Genes regulated exclusively by *MGV1* were involved in both primary and secondary metabolism, while those regulated by *TRI6* (independently or together with *MGV1*) were involved in pathways affecting virulence or those producing secondary metabolites or their precursors.

3.3 Results

3.3.1 *MGV1* transcriptionally regulates primary and secondary metabolic pathways.

To identify the SMCs affected by MGV1, gene expression profiling was performed with *F. graminearum* wild-type, strains devoid of *MGV1* (*Δmgv1*), and two independent strains where *MGV1* was constitutively expressed (*Δmgv1/MGV1_1* and

Δmgv1/MGV1_6). To mimic conditions conductive to SM production, the strains were grown in non-preferred nutrient conditions (NPN) for 24 hours.

A comparison of gene expression between the wild-type and the *Δmgv1* revealed 1,495 DEGs (Table S3.1). This dataset was compared to the 1,824 DEGs between the *Δmgv1* and *Δmgv1/MGV1_1*, which identified 1,207 genes regulated by *MGV1* (Table S3.1, Fig. 3.2A). A similar comparison of 1,495 DEGs to the 2,101 DEGs between *Δmgv1* and *Δmgv1/MGV1_6* identified 1,185 genes under *MGV1* control (Table S3.1, Fig. 3.2A). Lastly, a comparison of the 1,207 and 1,185 DEG dataset associated with *Δmgv1/MGV1_1* and *Δmgv1/MGV1_6*, respectively, revealed an overlap of 1,120 genes regulated by *MGV1* (Table S3.1, Fig. 3.2B). Of these, 485 were negatively regulated by *MGV1,* and 635 were positively regulated (Table S3.1).

A functional analysis of the *MGV1*-regulated genes revealed an enrichment of categories associated with both primary and secondary metabolism representative of the many pathways affected by the MGV1. The enriched categories include metabolism of amino acids, iron acquisition, transport systems, toxin production and detoxification, and cell type differentiation (Table S3.2) [142,173].

To validate the RNA sequencing results, a RT-qPCR was performed on six highly expressed SMC genes regulated by *MGV1* (Fig. S3.1). RNA-seq analysis indicated that *TRI5* and *TRI6* genes in the trichothecene SMC, and the *NPS5* and *NPS9* genes in the fusaoctaxin SMC are positively regulated by *MGV1.* Consistent with these results, RT-qPCR showed a significant decrease in the expression levels of these genes in the *mgv1*

mutant compared to the wild-type and both constitutive expressor strains (Fig. S3.1 A-D). In contrast, expression of *PKS12* and *GIP1* genes in the aurofusarin SMCs was significantly upregulated in the strain lacking *MGV1,* in agreement with the transcriptomics data (Fig. S3.1 E, F).

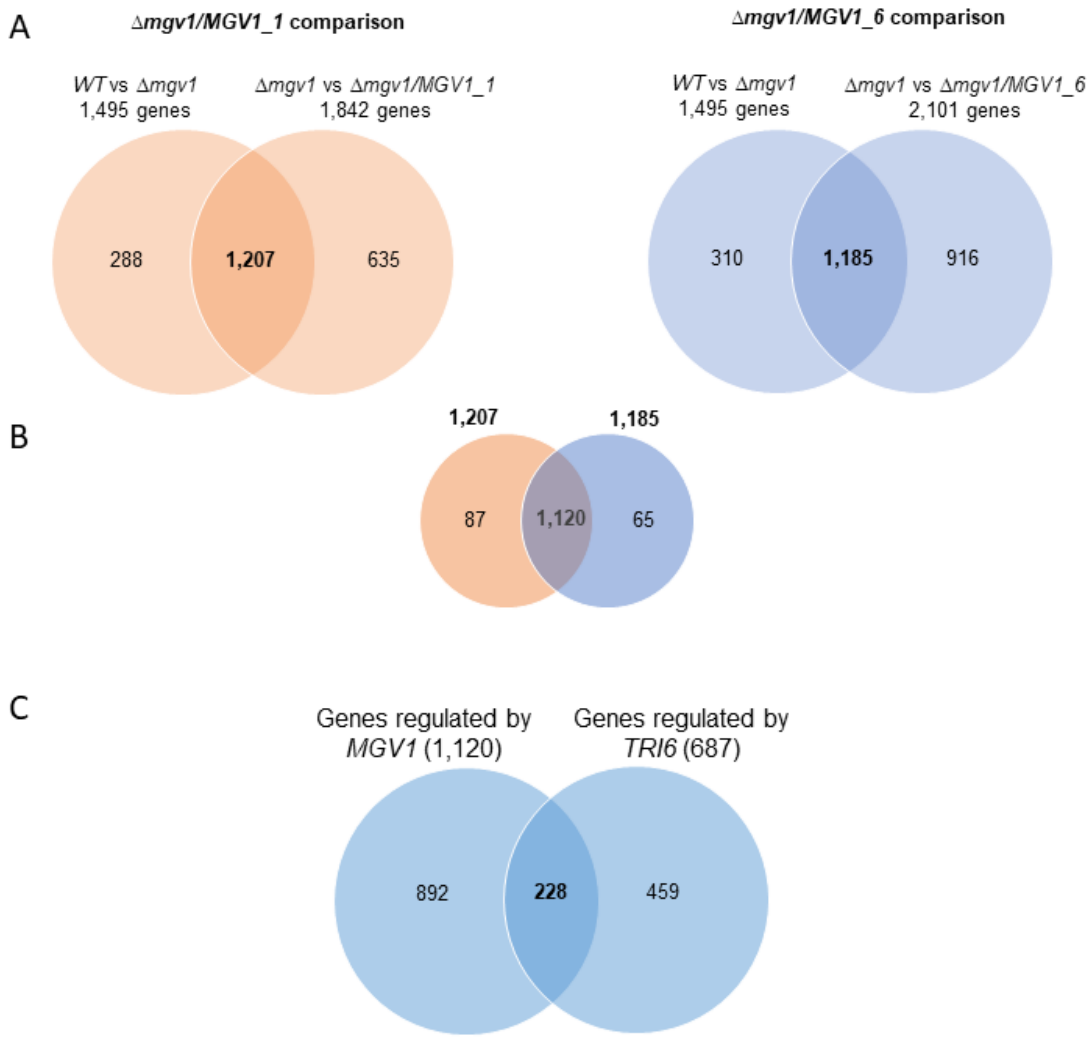

Fig 3.2. *MGV1* regulates genes in non-preferred nutrient conditions. (**A**) The Venn diagrams represent 1,495 genes differentially expressed in Δ*mgv1* strain relative to the wild-type and compares them to either 1,842 DEGs in the Δ*mgv1/MGV1_1* strain relative to the Δ*mgv1,* or 2,101 DEGs in in the Δ*mgv1/MGV1_6* strain relative to the Δ*mgv1.* (**B**) The Venn diagram represents the 1,120 genes that are specifically regulated by MGV1. (**C**) *MGV1* and *TRI6* regulate a subset of the same genes in NPN conditions.

3.3.2 *TRI6* and *MGV1* regulate different aspects of cellular metabolism

To explore the regulatory relationship between *MGV1* and *TRI6*, a comparison of the 687 genes regulated by *TRI6* in the NPN medium (chapter 2) and the 1,120 genes regulated by *MGV1* (present chapter) was performed, revealing an overlap of 228 genes under the control of both regulators (Fig. 3.2C). Of the 228 genes, 132 were positively regulated by *MGV1* and *TRI6*, and 96 were negatively regulated by both (Table S3.5). Of interest, *TRI6* was positively regulated by *MGV1* with a 5-fold decrease in expression in the *Δmgv1* strain (Tables 3.1, S3.5). On the other hand, we did not observe a significant change in the *MGV1* expression levels in the *Δtri6* strain (data not shown).

Functional analysis of genes co-regulated and exclusively regulated by *MGV1* and *TRI6* revealed clear differences between the two regulators. Genes exclusively regulated by *MGV1* are related to a wide variety of cellular metabolic pathways, such as cell cycle, endocytosis, transcription factor control, and oxidative phosphorylation (Tables S3.6, S3.7) [142,173]. In addition, *MGV1* regulated the expression of the four genes involved in the CWI and high osmolarity HOG1 MAPK pathway. These included the putative CWI cell surface receptor, the MGV1 inhibitor MSG5, MGV1 effector MIH1, and the HOG1 pathway effector CTT1 (Fig. 3.1, Table S3.1).

In yeast, the CWI pathway is activated through the cell membrane WSC1, WSC2, and WSC3 receptors, which mediate environmental changes in temperature, osmolarity, or presence of cell wall biosynthesis inhibitors [174,175]. Our data indicated that a gene (FGSG_03574) homologous to the yeast *WSC1/2/3*, was negatively regulated by *MGV1*

(Fig. 3.1, Table S3.1). Further, *F. graminearum* FGSG_06977, a homolog of yeast *MSG5*, was positively regulated by *MGV1* (Fig. 3.1, Table S3.1). In the yeast CWI pathway, the MGV1 homolog SLT2 reinforces its activation through deactivation of the MSG5 phosphatase. MSG5 phosphatase downregulates the activities of the MAPKs [68,171]. Our findings suggest that self-regulation of MGV1 is present in *F. graminearum* through transcriptional downregulation of the receptor and activation of the phosphatase that will dampen the signal leading to the CWI pathway activation.

Finally, *MGV1* regulated FGSG_00565, a homolog of the yeast MIH1 phosphatase (Fig. 3.1, Table S3.1). In yeast, MIH1 dephosphorylates cell cycle control proteins CLB1/2 and CDC28, leading to cell cycle arrest and is negatively regulated by the SLT2 kinase through phosphorylation [176,177]. In *F. graminearum*, FGSG_00565 was transcriptionally upregulated in the *mgv1* mutant, implicating MGV1 in cell cycle.

A potential crosstalk between the MGV1 and another MAPK module, HOG1, was identified, as *MGV1* positively regulated *FCA4* (FGSG_02881), a homolog of a yeast CTT1 catalase (Fig. 3.1, Table S3.1). Catalases decompose H_2O_2 into hydrogen and water, and are essential components in the osmotic and heat shock stress responses mediated by the HOG1 MAPK pathway [84]. FCA4 has been characterized as one of the six catalase-peroxidase enzymes encoded in the *F. graminearum* genome [178,179]. Targeted deletion of *FCA4* had no effect on oxidative stress response, virulence, or DON production, possibly due to the functional redundancy with the other catalases [178,179]. However, treatment of *F. graminearum* with a bacterial toxin bacillomycin D, which

induces extreme levels of reactive oxygen species (ROS) production and a decrease in *FCA4* expression, resulted in activation of both the MGV1 and the HOG1 pathways, implicating both circuitries in ROS defense [180].

Table 3.1. *MGV1* and *TRI6* both regulate aurofusarin, trichothecene, and fusaoctaxin SMCs.

Cluster_ID	Gene	Description	Role	MGV1‡			TRI6‡	
				WT vs Δmgv	*Δmgv1 vs Δmgv1/MGV 1_1*	*Δmgv1 vs Δmgv1/MGV 1_6*	*WT vs Δtri6*	*Δtri6 vs Δtri6/TRI6*
C03|C23 (trichothecene)	FGSG_00071	cytochrome P450 monooxygenase (TRI1)		5	-9	-7	1,613	-1,300
	FGSG_03532	trichothecene C-15 esterase (TRI8)		7	-9	-6	9	-9
	FGSG_03534	15-O-acetyl transferase		8	-13	-10	185	-123
	FGSG_03535	trichodiene oxygenase	potential detoxifying	5	-8	-6	3	-4
	FGSG_03537	trichodiene synthase (TRI5)	TPS	7	-13	-10	90	-85
	FGSG_03539	hypothetical protein (TRI9)		8	-13	-10	64	-52
	FGSG_03540	isotrichodermin C-15 hydroxylase		4	-6	-4	10	-10
	FGSG_03541	trichothecene efflux pump	transporter	3	-6	-4	14	-17
	FGSG_03542	cytochrome P450 (TRI13)		4	-6	-5	12	-27
	FGSG_03543	trichothecene biosynthesis gene(TRI14)		5	-9	-6	162	-148
	FGSG_16251	regulatory	TF	5	-8	-6	49	-50
C64 (fusaoctaxin A)	FGSG_10989	short-chain dehydrogenase reductase		7	-12	-12	16	-14
	FGSG_10990	non-ribosomal peptide synthetase	NPS	4	-7	-7	13	-10
	FGSG_10991	cytochrome p450 family	potential detoxifying	4	-8	-11	14	-13
	FGSG_10993	2-isopropylmalate synthase		3	-5	-5	8	-8
	FGSG_10994	A Chain Structure Of Ankyrin repeat	TF	4	-9	-7	5	-3
	FGSG_10995	hypothetical protein	transporter	3	-5	-4	5	-5
	FGSG_17487	non-ribosomal peptide synthetase	NPS	6	-16	-18	23	-26
C13 (aurofusarin)	FGSG_02320	transcription factor	TF	-4	3	3	-9	10
	FGSG_02321	6-hydroxy-d-nicotine oxidase		-4	3	4	-9	12
	FGSG_02322†	major facilitator super family transporter	transporter				-31	93
	FGSG_02324	polyketide synthase	PKS	-69	18	27	-132	435
	FGSG_02325	conidial pigment polyketide synthase	PKS	-55	17	39	-634	528
	FGSG_02326	sterigmatocystin 8-o-methyl transferase	potential detoxifying	-98	19	35	-446	306
	FGSG_02327	dimethylaniline monooxygenase 3		-82	17	28	-291	617
	FGSG_02328	conidial pigment biosynthesis oxidase Arb2/brown2		-74	20	37	-277	1,281
	FGSG_02329	fasciclin domain family		-83	20	36	-491	1,108
	FGSG_02330	L-ascorbate oxidase		-2	5	7	-6	2
C49 (butenolide)	FGSG_08077†	nadh-dependent flavin oxido reductase	biosynthetic				5	-8
	FGSG_08078	hypothetical protein	biosynthetic	2	-3	-2	4	-5
	FGSG_08079	benzoate-4-monooxygenase	biosynthetic	9	-19	-5	8	-9
	FGSG_08080†	transcription factor	TF				3	-3
	FGSG_08081†	2og-fe(II) oxygenase family	biosynthetic				8	-9
	FGSG_08082	gnat family n-acetyltransferase, putative		9	-15	-4	8	-8
	FGSG_08083	glutamate decarboxylase	biosynthetic	11	-21	-4	11	-11
	FGSG_08084	major facilitator super family transporter	transporter	8	-11	-4	6	-6

† genes from the aurofusarin and the butenolide clusters that are regulated by *TRI6*, but not *MGV1*.

‡ foldChange values

(*WT* vs Δ*gene* = fold change in the *WT* versus the mutant strain; Δ*gene* vs Δ*gene/GENE* = fold change in the gene mutant vs constitutive expressor)

A functional analysis of genes controlled by *TRI6,* whether exclusively or together with *MGV1,* implicated both regulators in metabolism of SMs and their precursors, such as biosynthesis and degradation of the amino acids, fatty acids, and terpene metabolism (Table S3.6) [142,173]. For example, we identified 19 genes involved in metabolism of branched-chain and aromatic amino acids, histidine, asparagine, and proline (Fig. S3.2). Further, we found ten genes regulated by *TRI6* associated with the fatty acid metabolic pathway (Fig. S3.3).

Among the *TRI6* and *MGV1* co-regulated genes, 50 were associated with SMCs (Table S3.5). In chapter 2, we established the criteria for SMC activation as expression of genes encoding the key biosynthetic, regulatory, transporter, and potential detoxifying enzymes. According to these criteria, trichothecene and fusaoctaxin SMCs were positively regulated by *MGV1* and *TRI6* (Table 3.1). When the analysis was performed with less stringent criteria, not requiring expression of all the key genes, the aurofusarin and butenolide SMCs were also revealed to be regulated by both *MGV1* and *TRI6* (Table 3.1). Of the ten aurofusarin genes in the cluster, nine were regulated by *MGV1;* the single orphan gene encoding a transporter protein (FGSG_02322) exhibited high levels of expression in all four strains (~39K-56K normalized gene reads, Table S3.4). In the butenolide SMC, expression of five of the eight genes was upregulated by *MGV1* (Table 3.1). These included three biosynthetic genes (FGSG_08078, FGSG_08079, and FGSG_08083) and the transporter (FGSG_08084). However, two biosynthetic genes

(FGSG_08077 and FGSG_08081) and the TF (FGSG_08080) were downregulated in the *Δmgv1* by less than 2-fold compared to the wild-type (Table S3.4).

Overall, MGV1 and TRI6 control different sets of pathways. MGV1 influences metabolism in *F. graminearum* on a broad scale, while TRI6 influences pathways related to secondary metabolism. Due to the functional overlap in the control of SM biosynthesis and the positive regulation of *TRI6* by *MGV1*, it is likely that *MGV1* indirectly regulates SMCs by influencing *TRI6* transcription.

3.3.3 *MGV1* regulates biosynthesis and accumulation of secondary metabolites

To further explore the regulation of secondary metabolism by *MGV1*, we performed metabolite profiling by UPLC-HRMS of four *F. graminearum* strains (wild-type and the three *MGV1* mutants Δ*mgv1,* Δ*mgv1/MGV1_1,* Δ*mgv1_MGV1_6*) from mycelia isolated at the time points of 3, 6, 9, and 12 days. As with *TRI6* regulation, we sought a link between the transcriptional changes induced by *MGV1* and the dynamics of SM biosynthesis and accumulation.

A principal component analysis (PCA) was performed to explore the variations in the metabolite accumulation. On day 3, the onset of SM production, 41% of the variation was explained by the differences in SM biosynthesis between biological and technical replicates, irrespective of the strain and can be observed as a separation of the replicates along the PC1 (Fig. 3.3 A). Only 32% of the variation was explained by the differences between strains, with the *Δmgv1* separating away from the wild-type, *Δmgv1/MGV1_1* and *Δmgv1/MGV1_6* along the PC2 (Fig. 3.3 A). On days 6, 9, and 12, the majority of the

differences between samples were attributable to the strains, with the samples from the *Δmgv1* strain separating away from the wild-type, *Δmgv1/MGV1_1* and *Δmgv1/MGV1_6* samples, explaining 55-62% of variation along PC1 (Fig. 3.3 B-D). Only 15-22% of the variation was explained by the differences between replicates, which were separated along PC2 (Fig. 3.3 B-D).

Mass features associated with several characterized compounds were responsible for the variances observed in the PCA. These included products of the trichothecene, fusaoctaxin A, fusarin, gramillin, aurofusarin, and ferricrocin SMCs (Table 3.2). Biosynthesis pattern analysis of these SMs across the four time points showed varying kinetic profiles. Fusarins A and C/D/B accumulated highly in the wild-type strain on day 3 and reduced production on consecutive time points (Fig. 3.4 A, B). Conversely, in the *mgv1* mutant the production of fusarins increased from day 3 to day 9 for fusarin A or day 6 for fusarin C/D/B, and then decreased on day 12 (Fig. 3.4 A, B). The accumulation of products of the fusaoctaxin A cluster, namely fusaoctaxin A, fusaoctaxin A analogs 1-4 described in Chapter 2, and two fusaoctaxin A cleavage products fusapentaxin and fusatrixin, peaked on day 9 in the wild-type strain (Fig. 3.4 C-I). In the *Δmgv1* mutant, biosynthesis pattern of fusapentaxin remained the same as in the wild-type, while the rest of the compounds peaked on day 12 (Fig. 3.4 C-I). The gramillins A and B, aurofusarin, and ferricrocin accumulated until day 12 in the wild-type. In the *mgv1* mutant, kinetics of gramillin accumulation remained the same over

the 12-day time period but aurofusarin and ferricrocin production peaked on day 6 (Fig. 3.4 J-M).

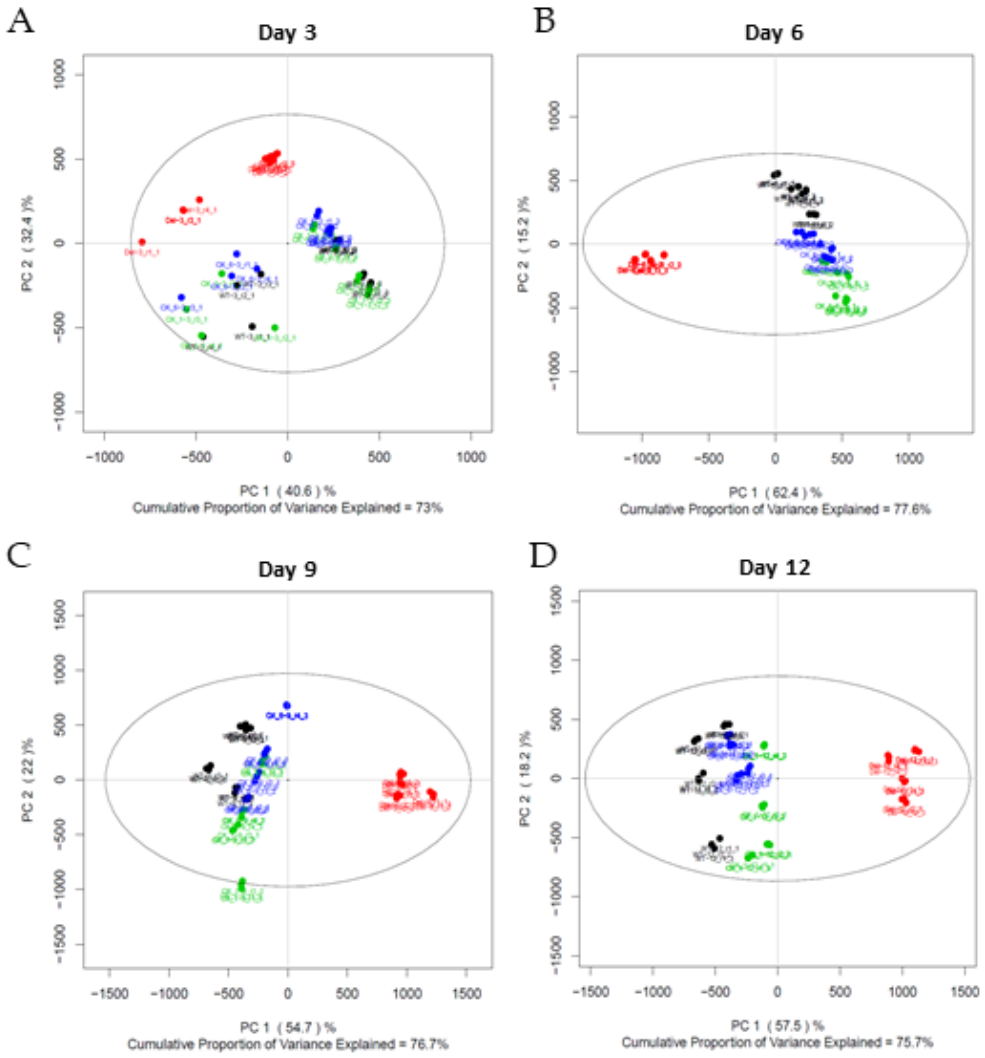

Fig. 3.3. Principal component analysis of metabolites regulated by *MGV1*. *MGV1* is responsible for majority of the variations in metabolomics profiles of *F. graminearum* wild-type, Δ*mgv1*, and Δ*mgv1/MGV1* strains grown in PN medium for 3, 6, 9, and 12 days (**A-D**). PC1 represents variation due to strain differences, PC2 – due to variability between samples in individual strains (exception – day 3, where this trend is reversed). Black dots = wild-type sample replicates; red = Δ*mgv1*; green = Δ*mgv1/MGV1_1*, blue = Δ*mgv1/MGV1_6*.

Table 3.2. MGV1 regulates several known secondary metabolites.

RT_m/z	Feature ID	Day with highest signal in WT	Regulation by *MGV1* †				Regulation by TRI6 (Chapter 2)†	SMC ID‡
			day 3	day 6	day 9	day 12		
RT4.93_438.1878	Fusarin A	3		-	-	-		C42
RT4.61_432.2001	Fusarin C/D/B*	3	+		-	-		
RT3.53_339.1427	15-ADON	6	+				+	C03 | C23
RT4.4_398.1966	isotrichodiol analog (1)*	6	+			-	+	
RT3.85_413.2102	isotrichodiol analog (2)	6	+	+			+	
RT3.78_269.1737	trichotriol	12	+	+	+	+		
RT3.99_414.1928	isotrichotriol analog (3)	9	+				+	
RT3.9_773.5116	Fusaoctaxin A	9	+	+			+	C64
RT3.31_474.2907	Fusapentaxin	9			-	-		
RT3.53_340.2198	Fusatrixin	9		-	-	-		
RT3.92_787.5012	Fusaoctaxin analog (1)	9	+	+			+	
RT3.95_757.5166	Fusaoctaxin analog (2)	9	+	+			+	
RT3.96_771.5069	Fusaoctaxin analog (3)	9	+	+			+	
RT4.01_801.5167	Fusaoctaxin analog (4)	9	+	+	+		+	
RT4.2_847.3672	Gramillin A	12	+	+	+	+	-	C02
RT4.22_861.3817	Gramillin B	12	+	+	+	+	-	
RT4.9_571.0851	Aurofusarin	12		-			-	C13
RT2.8_771.2459	Ferricrocin	12				+		C33

* fold Change not consistent across the timeline

† refers to positive (+) or negative (-) regulation by *MGV1 or TRI6*

‡ designated by Sieber *et. al.* 2014

In comparison, production of 15-ADON and the other trichothecene-related compounds showed greater variability. In the wild-type strain, accumulation of 15-ADON and the isotrichodiol analogs 1 and 2 were highest on day 6 (Fig. 3.4 N-P). However, isotrichotriol analog (3) biosynthesis accumulated until day 9, and the trichotriol production peaked on day 12 (Fig. 3.4 Q, R). In the *mgv1* mutant, biosynthesis of 15-ADON, isotrichodiol analog 2, isotrichotriol analog 3, and trichotriol was highest on day 9 (Fig. 3.4 N, P-R), while biosynthesis of isotrichodiol analog 1 peaked on day 12 (Fig. 3.4 O).

Fig. 3.4. (pgs. 99-100) Kinetics of secondary metabolite production in *F. graminearum* wild-type and Δ*mgv1* strains grown in PN conditions over the course of 3, 6, 9, and 12 days. Accumulation of fusarins (**A, B**), fusaoctaxin A (**C**) and is four analogs (**D-G**), fusapentaxin (**H**), and fusatrixin (**I**), gramillins (**J, K**), aurofusarin (**L**), ferricrocin (**M**), 15-ADON (**N**), isotrichodiol analogs 1 and 2 (**O, P**), isotrichotriol analog 3 (**Q**), and trichotriol (**R**). Box plots are representative of four biological replicates. Signal intensity was measured in counts per second (cps) and normalized to total ion current.

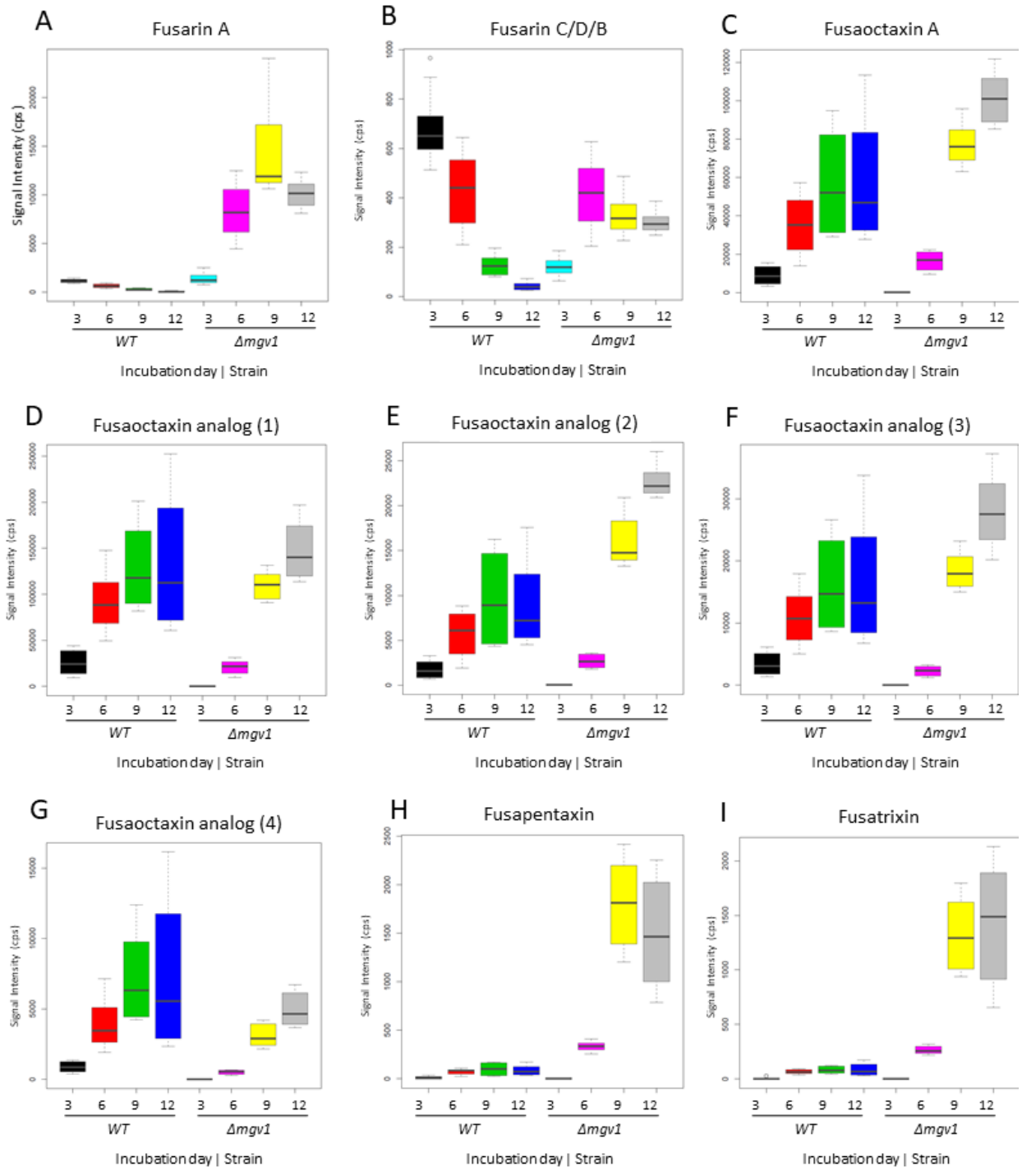
A
Fusarin A
B
Fusarin C/D/B
C
Fusaoctaxin A
D
Fusaoctaxin analog (1)
E
Fusaoctaxin analog (2)
F
Fusaoctaxin analog (3)
G
Fusaoctaxin analog (4)
H
Fusapentaxin
I
Fusatrixin
Signal Intensity (cps)
3 6 9 12 3 6 9 12
WT
Δmgv1
Incubation day | Strain

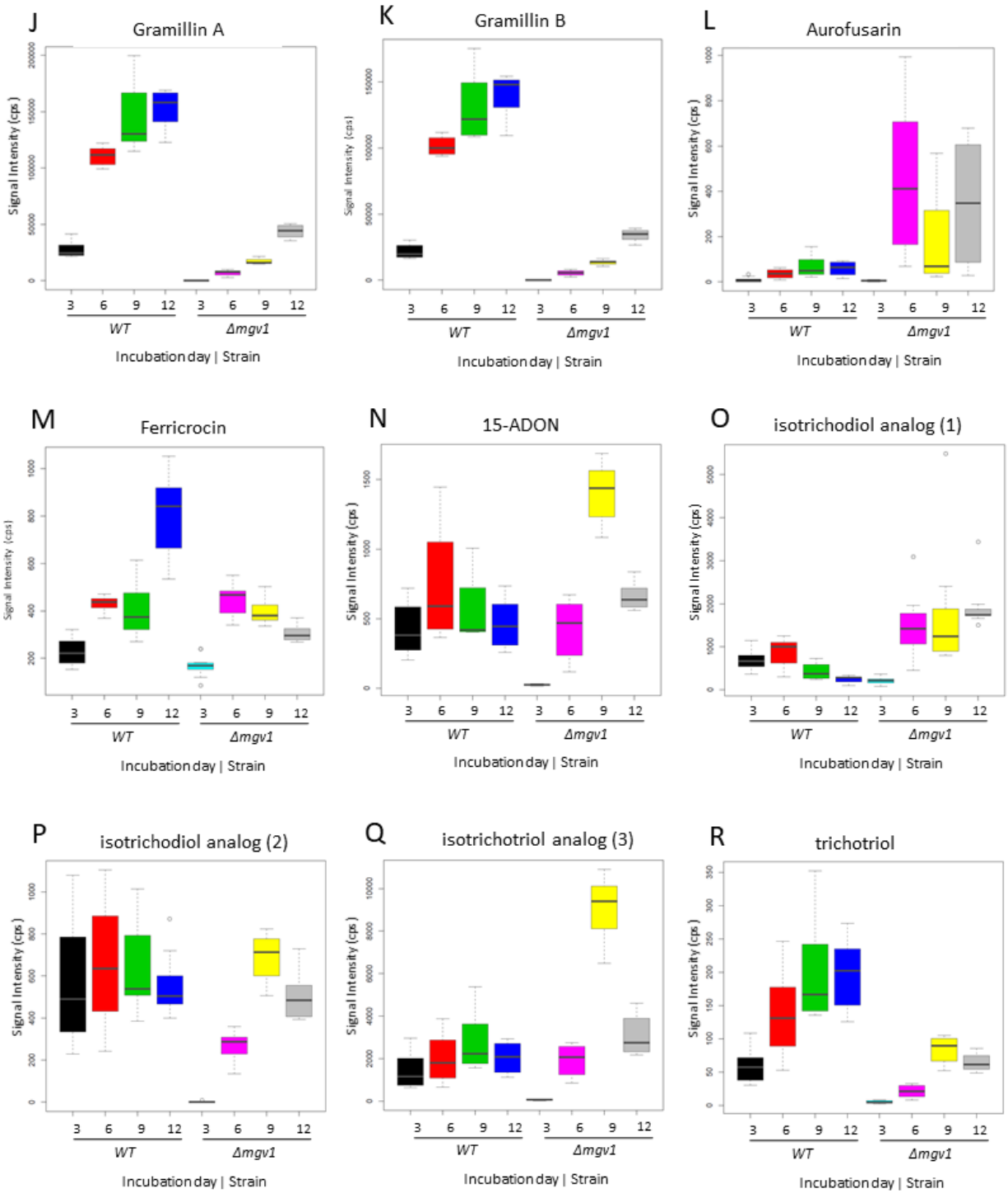
J
Gramillin A
K
Gramillin B
L
Aurofusarin
M
Ferricrocin
N
15-ADON
O
isotrichodiol analog (1)
P
isotrichodiol analog (2)
Q
isotrichotriol analog (3)
R
trichotriol
Signal Intensity (cps)
3 6 9 12 3 6 9 12
WT
Δmgv1
Incubation day | Strain

In order to validate if the observed differences in SM production was due to *MGV1*, SM profiles between the wild-type and the *mgv1* mutant were compared with the profiles from the two rescue mutant strains, *Δmgv1/MGV1_1* and Δ*mgv1/MGV1_6*, at each time point. Analysis indicated that 93-99% of the metabolites differentially produced in *Δmgv1* relative to the wild-type were rescued by both constitutive expressor strains. These included 231, 242, 266, and 242 compounds on days 3, 6 ,9 and 12, respectively (Fig. 3.5). There was a large overlap of the compounds regulated by *MGV1* at each timepoint, with only 37, 6, 22, and 12 metabolites unique to days 3, 6, 9, and 12, respectively. Overall, 99 metabolites were differentially produced on days 3, 6, 9, and 12 (Fig. 3.5). Of the 99, only gramillins A and B and isotrichotriol have been characterized, other metabolites remain uncharacterized (Table 3.2, Fig. 3.5).

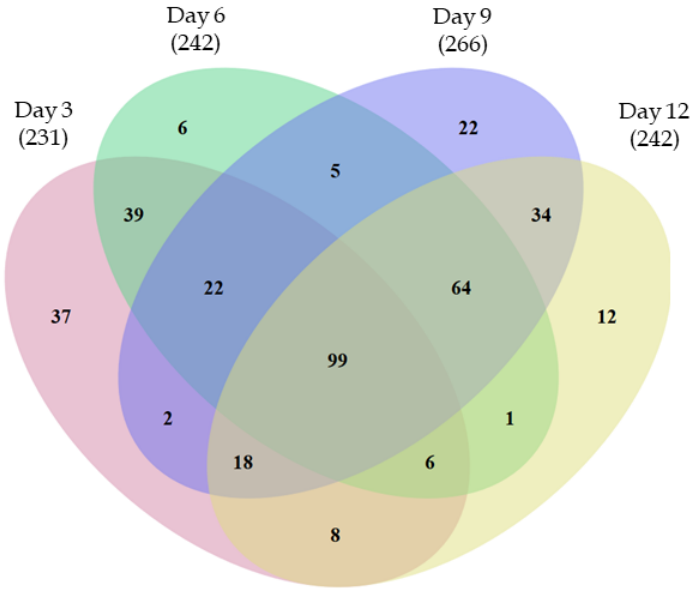

Fig. 3.5. *MGV1* regulates production of secondary metabolites. The Venn diagrams represent overlaps between metabolites differentially produced due to *MGV1* on day 3, 6, 9, and 12 with the number of compounds regulated by *MGV1* on each day in brackets. 99 compounds were regulated by *MGV1* at all time points.

Our analysis also indicated that the accumulation of gramillins A and B and ferricrocin was positively influenced by *MGV1*, while accumulation of fusarin A, fusarin C/D/B, and aurofusarin was negatively influenced by *MGV1* (Table 3.2). Fusarin, ferricrocin and gramillin SMCs were not detected in the analysis of transcriptional control by *MGV1*, suggesting post-translational regulation of gene products involved in the biosynthesis of these compounds. The negative effect on aurofusarin accumulation correlated with the gene expression changes in the aurofusarin SMC, suggesting that transcriptional re-programming is a dominant contributor of regulation of this gene cluster by *MGV1*.

Among the products of the fusaoctaxin SMC, production of fusaoctaxin A and its four analogs was positively influenced by both *MGV1* and *TRI6* (Tables 3.2, 2.3). However, *MGV1* had a negative effect on accumulation of fusapentaxin and fusatrixin (Table 3.2). A recent study revealed that fusaoctaxin A is cleaved to produce fusapentaxin and fusatrixin by an ABC-transporter with peptidase activity encoded by FGSG_10995 within the fusaoctaxin SMC [155]. Paradoxically, we observed that *MGV1* positively regulates the expression of FGSG_10995, while negatively influencing the accumulation of the cleavage products of fusaoctaxin A (Tables 3.1, 3.2). Together, these results indicate that *MGV1* regulation of the transporter occurs both at the transcriptional and post-transcriptional levels.

Regulation of trichothecene products exhibited a complex pattern. The biosynthesis of 15-ADON, trichotriol, isotrichodiol analog 2, and isotrichotriol analog 3

is positively influenced by *MGV1* (Table 3.2). However, the influence on the isotrichodiol analog 1 is inconsistent (Day 3 vs day 12, Table 3.2). In the wild-type strain, accumulation of all trichothecenes peaked on day 6, and then decreased in production between 9 and 12 days. This trend could be associated with the regulatory changes in response to the shifting conditions in the *F. graminearum* cultures incubated over the course of 12 days. Such changes could be attributed to a negative feedback loop between the various trichothecene analogs.

Transcription profiling indicated that *MGV1* regulation of the trichothecene, fusaoctaxin, butenolide, and aurofusarin SMCs is mediated through *TRI6*. HRMS-UPLC analysis confirmed the regulation of these clusters with the exception of the butenolide SMC (the mass feature associated with this compound was absent from the dataset). As well, products of the fusarin, gramillin, and ferricrocin SMCs were significantly differentially produced in the *mgv1* mutant strain, despite the lack of transcriptional regulation. Cumulatively, our data suggests that *MGV1* exerts its regulatory control of these metabolic gene clusters at the post-transcriptional level.

3.4 Discussion

Secondary metabolism regulation in filamentous fungi has a hierarchical organization with the protein kinases amplifying many signals through phosphorylation of transcriptional regulators [181]. MGV1 is a MAPK in *F. graminearum* that regulates the cell wall integrity pathway, though it is also implicated in sexual and asexual development and pathology on wheat [80]. Previous work implicated MGV1 in

the biosynthesis of SMs 15-ADON, butenolide, and other unknown compounds [94]. My thesis expanded the knowledge of regulation of SMs by MGV1 through genome wide transcriptomic and metabolomic analyses. We compared the regulation of SMs by *TRI6* to those regulated by *MGV1,* and together, the two analyses revealed that (a) a subset of SMCs are co-regulated by *MGV1* and *TRI6*; (b) a subset of SMCs regulated by *MGV1* is independent of *TRI6;* (c) genes within a cluster can be regulated by either *MGV* or *TRI6*, thus revealing coordination of regulatory pathways; and (d) *MGV1* regulates SM production post-transcriptionally.

We identified 1,120 genes under transcriptional control of the *MGV1*, including 228 genes that are co-regulated with *TRI6.* The co-regulated genes, along with those regulated exclusively by TRI6, were mostly involved in carbon and amino acids metabolism and secondary metabolism (Table S3.6, S3.7, Figs. S3.2, S3.3). The amino acid and fatty acid metabolic pathways provide structural constituents for the biosynthesis of non-ribosomal peptides (NPs) in the form of amino acid precursors, and for the biosynthesis of polyketides (PKs) in the form of acetyl- and malonyl-CoA precursors [12]. Therefore, the regulation of amino acid and fatty acid metabolic genes by *TRI6* suggests its involvement in the allocation of resources for biosynthesis of the PK and NP classes of secondary metabolic compounds.

Both regulators exerted positive control over the trichothecene, fusaoctaxin, and butenolide SMCs, and negative control over the aurofusarin cluster (Table 3.1). Since *MGV1* can potentially regulate *TRI6*, and influence the expression of the SMCs, it is not

too farfetched to suggest that *MGV1* controls these genes through TRI6. In support, we observed that most of the SMC genes under the control of both regulators exhibited less dramatic changes (increase or decrease) in expression in the Δ*mgv1,* relative to what we observed in the Δ*tri6* strains (Table 3.1). This could be attributed to the reduced expression of *TRI6* or low levels of TRI6 protein present in the *mgv1* mutant strain. Thus, lower levels of the TRI6 protein may be sufficient to repress aurofusarin genes and activate the trichothecene and fusaoctaxin SMCs. Reduced expression of *TRI6* in the Δ*mgv1* strain may also explain the apparent lack of *MGV1* control over the gramillin genes. The differences in expression of the gramillin cluster genes between the *Δtri6* and the wild-type strains were 3-fold or less (Table S2.3). Therefore, low TRI6 levels in the *mgv1* mutant may be insufficient to repress the gramillin cluster genes to a degree significantly different from the wild-type strain.

Our metabolomics data supported the positive regulation of the trichothecene, fusaoctaxin, and aurofusarin SMCs by *MGV1.* Fusaoctaxin A and its four analogs were highly accumulated in presence of *MGV1.* In contrast, fusaoctaxin A cleavage products, fusapentaxin and fusatrixin, were produced in smaller quantities in the wildtype and both *Δmgv1/MGV1* strains when compared with the *Δmgv1* strain (Table 3.2). Prior work has indicated that the cleavage mechanism of fusaoctaxin A is mediated by an ABC transporter with peptidase activity encoded within the fusaoctaxin SMC [155]. Proteolytic cleavage as a method for detoxification is common in bacterial systems, and has been suggested as a mechanism to detoxify fusaoctaxin A [155,182]. However, the

comparative toxicity studies with fusaoctaxin A and its cleavage products, fusapentaxin and fusatrixin, have not been performed in wheat to test this scenario. Alternatively, *MGV1* may regulate the expression of the ABC transporter differentially such that the proteolytic products are used in a feedback mechanism to regulate the production of fusaoctaxin A. Thus, *MGV1* positively influences production of fusaoctaxin A and concomitantly downregulates its cleavage into the fusapentaxin and fusatrixin. The advantage of this regulatory mechanism for *F. graminearum* is not apparent and is a subject for future studies.

One of the interesting findings from this study was that *MGV1* had profound effect on the biosynthesis of the gramillins A and B, ferricrocin and the fusarins A and B/C/D, but had no effect on the transcription of genes associated with these metabolites (Table 3.2). This contrasted with our prior observations, which showed *TRI6* to be a negative regulator of gramillin both at transcriptional and biosynthetic levels (Tables 2.2, 2.3). The differential effect of *MGV1* and *TRI6* on the gramillin SMC expression and metabolite biosynthesis underscores the fact that there are a multitude of regulatory circuits influencing SMCs. It is tempting to speculate that while gramillin gene cluster is repressed transcriptionally by *TRI6*, biosynthesis of gramillin is modulated by *MGV1* at the post-transcriptional level. We have previously shown that TRI6 can interact with GRA2, a gramillin cluster-specific transcriptional regulator (Chapter 2). Therefore, it is conceivable that post-transcriptional regulation could occur

via phosphorylation of either TRI6 or GRA2 by MGV1, resulting in modification of protein complexes involved in the production of gramillin.

Consistent with the regulatory hierarchy, genes controlled by *MGV1*, independent of *TRI6*, belong to a wide variety of cellular processes such as cell transport systems, cell type differentiation and mismatch repair (Tables S3.6, S3.7). Of interest is the transcriptional regulation by *MGV1* of the three members of the CWI pathway – the cell surface receptor FGSG_03574, a MAP kinase inhibitor MSG5, and a cell cycle regulator MIH1 (Fig. 3.1B). The cell surface receptor is responsible for receiving and transducing the environmental signals to the MAPK cascade, activating MGV1, while MSG5 is involved in downregulation of MGV1 through phosphorylation [68,174]. This study might have uncovered a strategy of MGV1 modulating the activity of the CWI pathway in *F. graminearum* at the transcriptional level.

We also identified a crosstalk between two MAPK pathways, as *MGV1* positively regulated *FCA4,* which encodes the catalase induced by HOG1 MAPK in response to oxidative stress. Prior to this study, the only demonstrated relationship between these two MAPK pathways in *F. graminearum* was the MKK1 phosphorylation of both HOG1 and MGV1 [170]. Studies in yeast determined that *FCA4* homolog *CTT1* was transcriptionally regulated by the MGV1 homolog SLT2 in response to the toxic metalloid arsenate [183]. However, the role of CTT1 in either arsenate response or in the SLT2 pathway remains unexplored.

3.5 Conclusion

MAPKs are essential for transduction of environmental signals to the global regulators of primary and secondary metabolism. Here, we explored the regulatory interaction between the MAPK, *MGV1*, and the global regulator of secondary metabolism, *TRI6*. Our findings indicate that *MGV1* exclusively controls a wide variety of primary and secondary metabolic pathways, while co-regulating SM-specific genes together with *TRI6*. We also determined that transcriptional regulation of the trichothecene, aurofusarin, and fusaoctaxin A SMCs by *TRI6* is likely coordinated through *MGV1*. Meanwhile, *MGV1* regulates the gramillin, fusarin, and ferricrocin production post-transcriptionally.

3.6 Materials and Methods

3.6.1 *F. graminearum* strain construction

F. graminearum NRRL29169 is the wild-type strain and was used as the parental strain for all transgenic strains used. The construction of *Δmgv1* strain has been previously described [94].

Strains *Δmgv1/MGV1_1* and *Δmgv1/MGV1_6* were constructed using *Agrobacterium*-mediated transformation as per Frandsen *et al.* [160]. Briefly, the pRF-HU2E vector was used for *in locus* constitutive expression, which is driven by the constitutive *Aspergillus nidulans* promoter (PgpdA) [160]. Primers P28-31 were used to amplify a fragment of the *MGV1* gene and a fragment of its upstream region from genomic DNA (gDNA) of *F. graminearum*. Correct insertion of the cassette into *F. graminearum* was

corroborated using the primers P32-P37, and the *MGV1* sequence was confirmed through the Genome Quebec service lab (Montréal, Québec, Canada). All primers are listed in Table S2.9).

The over-expression of *MGV1* was corroborated through reverse-transcription qPCR (RT-qPCR). RNA extraction, cDNA synthesis and qPCR were carried out as previously described [184]. The qPCR reaction was performed in 10 µL with PerfeCTa® SYBR® Green SuperMix Low ROX (Quantabio) and primers P38-P41. Three biological replicates with three technical replicates were included in each reaction along with the negative controls. Standard curve calculations were used to normalize the data to housekeeping genes and to estimate the relative expression of *MGV1* compared to the wild-type using the Qiagen's Relative Expression Software Tool (REST©) ($p < 0.05$).

3.6.2 Culturing conditions

Culturing conditions were identical to those described in Chapter 2, section 2.6.1.

3.6.3 Gene expression analysis (RNAseq, RT-qPCR)

Gene expression analysis of the *F. graminearum* wild-type, *Δmgv1, Δmgv1/MGV1_1,* and *Δmgv1/MGV1_6* strains was carried out as described in Chapter 2, section 2.6.2, with one exception. The total RNA was sequenced using Illumina NovaSeq 6000 platform at the Centre d'expertise et de services Génome Québec.

3.6.4 Metabolomic analysis

Metabolomic analysis was conducted as described in Chapter 2, section 2.6.3, with the exception of additional processing of the dataset prior to the statistical analysis

in *muma.* Pearson correlation analysis was carried out to group the metabolites together with their fragments and adducts based on the retention time window of 0.1 minutes, thus eliminating duplicate variables representing the same compound. For each group, mass features with the highest total signal were chosen as representative variables. The script to perform correlation analysis is part of the supplementary files (S_file_1_Polished_correlation_script.R).

Chapter 4. Perspectives and future directions

4.1 Cryptic activation of secondary metabolism in *Fusarium graminearum*

Filamentous fungi have the potential to produce a diverse set of secondary metabolites. Some of these natural products are beneficial to humanity, such as the antibiotic penicillin and the immunosuppressant cyclosporine [148]. Others are harmful, such as the estrogen mimic zearalenone and the "vomitoxin" DON [3].

To date, 76 SMCs have been identified in the *F. graminearum* genome [24]. Due to high functional specificity and energetic requirements, biosynthesis of these natural products is "silent" in the majority of standard laboratory conditions. This "cryptic" status hinders characterization of many known SMCs. Over the last couple of decades, a variety of methods have been developed to successfully induce production of SMs from the cryptic clusters. For instance, a method termed OSMAC (one strain – many compounds) involves systematic variation of the fermentation conditions to induce production of as many compounds as possible from a single microbial strain [185]. In a different method, the fungal strain of interest is co-cultured with another microorganism. This strategy is aimed at inducing the production of SMs in the microorganisms that have a role in inter- or intra- species interactions [186,187].

Other methods of inducing cryptic activation are based on molecular manipulation of the cellular machinery. In cases where an SMC contains a cluster-specific transcriptional regulator, its overexpression can result in the activation of the

compound biosynthesis [131,148]. In fact, fusaoctaxin A characterization was achieved through constitutive expression of the cluster-specific regulator *FGM4* [15].

As discussed in Chapter 1, manipulation of the global regulators, such as AreA, PacC and CreA leads to gene expression changes in multiple SMCs. Similarly, epigenetic alterations result in an altered metabolic profile. This has been demonstrated by chemical inhibition, or targeted deletion or constitutive expression of the chromatin modifying enzymes, such as histone acetyltransferases, deacetylases, and methyltransferases [131,148]. For example, targeted deletion of KMT6, the H3K27me3 methyltransferase, relieved repression of 20% of the genome and led to identification of 9 novel SMCs in *F. graminearum* [24].

This dissertation describes cryptic activation of the secondary metabolite biosynthesis in *F. graminearum* by altering the expression of regulators TRI6 and MGV1. To identify the SMCs controlled by *TRI6* and *MGV1*, we studied the strains deficient in expression of these regulators. We then combined this data with analysis of strains constitutively expressing *TRI6* and *MGV1*. This approach gave us insight into biosynthesis of phytotoxins 15-ADON, gramillins A and B, and fusaoctaxin A, as well as compounds with other roles in *F. graminearum* life cycle – fusarins, ferricrocin, aurofusarin, and butenolide. Finally, we identified many novel SMs whose structures and roles in fungal physiology will be subjects for future studies. Overall, our results support the hypotheses that TRI6 and MGV1 regulate multiple secondary metabolism gene clusters in *F. graminearum*.

Aside from further identification and characterization of novel compounds, we also need to understand the regulatory relationship between MGV1 and TRI6. One way to achieve this would be to constitutively express *TRI6* in the *mgv1* mutant to identify pathways specifically regulated by *TRI6* without the influence of *MGV1*.

An alternate approach would be to use the large-scale genomic and proteomic datasets available to construct the molecular interaction networks. Apart from revealing the regulatory relationships between MGV1 and TRI6, this approach would have an additional advantage of exploring how TRI6 and MGV1 relate to the other signalling pathways.

4.2 Beyond regulation of secondary metabolism – construction of a global regulatory network in *F. graminearum*

The individual pathways in cellular networks are connected in a complex manner to perceive multiple stimuli and integrate them for the cellular machinery to elicit an appropriate response. Integration of cellular circuitries can help us comprehend the biological significance of the individual signalling pathways.

Several networks have been constructed in *F. graminearum* based on the interologs and domain-domain interaction approaches from seven species to predict protein interactions in *F. graminearum* [188]. This led to 27,102 predicted interactions among 3,745 proteins, and construction of the first Protein-Protein Interaction (FPPI) database (data collected from http://comp-sysbio.org/efg/) [188]. More recently, a dedicated PPI network of proteins differentially expressed during DON inducing

conditions was constructed in *F. graminearum* using the yeast-two-hybrid approach. This *Fusarium* network of trichothecene associated proteins (FuNTAP) was based on 90,000 interactions and identified 192 nodes with 520 interactions (personal communications, R. Subramaniam) [189]. Studies are underway to validate the construction of such dedicated PPI network with respect to overall cellular network.

Another way to model cellular networks is through integration of gene expression profiles using microarray and transcriptomics datasets. For *F. graminearum*, such a network was constructed for genes involved in pathogenicity [190]. The resultant network was then combined with the PPI data to narrow down the genes physically interacting with the known pathogenic factors during the infection process [190]. In this manner, authors identified novel genes interacting with the regulatory proteins GPCRs and MAPKs that are important for *F. graminearum* pathogenicity on wheat. One of the network hubs identified in this study was the MGV1 kinase [190]. Of interest is that TRI6, though essential for pathogenicity, was not a part of the MGV1 subnetwork, underscoring the limitations of this approach. To construct a model that represents the biological system accurately, integration of multiple datasets is necessary.

Towards developing an accurate model of the *F. graminearum* cellular network, one of the propositions is to construct a dedicated network based on the key regulators of cellular processes, such as TRI6, MGV1, AreA, LaeA and PacC. Such network would identify novel interactions between the key regulators, but also integrate pathways involved in various environmental inputs. The resultant network can then be integrated

into transcriptomics datasets and protein interaction datasets such as FPPI and FuNTAP. Importantly, this network could be used to predict function of approximately ~65% of the currently uncharacterized "hypothetical proteins" in *F. graminearum,* thus enhancing our understanding of the individual regulatory elements within the cellular network of this fungal pathogen.

Bibliography

1. Trail, F. For blighted waves of grain: *Fusaraium graminearum* in the postgenomics era. *Plant Physiol.* **149**, 103–110 (2009).

2. Xue, A. G. *et al.* Prevalence of *Fusarium* species causing head blight of spring wheat, barley and oat in Ontario during 2001–2017. *Can. J. Plant Pathol.* **41**, 392–402 (2019).

3. Goswami, R. S. & Kistler, H. C. Heading for disaster: *Fusarium graminearum* on cereal crops. *Mol. Plant Pathol.* **5**, 515–525 (2004).

4. Tudzynski, B. Nitrogen regulation of fungal secondary metabolism in fungi. *Front. Microbiol.* **5**, 1–15 (2014).

5. Kimura, M., Tokai, T., Takahashi-Ando, N., Ohsato, S. & Fujimura, M. Molecular and genetic studies of *Fusarium* trichothecene biosynthesis: pathways, genes, and evolution. *Biosci. Biotechnol. Biochem.* **71**, 2105–2123 (2007).

6. Menke, J., Weber, J., Broz, K. & Kistler, H. C. Cellular development associated with induced mycotoxin synthesis in the filamentous fungus *Fusarium graminearum*. *PLoS One* **8**, 1–12 (2013).

7. Hoffmeister, D. & Keller, N. P. Natural products of filamentous fungi: enzymes, genes, and their regulation. *Nat. Prod. Rep.* **24**, 393–416 (2007).

8. Keller, N. P., Turner, G. & Bennett, J. W. Fungal secondary metabolism - from

biochemistry to genomics. *Nat. Rev. Microbiol.* **3**, 937–947 (2005).

9. Lim, F. Y. & Keller, N. P. Spatial and temporal control of fungal natural product synthesis. *Nat. Prod. reports* **31**, 1277–1286 (2015).

10. Venkatesh, N. & Keller, N. P. Mycotoxins in conversation with bacteria and fungi. *Front. Microbiol.* **10**, 1–10 (2019).

11. Adam, G., Wiesenberger, G. & Güldener, U. *Biosynthesis and Molecular Genetics of Fungal Secondary Metabolites, Volume 2*. (Springer New York, 2015).

12. Hansen, F. T. *et al.* An update to polyketide synthase and non-ribosomal synthetase genes and nomenclature in *Fusarium*. *Fungal Genet. Biol.* **75**, 20–29 (2015).

13. Hansen, F. T., Sorensen, J. L., Giese, H., Sondergaard, T. E. & Frandsen, R. J. N. Quick guide to polyketide synthase and nonribosomal synthetase genes in *Fusarium*. *Int. J. Food Microbiol.* **155**, 128–136 (2012).

14. Bahadoor, A. *et al.* Gramillin A and B: cyclic lipopeptides identified as the nonribosomal biosynthetic products of *Fusarium graminearum*. *J. Am. Chem. Soc.* **140**, 16783–16791 (2018).

15. Jia, L.-J. *et al.* A linear nonribosomal octapeptide from *Fusarium graminearum* facilitates cell-to-cell invasion of wheat. *Nat. Commun.* **10**, 1–20 (2019).

16. Flynn, C. M., Broz, K., Jonkers, W., Schmidt-Dannert, C. & Kistler, H. C.

Expression of the *Fusarium graminearum* terpenome and involvement of the endoplasmic reticulum-derived toxisome. *Fungal Genet. Biol.* **124**, 78–87 (2019).

17. Yin, W. & Keller, N. P. Transcriptional regulatory elements in fungal secondary metabolism. *J. Microbiol.* **49**, 329–339 (2013).

18. Desjardins, A. E. & Proctor, R. H. Molecular biology of *Fusarium* mycotoxins. *Int. J. Food Microbiol.* **119**, 47–50 (2007).

19. Brakhage, A. A. Regulation of fungal secondary metabolism. *Nat. Rev. Microbiol.* **11**, 21–32 (2013).

20. Sieber, C. M. K. *et al.* The *Fusarium graminearum* genome reveals more secondary metabolite gene clusters and hints of horizontal gene transfer. *PLoS One* **9**, 1–22 (2014).

21. Connolly, L. R., Smith, K. M. & Freitag, M. The *Fusarium graminearum* histone H3 K27 methyltransferase KMT6 regulates development and expression of secondary metabolite gene clusters. *PLoS Genet.* **9**, 1–18 (2013).

22. Reyes-Dominguez, Y. *et al.* Heterochromatic marks are associated with the repression of secondary metabolism clusters in *Aspergillus nidulans*. *Mol. Microbiol.* **76**, 1376–1386 (2010).

23. Palmer, J. M. & Keller, N. P. Secondary metabolism in fungi: does chromosomal location matter? *Curr. Opin. Microbiol.* **13**, 431–436 (2011).

24. Adpressa, D. A. *et al.* A metabolomics-guided approach to discover *Fusarium graminearum* metabolites after removal of a repressive histone modification. *Fungal Genet. Biol.* **132**, 1–14 (2019).

25. Spraker, J. E. *et al.* Conserved responses in a war of small molecules between a plant-pathogenic bacterium and fungi. *MBio* **9**, 1–14 (2018).

26. Haas, H., Eisendle, M. & Turgeon, B. G. Siderophores in fungal physiology and virulence. *Annu. Rev. Phytopathol.* **46**, 149–187 (2008).

27. Oide, S., Berthiller, F., Wiesenberger, G., Adam, G. & Turgeon, B. G. Individual and combined roles of malonichrome, ferricrocin, and TAFC siderophores in *Fusarium graminearum* pathogenic and sexual development. *Front. Microbiol.* **5**, 1–15 (2014).

28. Oide, S. *et al. NPS6*, encoding a nonribosomal peptide synthetase involved in siderophore-mediated iron metabolism, is a conserved virulence determinant of plant pathogenic ascomycetes. *Plant Cell* **18**, 2836–2853 (2006).

29. Notz, R., Maurhofer, M., Dubach, H. & Haas, D. Fusaric acid-producing strains of *Fusarium oxysporum* alter 2,4-diacetylphloroglucinol biosynthetic gene expression in *Pseudomonas fluorescens* CHA0 *in vitro* and in the rhizosphere of wheat. *Society* **68**, 2229–2235 (2002).

30. van Rij, E. T., Girard, G., Lugtenberg, B. J. J. & Bloemberg, G. V. Influence of fusaric acid on phenazine-1-carboxamide synthesis and gene expression of

Pseudomonas chlororaphis strain PCL1391. *Microbiology* **151**, 2805–2814 (2005).

31. Quecine, M. C. *et al.* An interspecies signaling system mediated by fusaric acid has parallel effects on antifungal metabolite production by *Pseudomonas protegens* strain Pf-5 and antibiosis of *Fusarium* spp. *Appl. Environ. Microbiol.* **82**, 1372–1382 (2016).

32. Lee, K., Pan, J. J. & May, G. Endophytic *Fusarium verticillioides* reduces disease severity caused by *Ustilago maydis* on maize. *FEMS Microbiol. Lett.* **299**, 31–37 (2009).

33. Jonkers, W. *et al.* Metabolome and transcriptome of the interaction between *Ustilago maydis* and *Fusarium verticillioides in vitro*. *Appl. Environ. Microbiol.* **78**, 3656–3667 (2012).

34. Lutz, M. P., Feichtinger, G., Défago, G. & Duffy, B. Mycotoxigenic *Fusarium* and deoxynivalenol production repress chitinase gene expression in the biocontrol agent *Trichoderma atroviride* P1. *Appl. Environ. Microbiol.* **69**, 3077–3084 (2003).

35. Seong, K. *et al.* Global gene regulation by *Fusarium* transcription factors *Tri6* and *Tri10* reveals adaptations for toxin biosynthesis. *Mol. Microbiol.* **72**, 354–367 (2009).

36. Brown, D. W., Proctor, R. H., Dyer, R. B. & Plattner, R. D. Characterization of a *Fusarium* 2-gene cluster involved in trichothecene C-8 modification. *J. Agric. Food Chem.* **51**, 7936–7944 (2003).

37. Basenko, E. Y. *et al.* FungiDB: An integrated bioinformatic resource for fungi and oomycetes. *J. Fungi* **4**, 1–28 (2018).

38. Crippin, T., Renaud, J. B., Sumarah, M. W. & David Miller, J. Comparing genotype and chemotype of *Fusarium graminearum* from cereals in Ontario, Canada. *PLoS One* **14**, 1–18 (2019).

39. Alexander, N. J., McCormick, S. P., Waalwijk, C., van der Lee, T. & Proctor, R. H. The genetic basis for 3-ADON and 15-ADON trichothecene chemotypes in *Fusarium*. *Fungal Genet. Biol.* **48**, 485–495 (2011).

40. Varga, E. *et al.* New tricks of an old enemy: isolates of *Fusarium graminearum* produce a type A trichothecene mycotoxin. *Environ. Microbiol.* **17**, 2588–2600 (2015).

41. Jansen, C. *et al.* Infection pattern in barley and wheat spikes inoculated with wild-type and trichodiene synthase gene disrupted *Fusarium graminearum*. *Proc. Natl. Acad. Sci. U. S. A.* **102**, 16892–16897 (2005).

42. Garreau De Loubresse, N. *et al.* Structural basis for the inhibition of the eukaryotic ribosome. *Nature* **513**, 517–522 (2014).

43. Foroud, N. A., Shank, R. A., Kiss, D., Eudes, F. & Hazendonk, P. Solvent and water mediated structural variations in deoxynivalenol and their potential implications on the disruption of ribosomal function. *Front. Microbiol.* **7**, 1–15 (2016).

44. Zhang, X.-W. *et al.* In planta stage-specific fungal gene profiling elucidates the molecular strategies of *Fusarium graminearum* growing inside wheat coleoptiles. *Plant Cell* **24**, 5159–5176 (2012).

45. Macheleidt, J. *et al.* Regulation and role of fungal secondary metabolites. *Annu. Rev. Genet.* **50**, 371–392 (2016).

46. Lyu, H.-N., Liu, H.-W., Keller, N. P. & Yin, W.-B. Harnessing diverse transcriptional regulators for natural product discovery in fungi. *Nat. Prod. Rep.* **37**, 1–11 (2019).

47. Hou, R., Jiang, C., Zheng, Q., Wang, C. & Xu, J. R. The AreA transcription factor mediates the regulation of deoxynivalenol (DON) synthesis by ammonium and cyclic adenosine monophosphate (cAMP) signalling in *Fusarium graminearum*. *Mol. Plant Pathol.* **16**, 987–999 (2015).

48. Chang, P. K. The *Aspergillus parasiticus* protein AFLJ interacts with the aflatoxin pathway-specific regulator AFLR. *Mol. Genet. Genomics* **268**, 711–719 (2003).

49. Shwab, E. K. & Keller, N. P. Regulation of secondary metabolite production in filamentous ascomycetes. *Mycol. Res.* **112**, 225–230 (2008).

50. Yu, J. H. & Alkhayyat, F. Upstream regulation of mycotoxin biosynthesis. in *Advances in Applied Microbiology* **86**, 251–278 (Copyright © 2014 Elsevier Inc. All rights reserved., 2014).

51. Brodhagen, M. & Keller, N. P. Signalling pathways connecting mycotoxin production and sporulation. *Mol. Plant Pathol.* **7**, 285–301 (2006).

52. Dilks, T., Halsey, K., De Vos, R. P., Hammond-Kosack, K. E. & Brown, N. A. Non-canonical fungal G-protein coupled receptors promote *Fusarium* head blight on wheat. *PLoS Pathog.* **15**, 1–26 (2019).

53. Yu, H. Y. *et al.* Functional analyses of heterotrimeric G protein Gα and Gβ subunits in *Gibberella zeae*. *Microbiology* **154**, 392–401 (2008).

54. Lee, J., Leslie, J. F. & Bowden, R. L. Expression and function of sex pheromones and receptors in the homothallic ascomycete *Gibberella zeae*. *Eukaryot. Cell* **7**, 1211–1221 (2008).

55. Bayram, Ö. & Braus, G. H. Coordination of secondary metabolism and development in fungi: The velvet family of regulatory proteins. *FEMS Microbiol. Rev.* **36**, 1–24 (2012).

56. Adnan, M. *et al.* Carbon catabolite repression in filamentous fungi. *Int. J. Mol. Sci.* **19**, 1–23 (2018).

57. Jiang, C. *et al.* An expanded subfamily of G-protein-coupled receptor genes in *Fusarium graminearum* required for wheat infection. *Nat. Microbiol.* **4**, 1582–1591 (2019).

58. Turrà, D., Segorbe, D. & Di Pietro, A. Protein kinases in plant-pathogenic fungi:

conserved regulators of infection. *Annu. Rev. Phytopathol.* **52**, 267–288 (2014).

59. Jacinto, E. & Hall, M. N. TOR signalling in bugs, brain and brawn. *Nat. Rev. Mol. Cell Biol.* **4**, 117–126 (2003).

60. González, A. & Hall, M. N. Nutrient sensing and TOR signaling in yeast and mammals . *EMBO J.* **36**, 397–408 (2017).

61. Sutter, B. M., Wu, X., Laxman, S. & Tu, B. P. Methionine inhibits autophagy and promotes growth by inducing the SAM-responsive methylation of PP2A. *Cell* **154**, 403 (2013).

62. Bonfils, G. *et al.* Leucyl-tRNA Synthetase Controls TORC1 via the EGO Complex. *Mol. Cell* **46**, 105–110 (2012).

63. Stracka, D., Jozefczuk, S., Rudroff, F., Sauer, U. & Hall, M. N. Nitrogen source activates TOR (Target of Rapamycin) complex 1 via glutamine and independently of Gtr/Rag proteins. *J. Biol. Chem.* **289**, 25010–25020 (2014).

64. Hughes Hallett, J. E., Luo, X. & Capaldi, A. P. State transitions in the TORC1 signaling pathway and information processing in *Saccharomyces cerevisiae*. *Genetics* **198**, 773–786 (2014).

65. López-Berges, M. S., Rispail, N., Prados-Rosales, R. C. & di Pietro, A. A nitrogen response pathway regulates virulence functions in *Fusarium oxysporum* via the protein kinase TOR and the bZIP protein MeaB. *Plant Cell* **22**, 2459–2475 (2010).

66. Teichert, S., Wottawa, M., Schönig, B. & Tudzynski, B. Role of the *Fusarium fujikuroi* TOR kinase in nitrogen regulation and secondary metabolism. *Eukaryot. Cell* **5**, 1807–1819 (2006).

67. Chen, Y., Kistler, H. C. & Ma, Z. *Fusarium graminearum* trichothecene mycotoxins: biosynthesis, regulation, and management. *Annu. Rev. Phytopathol.* **57**, 1–25 (2019).

68. Yu, F. *et al.* The TOR signaling pathway regulates vegetative development and virulence in *Fusarium graminearum*. *New Phytol.* **203**, 219–232 (2014).

69. Boenisch, M. J. *et al.* Structural reorganization of the fungal endoplasmic reticulum upon induction of mycotoxin biosynthesis. *Sci. Rep.* **7**, 1–13 (2017).

70. Gu, Q. *et al.* Protein kinase FgSch9 serves as a mediator of the target of rapamycin and high osmolarity glycerol pathways and regulates multiple stress responses and secondary metabolism in *Fusarium graminearum*. *Environ. Microbiol.* **17**, 2661–2676 (2015).

71. Divon, H. H., Ziv, C., Davydov, O., Yarden, O. & Fluhr, R. The global nitrogen regulator, FNR1, regulates fungal nutrition-genes and fitness during *Fusarium oxysporum* pathogenesis. *Mol. Plant Pathol.* **7**, 485–497 (2006).

72. Brauer, E. K., Manes, N., Bonner, C. & Subramaniam, R. Two 14-3-3 proteins contribute to nitrogen sensing through the TOR and glutamine synthetase-dependent pathways in *Fusarium graminearum*. *Fungal Genet. Biol.* **134**, 1–9 (2020).

73. Bormann, J., Boenisch, M. J., Brückner, E., Firat, D. & Schäfer, W. The adenylyl cyclase plays a regulatory role in the morphogenetic switch from vegetative to pathogenic lifestyle of *Fusarium graminearum* on wheat. *PLoS One* **9**, 1–13 (2014).

74. Yang, K. *et al.* Adenylate cyclase AcyA regulates development, aflatoxin biosynthesis and fungal virulence in *Aspergillus flavus*. *Front. Cell. Infect. Microbiol.* **6**, 1–14 (2016).

75. Hu, S. *et al.* The cAMP-PKA pathway regulates growth, sexual and asexual differentiation, and pathogenesis in *Fusarium graminearum*. *Mol. Plant-Microbe Interact.* **27**, 557–566 (2014).

76. Li, C. *et al.* The PKR regulatory subunit of protein kinase A (PKA) is involved in the regulation of growth, sexual and asexual development, and pathogenesis in *Fusarium graminearum*. *Mol. Plant Pathol.* **19**, 909–921 (2018).

77. Guo, L. *et al.* Conservation and divergence of the cyclic adenosine monophosphate-protein kinase A (cAMP-PKA) pathway in two plant-pathogenic fungi: *Fusarium graminearum* and *F.verticillioides*. *Mol. Plant Pathol.* **17**, 196–209 (2016).

78. Jiang, C. *et al.* TRI6 and TRI10 play different roles in the regulation of DON production by cAMP signaling in *Fusarium graminearum*. *Environ. Microbiol.* **18**, 3689–3701 (2016).

79. Xu, J. MAP kinases in fungal pathogens. *Fungal Genet. Biol.* **152**, 137–152 (2001).

80. Hou, Z. *et al.* A mitogen-activated protein kinase gene (MGV1) in *Fusarium graminearum* is required for female fertility , heterokaryon formation , and plant infection. *Mol. Plant. Microbe. Interact.* **15**, 1119–1127 (2002).

81. Van Nguyen, T., Schöfer, W. & Bormann, J. The stress-activated protein kinase FgOS-2 is a key regulator in the life cycle of the cereal pathogen *Fusarium graminearum*. *Mol. Plant-Microbe Interact.* **25**, 1142–1156 (2012).

82. Jenczmionka, N. J., Maier, F. J., Lösch, A. P. & Schäfer, W. Mating, conidiation and pathogenicity of *Fusarium graminearum*, the main causal agent of the head-blight disease of wheat, are regulated by the MAP kinase gpmk1. *Curr. Genet.* **43**, 87–95 (2003).

83. Gustin, M. C., Albertyn, J., Alexander, M. & Davenport, K. MAP kinase pathways in the yeast *Saccharomyces cerevisiae*. *Microbiol. Mol. Biol. Rev.* **62**, 1264–1300 (1998).

84. Schüller, C., Brewster, J. L., Alexander, M. R., Gustin, M. C. & Ruis, H. The HOG pathway controls osmotic regulation of transcription via the stress response element (STRE) of the *Saccharomyces cerevisiae CTT1* gene. *EMBO J.* **13**, 4382–4389 (1994).

85. Degols, G., Shiozaki, K. & Russell, P. Activation and regulation of the Spc1 stress-activated protein kinase in *Schizosaccharomyces pombe*. *Mol. Cell. Biol.* **16**, 2870–2877 (1996).

86. Zheng, D. *et al.* The FgHOG1 pathway regulates hyphal growth, stress responses,

and plant infection in *Fusarium graminearum*. *PLoS One* **7**, 1–12 (2012).

87. Wang, C. *et al.* Functional analysis of the kinome of the wheat scab fungus *Fusarium graminearum*. *PLoS Pathog.* **7**, 1–21 (2011).

88. Van Nguyen, T., Kröger, C., Bönnighausen, J., Schäfer, W. & Bormann, J. The ATF/CREB transcription factor Atf1 is essential for full virulence, deoxynivalenol production, and stress tolerance in the cereal pathogen *Fusarium graminearum*. *Mol. Plant-Microbe Interact.* **26**, 1379–1394 (2013).

89. Gu, Q., Chen, Y., Liu, Y., Zhang, C. & Ma, Z. The transmembrane protein FgSho1 regulates fungal development and pathogenicity via the MAPK module Ste50-Ste11-Ste7 in *Fusarium graminearum*. *New Phytol.* **206**, 315–328 (2015).

90. Córcoles-Sáez, I., Ballester-Tomas, L., De La Torre-Ruiz, M. A., Prieto, J. A. & Randez-Gil, F. Low temperature highlights the functional role of the cell wall integrity pathway in the regulation of growth in *Saccharomyces cerevisiae*. *Biochem. J.* **446**, 477–488 (2012).

91. Kim, K.-Y., Truman, A. W., Ceasar, S., Schlenstedt, G. & Levin, D. E. Yeast Mpk1 cell wall integrity mitogen-activated protein kinase regulates nucleocytoplasmic shuttling of the Swi6 transcriptional regulator. *Mol. Biol. Cell* **21**, 1609–1619 (2010).

92. Mao, K., Wang, K., Zhao, M., Xu, T. & Klionsky, D. J. Two MAPK-signaling pathways are required for mitophagy in *Saccharomyces cerevisiae*. *J. Cell Biol.* **193**, 755–767 (2011).

93. Rousseau, A. & Bertolotti, A. An evolutionarily conserved pathway controls proteasome homeostasis. *Nature* **536**, 184–189 (2016).

94. Rampitsch, C., Leung, W., Blackwell, B. & Subramaniam, R. MAP kinase MGV1: a potential shared control point of butenolide and deoxynivalenol biosynthesis in *Fusarium graminearum*. *Plant Breed. Seed Sci.* **64**, 81–88 (2011).

95. Fedotova, A. A., Bonchuk, A. N., Mogila, V. A. & Georgiev, P. G. C2H2 zinc finger proteins : the largest but poorly explored family of higher eukaryotic transcription factors. *Acta Naturae* **9**, 47–58 (2017).

96. Gallego, C., Garí, E., Colomina, N., Herrero, E. & Aldea, M. The Cln3 cyclin is down-regulated by translational repression and degradation during the G1 arrest caused by nitrogen deprivation in budding yeast. *EMBO J.* **16**, 7196–206 (1997).

97. Kim, H. & Woloshuk, C. P. Role of AREA, a regulator of nitrogen metabolism, during colonization of maize kernels and fumonisin biosynthesis in *Fusarium verticillioides*. *Fungal Genet. Biol.* **45**, 947–953 (2008).

98. Kim, H., Son, H. & Lee, Y. W. Effects of light on secondary metabolism and fungal development of *Fusarium graminearum*. *J. Appl. Microbiol.* **116**, 380–389 (2014).

99. Hou, R. & Wang, C. The function of the carbon metabolism regulator FgCreA in *Fusarium graminearum*. *Sci. Agric. Sin.* **51**, 257–267 (2017).

100. Merhej, J., Richard-Forget, F. & Barreau, C. The pH regulatory factor Pac1

regulates *Tri* gene expression and trichothecene production in *Fusarium graminearum*. *Fungal Genet. Biol.* **48**, 275–284 (2011).

101. Ries, L. N. A., Beattie, S. R., Espeso, E. A., Cramer, R. A. & Goldman, G. H. Diverse regulation of the CreA carbon catabolite repressor in *Aspergillus nidulans*. *Genetics* **203**, 335–352 (2016).

102. Jiao, F., Kawakami, A. & Nakajima, T. Effects of different carbon sources on trichothecene production and *Tri* gene expression by *Fusarium graminearum* in liquid culture. *FEMS Microbiol. Lett.* **285**, 212–219 (2008).

103. Janus, D., Hortschansky, P. & Kück, U. Identification of a minimal cre1 promoter sequence promoting glucose-dependent gene expression in the β-lactam producer *Acremonium chrysogenum*. *Curr. Genet.* **53**, 35–48 (2008).

104. Sørensen, J. L. & Giese, H. Influence of carbohydrates on secondary metabolism in *Fusarium avenaceum*. *Toxins (Basel).* **5**, 1655–1663 (2013).

105. Yu, J.-H. & Keller, N. P. Regulation of secondary metabolism in filamentous fungi. *Annu. Rev. Phytopathol.* **43**, 437–458 (2005).

106. Chang, K. P., Yu, J., Bhatnagar, D. & Cleveland, T. E. Characterization of the *Aspergillus parasiticus* major nitrogen regulatory gene, *areA*. *Biochim. Biophys. Acta - Gene Struct. Expr.* **1491**, 263–266 (2000).

107. Schönig, B., Brown, D. W., Oeser, B. & Tudzynski, B. Cross-species hybridization

with *Fusarium verticillioides* microarrays reveals new insights into F*usarium fujikuroi* nitrogen regulation and the role of AreA and NMR. *Eukaryot. Cell* **7**, 1831–1846 (2008).

108. Giese, H., Sondergaard, T. E. & Sørensen, J. L. The AreA transcription factor in *Fusarium graminearum* regulates the use of some nonpreferred nitrogen sources and secondary metabolite production. *Fungal Biol.* **117**, 814–821 (2013).

109. Biswas, K. & Morschhäuser, J. The Mep2p ammonium permease controls nitrogen starvation-induced filamentous growth in *Candida albicans*. *Mol. Microbiol.* **56**, 649–669 (2005).

110. Pfannmüller, A. *et al.* Comparative transcriptome and proteome analysis reveals a global impact of the nitrogen regulators AreA and AreB on secondary metabolism in *Fusarium fujikuroi*. *PLoS One* **12**, 1–27 (2017).

111. Rösler, S. M., Sieber, C. M. K., Humpf, H. U. & Tudzynski, B. Interplay between pathway-specific and global regulation of the fumonisin gene cluster in the rice pathogen *Fusarium fujikuroi*. *Appl. Microbiol. Biotechnol.* **100**, 5869–5882 (2016).

112. Bok, J. W. & Keller, N. P. LaeA, a regulator of secondary metabolism in *Aspergillus* spp. *Eukaryot. Cell* **3**, 527–535 (2004).

113. Bayram, Ö. *et al.* VelB/VeA/LaeA complex coordinates light signal with fungal development and secondary metabolism. *Science (80-.).* **320**, 1504–1506 (2008).

114. Jiang, J., Liu, X., Yin, Y. & Ma, Z. Involvement of a velvet protein FgVeA in the regulation of asexual development, lipid and secondary metabolisms and virulence in *Fusarium graminearum*. *PLoS One* **6**, 1–15 (2011).

115. Wiemann, P. *et al.* FfVel1 and fflae1, components of a velvet-like complex in *Fusarium fujikuroi*, affect differentiation, secondary metabolism and virulence. *Mol. Microbiol.* **77**, 972–994 (2010).

116. Stinnett, S. M., Espeso, E. A., Cobeño, L., Araújo-Bazán, L. & Calvo, A. M. *Aspergillus nidulans* VeA subcellular localization is dependent on the importin α carrier and on light. *Mol. Microbiol.* **63**, 242–255 (2007).

117. Niehaus, E. M. *et al.* Analysis of the global regulator Lae1 uncovers a connection between Lae1 and the histone acetyltransferase HAT1 in *Fusarium fujikuroi*. *Appl. Microbiol. Biotechnol.* **102**, 279–295 (2018).

118. Merhej, J. *et al.* The velvet gene, FgVe1, affects fungal development and positively regulates trichothecene biosynthesis and pathogenicity in *Fusarium graminearum*. *Mol. Plant Pathol.* **13**, 363–374 (2012).

119. Kim, H. K. *et al.* Functional roles of FgLaeA in controlling secondary metabolism, sexual development, and virulence in *Fusarium graminearum*. *PLoS One* **8**, 1–15 (2013).

120. Keller, N. P., Nesbitt, C., Sarr, B., Phillips, T. D. & Burow, G. B. pH regulation of sterigmatocystin and aflatoxin biosynthesis in *Aspergillus* spp. *Phytopathology* **87**,

643–648 (1997).

121. Gardiner, D. M., Osborne, S., Kazan, K. & Manners, J. M. Low pH regulates the production of deoxynivalenol by *Fusarium graminearum*. *Microbiology* **155**, 3149–3156 (2009).

122. Merhej, J., Richard-Forget, F. & Barreau, C. Regulation of trichothecene biosynthesis in *Fusarium*: Recent advances and new insights. *Appl. Microbiol. Biotechnol.* **91**, 519–528 (2011).

123. Peñalva, M. A., Tilburn, J., Bignell, E. & Arst, H. N. Ambient pH gene regulation in fungi: making connections. *Trends Microbiol.* **16**, 291–300 (2008).

124. Hervás-Aguilar, A., Rodríguez, J. M., Tilburn, J., Arst, H. N. & Peñalva, M. A. Evidence for the direct involvement of the proteasome in the proteolytic processing of the *Aspergillus nidulans* zinc finger transcription factor PacC. *J. Biol. Chem.* **282**, 34735–34747 (2007).

125. Flaherty, J. E., Pirttila, A. M., Bluhm, B. H. & Woloshuk, C. P. *PAC1*, a pH-regulatory gene from *Fusarium verticillioides*. *Appl. Environ. Microbiol.* **69**, 5222–5227 (2003).

126. Wiemann, P. *et al.* Biosynthesis of the red pigment bikaverin in *Fusarium fujikuroi*: genes, their function and regulation. *Mol. Microbiol.* **72**, 931–946 (2009).

127. Caracuel, Z. *et al.* The pH signalling transcription factor PacC controls virulence in

the plant pathogen *Fusarium oxysporum*. *Mol. Microbiol.* **48**, 765–779 (2003).

128. Merhej, J., Boutigny, A. L., Pinson-Gadais, L., Richard-Forget, F. & Barreau, C. Acidic pH as a determinant of TRI gene expression and trichothecene B biosynthesis in *Fusarium graminearum*. *Food Addit. Contam. - Part A Chem. Anal. Control. Expo. Risk Assess.* **27**, 710–717 (2010).

129. Son, H. *et al.* A phenome-based functional analysis of transcription factors in the cereal head blight fungus, *Fusarium graminearum*. *PLoS Pathog.* **7**, 1–10 (2011).

130. El-Gebli, S. *et al.* The Pfam protein families database in 2019. *Nucleic Acids Res.* **8**, D427–D432 (2019).

131. Pfannenstiel, B. T. & Keller, N. P. On top of biosynthetic gene clusters: how epigenetic machinery influences secondary metabolism in fungi. *Biotechnol Adv* **37**, 1–35 (2019).

132. Hallen-Adams, H. E., Wenner, N., Kuldau, G. A. & Trail, F. Deoxynivalenol biosynthesis-related gene expression during wheat kernel colonization by *Fusarium graminearum*. *Phytopathology* **101**, 1091–1096 (2011).

133. Audenaert, K., Vanheule, A., Höfte, M. & Haesaert, G. Deoxynivalenol: A major player in the multifaceted response of *Fusarium* to its environment. *Toxins (Basel).* **6**, 1–19 (2013).

134. Tilburn, J. *et al.* The *Aspergillus* PacC zinc finger transcription factor mediates

regulation of both acid- and alkaline-expressed genes by ambient pH. *EMBO J.* **14**, 779–790 (1995).

135. Dowzer, C. E. A. & Kelly, J. M. Analysis of the creA gene, a regulator of carbon catabolite repression in *Aspergillus nidulans*. *Mol. Cell. Biol.* **11**, 5701–5709 (1991).

136. Conlon, H. *et al.* The *Aspergillus nidulans* GATA transcription factor gene *areB* encodes at least three proteins and features three classes of mutation. *Mol. Microbiol.* **40**, 361–375 (2001).

137. Mihlan, M., Homann, V., Liu, T. W. D. & Tudzynski, B. AREA directly mediates nitrogen regulation of gibberellin biosynthesis in *Gibberella fujikuroi*, but its activity is not affected by NMR. *Mol. Microbiol.* **47**, 975–991 (2003).

138. Lee, J. *et al.* FgVelB globally regulates sexual reproduction, mycotoxin production and pathogenicity in the cereal pathogen *Fusarium graminearum*. *Microbiol. (United Kingdom)* **158**, 1723–1733 (2012).

139. Nasmith, C. G. *et al.* Tri6 is a global transcription regulator in the phytopathogen *Fusarium graminearum*. *PLoS Pathog.* **7**, 1–12 (2011).

140. Subramaniam, R. *et al.* Leucine metabolism regulates *TRI6* expression and affects deoxynivalenol production and virulence in *Fusarium graminearum*. *Mol. Microbiol.* **98**, 760–769 (2015).

141. Gardiner, D. M., Kazan, K. & Manners, J. M. Novel genes of *Fusarium graminearum*

that negatively regulate deoxynivalenol production and virulence. *Mol. Plant. Microbe. Interact.* **22**, 1588–1600 (2009).

142. Priebe, S., Kreisel, C., Horn, F., Guthke, R. & Linde, J. FungiFun2: a comprehensive online resource for systematic analysis of gene lists from fungal species. *Bioinformatics* **31**, 445–446 (2015).

143. Honjo, M. *et al.* A novel *Bacillus subtilis* gene involved in negative control of sporulation and degradative-enzyme production. *J. Bacteriol.* **172**, 1783–1790 (1990).

144. Walkowiak, S. & Subramaniam, R. A nitrogen-responsive gene affects virulence in *Fusarium graminearum*. *Can. J. Plant Pathol.* **36**, 224–234 (2014).

145. Gacek-Matthews, A. *et al.* KdmB, a Jumonji histone H3 demethylase, regulates genome-wide H3K4 trimethylation and is required for normal induction of secondary metabolism in *Aspergillus nidulans*. *PLoS Genet.* **12**, 1–29 (2016).

146. Shelest, E. Transcription factors in fungi. *FEMS Microbiol. Lett.* **286**, 145–151 (2008).

147. Mogg, C. *et al.* Genomic identification of the TOR signaling pathway as a target of the plant alkaloid antofine in the phytopathogen *Fusarium graminearum*. *MBio* **10**, 1–10 (2019).

148. Chiang, Y.-M., Lee, K.-H., Sanchez, J. F., Keller, N. P. & Wang, C. C. C. Unlocking fungal cryptic natural products. *Nat. Prod. Commun.* **4**, 1505–1510 (2009).

149. Proctor, R. H. *et al.* Evolution of structural diversity of trichothecenes, a family of toxins produced by plant pathogenic and entomopathogenic fungi. *PLoS Pathog.* **14**, 1–38 (2018).

150. Gardiner, S. A. *et al.* Transcriptome analysis of the barley-deoxynivalenol interaction: evidence for a role of glutathione in deoxynivalenol detoxification. *Mol. Plant-Microbe Interact.* **23**, 962–976 (2010).

151. Sevastos, A., Labrou, N. E., Flouri, F. & Malandrakis, A. Glutathione transferase-mediated benzimidazole-resistance in *Fusarium graminearum*. *Pestic. Biochem. Physiol.* **141**, 23–28 (2017).

152. Stanic, A. *et al.* Preparation and characterization of cysteine adducts of deoxynivalenol. *J. Agric. Food Chem.* **64**, 4777–4785 (2016).

153. Kluger, B. *et al.* Biotransformation of the mycotoxin deoxynivalenol in *Fusarium* resistant and susceptible near isogenic wheat lines. *PLoS One* **10**, (2015).

154. Uhlig, S. *et al.* Glutathione-conjugates of deoxynivalenol in naturally contaminated grain are primarily linked via the epoxide group. *Toxins (Basel).* **8**, 1–12 (2016).

155. Westphal, K. R. *et al.* Fusaoctaxin A, an example of a two-step mechanism for non-ribosomal peptide assembly and maturation in fungi. *Toxins (Basel).* **11**, 1–12 (2019).

156. Peplow, A. W., Tag, A. G., Garifullina, G. F. & Beremand, M. N. Identification of new genes positively regulated by Tri10 and a regulatory network for trichothecene mycotoxin production. *Appl. Environ. Microbiol.* **69**, 2731–2736 (2003).

157. Chang, K. P., Yu, J., Bhatnagar, D. & Cleveland, T. E. Repressor-AFLR interaction modulates aflatoxin biosynthesis in *Aspergillus parasiticus*. *Mycopathologia* **147**, 105–112 (1999).

158. Amoutzias, G. D., Robertson, D. L., Oliver, S. G. & Bornberg-Bauer, E. Convergent evolution of gene networks by single-gene duplications in higher eukaryotes. *EMBO Rep.* **5**, 274–279 (2004).

159. Cappellini, R. A. & Peterson, J. L. Macroconidium formation in submerged cultures by a non-sporulating strain of *Gibberella zeae*. *Mycologia* **57**, 962–966 (1965).

160. Frandsen, R. J. N., Andersson, J. A., Kristensen, M. B. & Giese, H. Efficient four fragment cloning for the construction of vectors for targeted gene replacement in filamentous fungi. *BMC Mol. Biol.* **9**, 1–11 (2008).

161. Ching, T., Huang, S. & Garmire, L. X. Power analysis and sample size estimation for RNA-Seq differential expression. *RNA* **20**, 1684–1696 (2014).

162. Michael W. Pfaffl. A new mathematical model for relative quantification in real-time RT-PCR. *Nucleic Acids Res.* **29**, 1–6 (2001).

163. Overy, D. *et al.* Does osmotic stress affect natural product expression in fungi? *Mar. Drugs* **15**, 1–19 (2017).

164. Pluskal, T., Castillo, S., Villar-Briones, A. & Orešič, M. MZmine 2: Modular framework for processing, visualizing, and analyzing mass spectrometry-based molecular profile data. *BMC Bioinformatics* **11**, 1–11 (2010).

165. Gaude, E. *et al. muma*, an R package for metabolomics univariate and multivariate statistical analysis. *Curr. Metabolomics* **1**, 180–189 (2013).

166. Xiao, W. *Yeast Protocols*. **313**, (Humana Press, 2006).

167. Zhang, T., Xu, Q., Chen, F. R., Han, Q. De & Zhang, Y. Y. Yeast two-hybrid screening for proteins that interact with α1-adrenergic receptors. *Acta Pharmacol. Sin.* **25**, 1471–1478 (2004).

168. Ochiai, N. *et al.* Involvement of the osmosensor histidine kinase and osmotic stress-activated protein kinases in the regulation of secondary metabolism in *Fusarium graminearum*. *Biochem. Biophys. Res. Commun.* **363**, 639–644 (2007).

169. Oide, S. *et al.* Histidine kinase two-component response regulator proteins regulate reproductive development, virulence, and stress responses of the fungal cereal pathogens *Cochliobolus heterostrophus* and *Gibberella zeae*. *Eukaryot. Cell* **9**, 1867–1880 (2010).

170. Yun, Y. *et al.* The MAPKK FgMkk1 of *Fusarium graminearum* regulates vegetative

differentiation, multiple stress response, and virulence via the cell wall integrity and high-osmolarity glycerol signaling pathways. *Environ. Microbiol.* **16**, 2023–2037 (2014).

171. Flández, M., Cosano, I. C., Nombela, C., Martín, H. & Molina, M. Reciprocal regulation between Slt2 MAPK and isoforms of Msg5 dual-specificity protein phosphatase modulates the yeast cell integrity pathway. *J. Biol. Chem.* **279**, 11027–11034 (2004).

172. Jiang, J. *et al.* A type 2C protein phosphatase FgPtc3 is involved in cell wall integrity, lipid metabolism, and virulence in *Fusarium graminearum*. *PLoS One* **6**, 1–14 (2011).

173. Kanehisa, M., Goto, S., Kawashima, S. & Nakaya, A. The KEGG databases at GenomeNet. *Nucleic Acids Res.* **30**, 42–6 (2002).

174. Verna, J., Lodder, A., Lee, K., Vagts, A. & Ballester, R. A family of genes required for maintenance of cell wall integrity and for the stress response in *Saccharomyces cerevisiae*. *Proc. Natl. Acad. Sci. U. S. A.* **94**, 13804–13809 (1997).

175. Alonso-Monge, R. *et al.* Hyperosmotic stress response and regulation of cell wall integrity in *Saccharomyces cerevisiae* share common functional aspects. *Mol. Microbiol.* **41**, 717–730 (2001).

176. Sia, R. A. L., Herald, H. A. & Lew, D. J. Cdc28 tyrosine phosphorylation and the morphogenesis checkpoint in budding yeast. *Mol. Biol. Cell* **7**, 1657–1666 (1996).

177. Chen, R. E. & Thorner, J. Function and regulation in MAPK signaling pathways: lessons learned from the yeast *Saccharomyces cerevisiae*. *Biochim. Biophys. Acta - Mol. Cell Res.* **1773**, 1311–1340 (2007).

178. Lee, Y., Son, H., Shin, J. Y., Choi, G. J. & Lee, Y. W. Genome-wide functional characterization of putative peroxidases in the head blight fungus *Fusarium graminearum*. *Mol. Plant Pathol.* **19**, 715–730 (2018).

179. Lee, Y. *et al.* ELP3 is involved in sexual and asexual development, virulence, and the oxidative stress response in *Fusarium graminearum*. *Mol. Plant-Microbe Interact.* **27**, 1344–1355 (2014).

180. Gu, Q. *et al.* Bacillomycin D produced by *Bacillus amyloliquefaciens* is involved in the antagonistic interaction with the plant-pathogenic fungus *Fusarium graminearum*. *Appl. Environ. Microbiol.* **83**, 1075–1092 (2017).

181. Fox, E. M. & Howlett, B. J. Secondary metabolism: regulation and role in fungal biology. *Curr. Opin. Microbiol.* **11**, 481–487 (2008).

182. Reimer, D. & Bode, H. B. A natural prodrug activation mechanism in the biosynthesis of nonribosomal peptides. *Nat. Prod. Rep.* **31**, 154–159 (2014).

183. Matia-Gonzalez, A. M. & Rodriguez-Gabriel, M. A. Slt2 MAPK pathway is essential for cell integrity in the presence of arsenate. *Yeast* **28**, 9–17 (2011).

184. Eranthodi, A. *et al.* Enniatin production influences *Fusarium avenaceum* virulence

on potato tubers, but not on durum wheat or peas. *Pathogens* **9**, 1–20 (2020).

185. Bode, H. B., Bethe, B., Höfs, R. & Zeeck, A. Big effects from small changes: possible ways to explore nature's chemical diversity. *ChemBioChem* **3**, 619–627 (2002).

186. Losada, L., Ajayi, O., Frisvad, J. C., Yu, J. & Nierman, W. C. Effect of competition on the production and activity of secondary metabolites in *Aspergillus* species. *Med. Mycol.* **47**, 88–96 (2009).

187. Arora, D. *et al.* Expanding the chemical diversity through microorganisms co-culture: current status and outlook. *Biotechnol. Adv.* **40**, 1–14 (2020).

188. Zhao, X. M., Zhang, X. W., Tang, W. H. & Chen, L. FPPI: *Fusarium graminearum* protein-protein interaction database. *J. Proteome Res.* **8**, 4714–4721 (2009).

189. Mirmiran, A., Desveaux, D. & Subramaniam, R. Building a protein-interaction network to study *Fusarium graminearum* pathogenesis. *Can. J. Plant Pathol.* **40**, 172–178 (2018).

190. Liu, X., Tang, W. H., Zhao, X. M. & Chen, L. A network approach to predict pathogenic genes for *Fusarium graminearum*. *PLoS One* **5**, 1–12 (2010).

Appendix A: Supplementary figures.

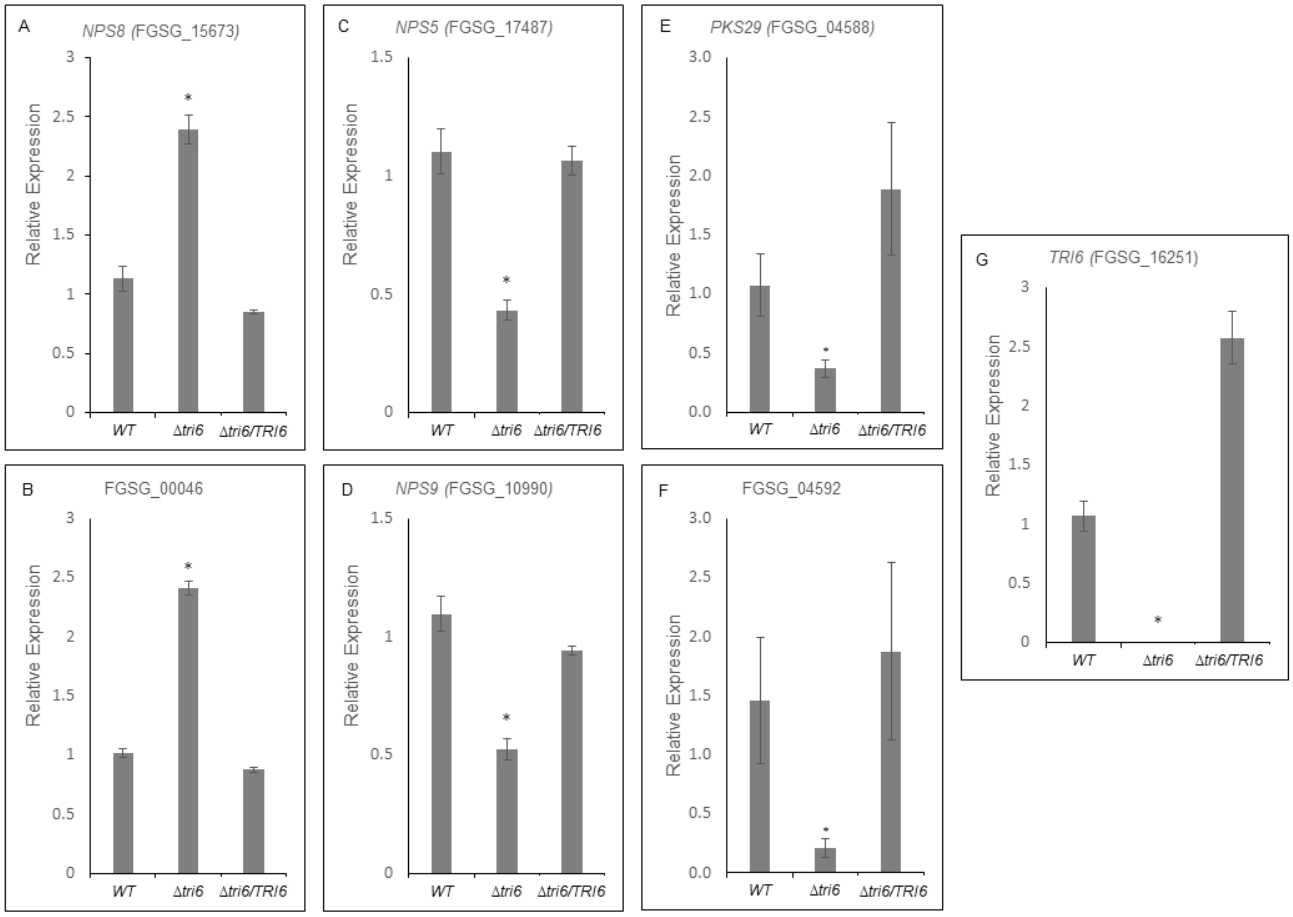

Fig. S2.1. *TRI6* affects expression of SMC genes. The wildtype (*WT*), the Δ*tri6* and the Δ*tri6/TRI6* strains were grown in NPN conditions for 24 hours and total RNA was isolated and RT-qPCR was performed with seven genes that are differentially expressed in the RNA-seq analysis. All genes except FGSG_00046 and *NPS8* are positively regulated by TRI6. The RT-qPCR reactions were performed in technical triplicates using Applied Biosystems PowerUp SYBR Green reaction mix and QuantStudio Real-Time PCR system. Relative expression was calculated using Pfaffl method with *EF1a (*FGSG_08811*)* and *β-tubulin (*FGSG_09530*)* as reference genes. Bars represent a mean of three biological replicates with error bars representing standard deviation. Significance was determined by Student's *t*-test at $p \leq 0.05$.

Fig. S2.2. (pgs. 142-143) Kinetics of secondary metabolite production in *F. graminearum* wildtype and Δ*tri6* strains grown in PN conditions over the course of 9 days. Accumulation of 15-ADON (**A**), and related analogs (**B-D**); gramillins A and B (**E,F**); fusaoctaxin A and related analogs (**G-K**, following page). Box plots are representative of four biological replicates. Signal intensity was measured in counts per second (cps) and normalized to total ion current.

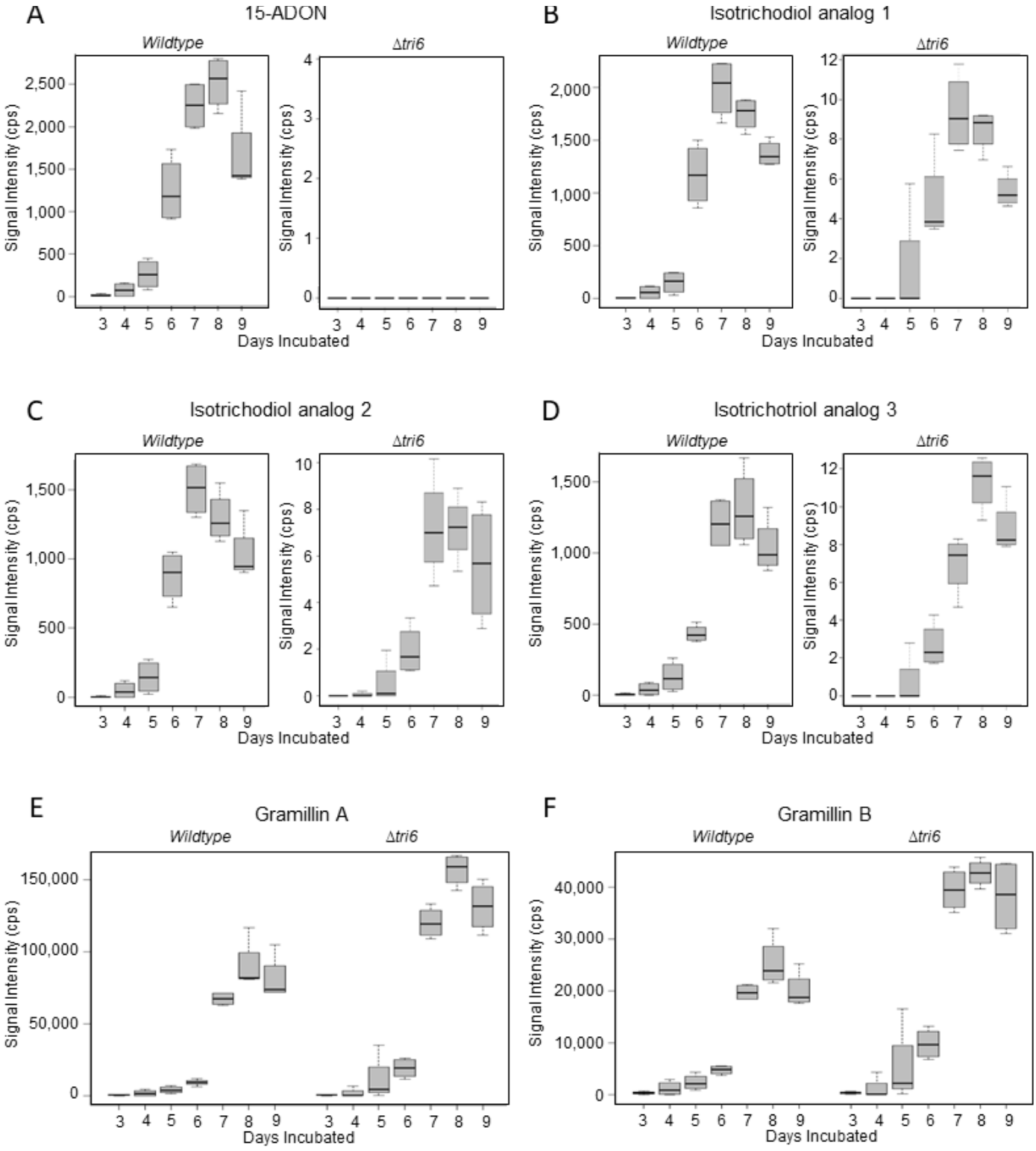

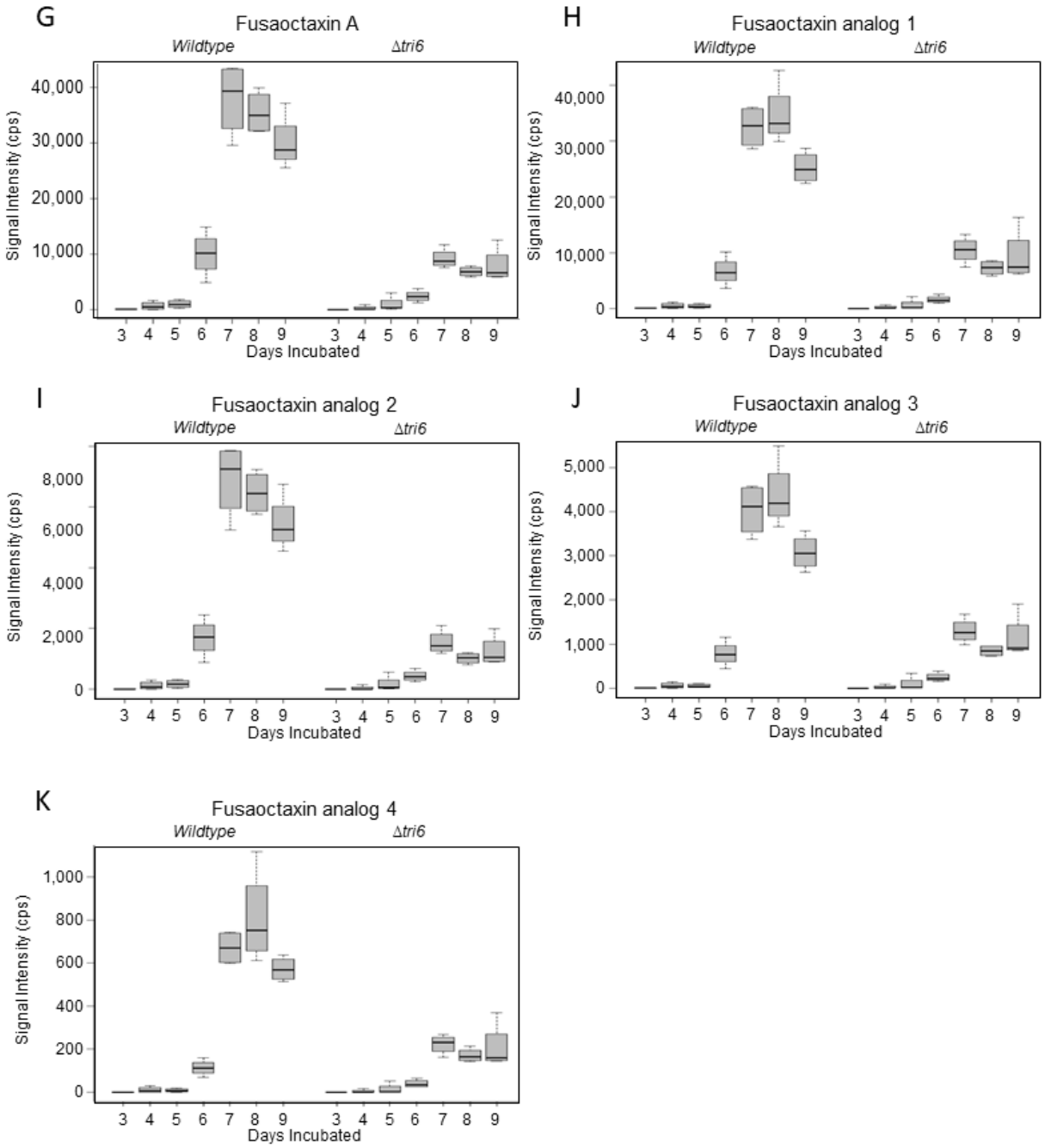
G
Fusaoctaxin A
Wildtype
Δtri6
Signal Intensity (cps)
40,000
30,000
20,000
10,000
0
3 4 5 6 7 8 9 3 4 5 6 7 8 9
Days Incubated
H
Fusaoctaxin analog 1
Wildtype
Δtri6
Signal Intensity (cps)
40,000
30,000
20,000
10,000
0
3 4 5 6 7 8 9 3 4 5 6 7 8 9
Days Incubated
I
Fusaoctaxin analog 2
Wildtype
Δtri6
Signal Intensity (cps)
8,000
6,000
4,000
2,000
0
3 4 5 6 7 8 9 3 4 5 6 7 8 9
Days Incubated
J
Fusaoctaxin analog 3
Wildtype
Δtri6
Signal Intensity (cps)
5,000
4,000
3,000
2,000
1,000
0
3 4 5 6 7 8 9 3 4 5 6 7 8 9
Days Incubated
K
Fusaoctaxin analog 4
Wildtype
Δtri6
Signal Intensity (cps)
1,000
800
600
400
200
0
3 4 5 6 7 8 9 3 4 5 6 7 8 9
Days Incubated

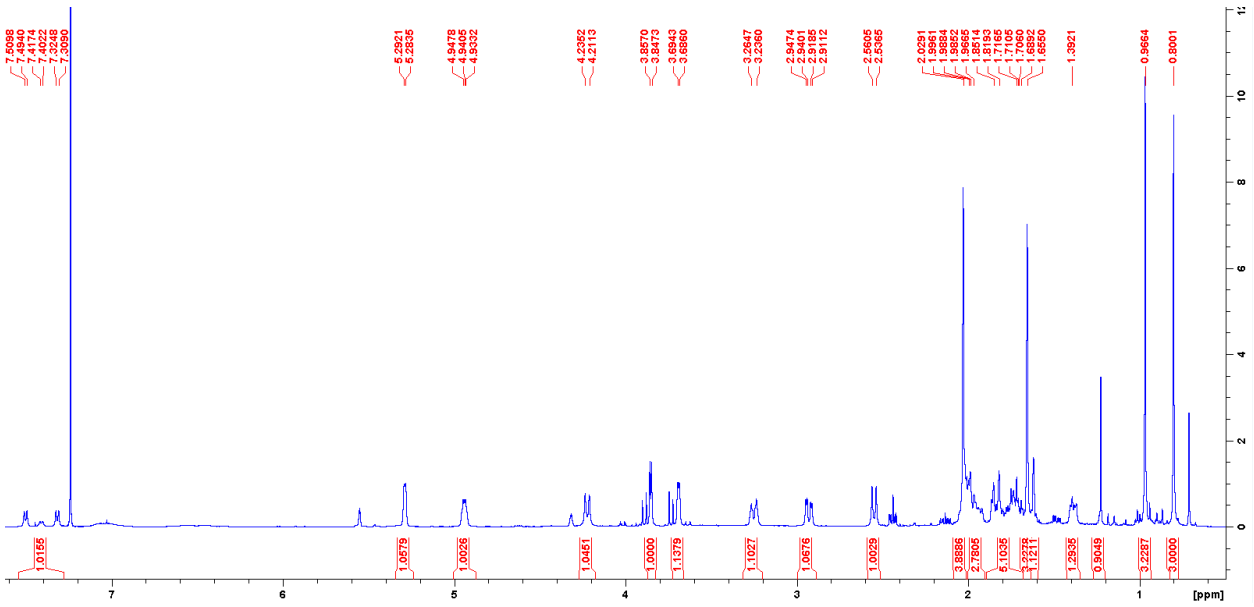

Fig. S2.3. 500 MHz ^{1}H spectrum of 12, 13-N-acetylcystidyl -isotrichodiol (**1**) in $CDCl_3$.

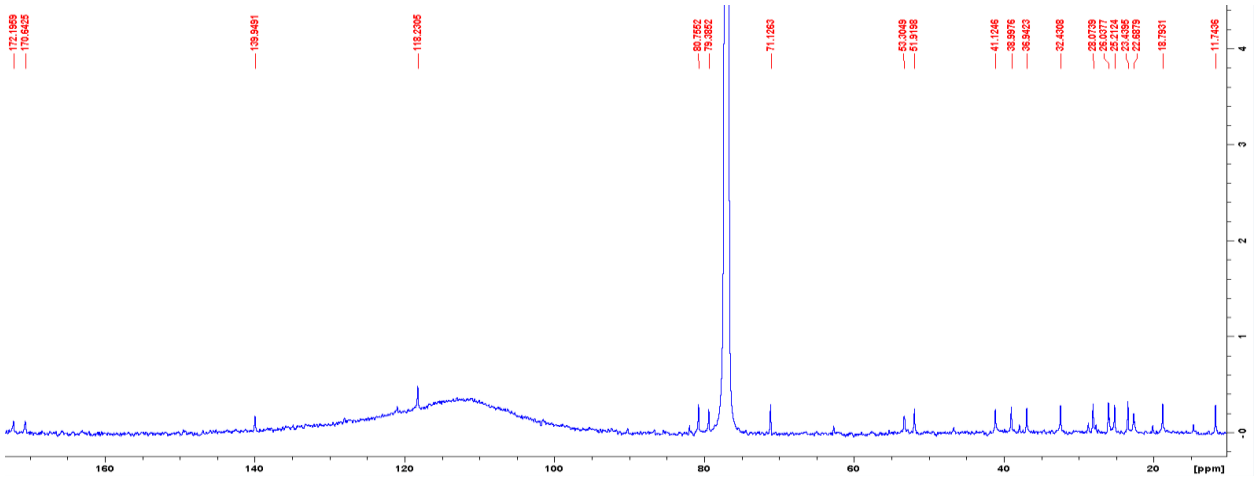

Fig. S2.4. 125 MHz ^{13}C spectrum of 12, 13-N-acetylcystidyl-isotrichodiol (**1**) in $CDCl_3$.

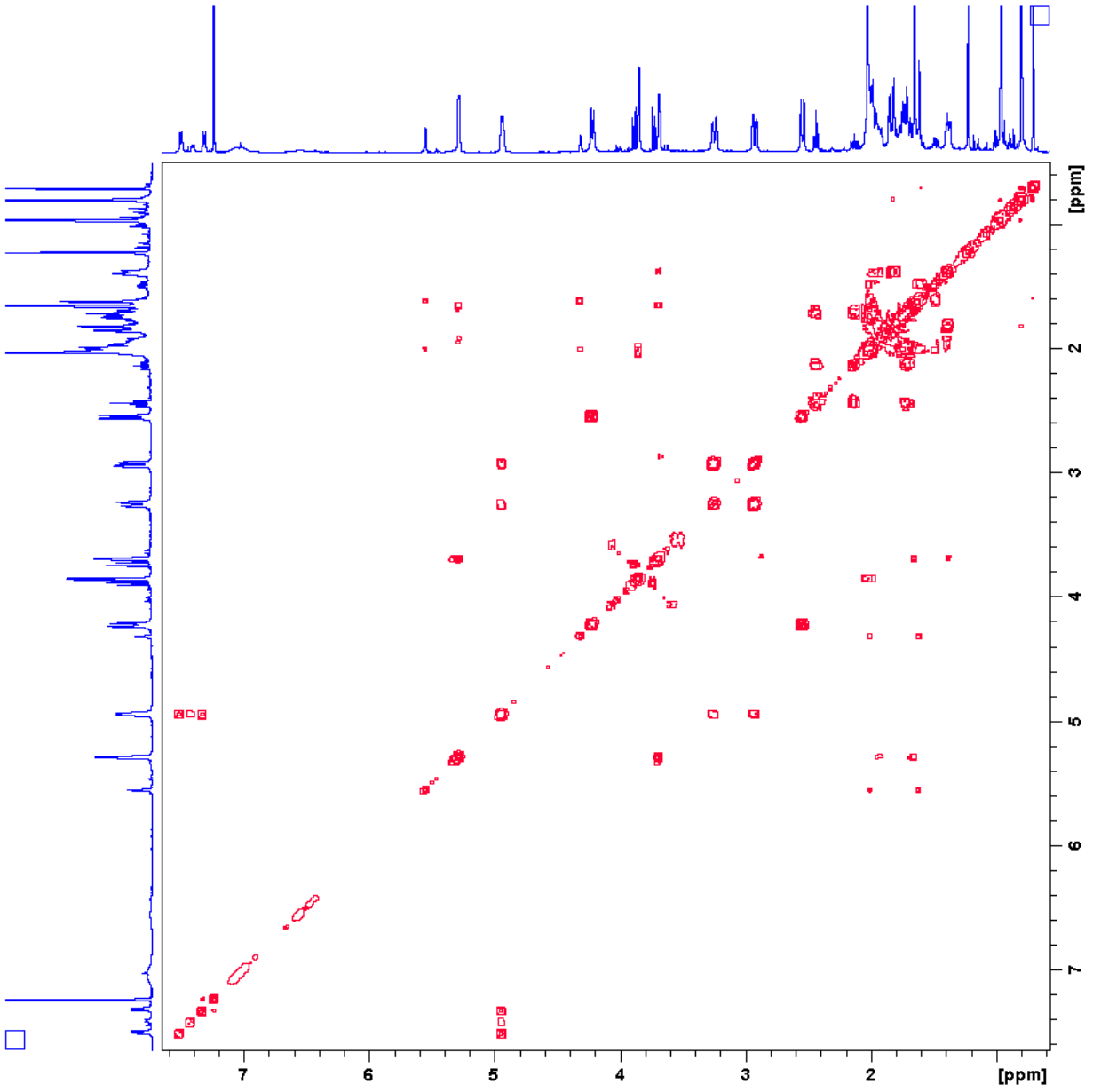

Fig. S2.5. 500 MHz COSY spectrum of 12, 13-N-acetylcystidyl-isotrichodiol (**1**) in $CDCl_3$.

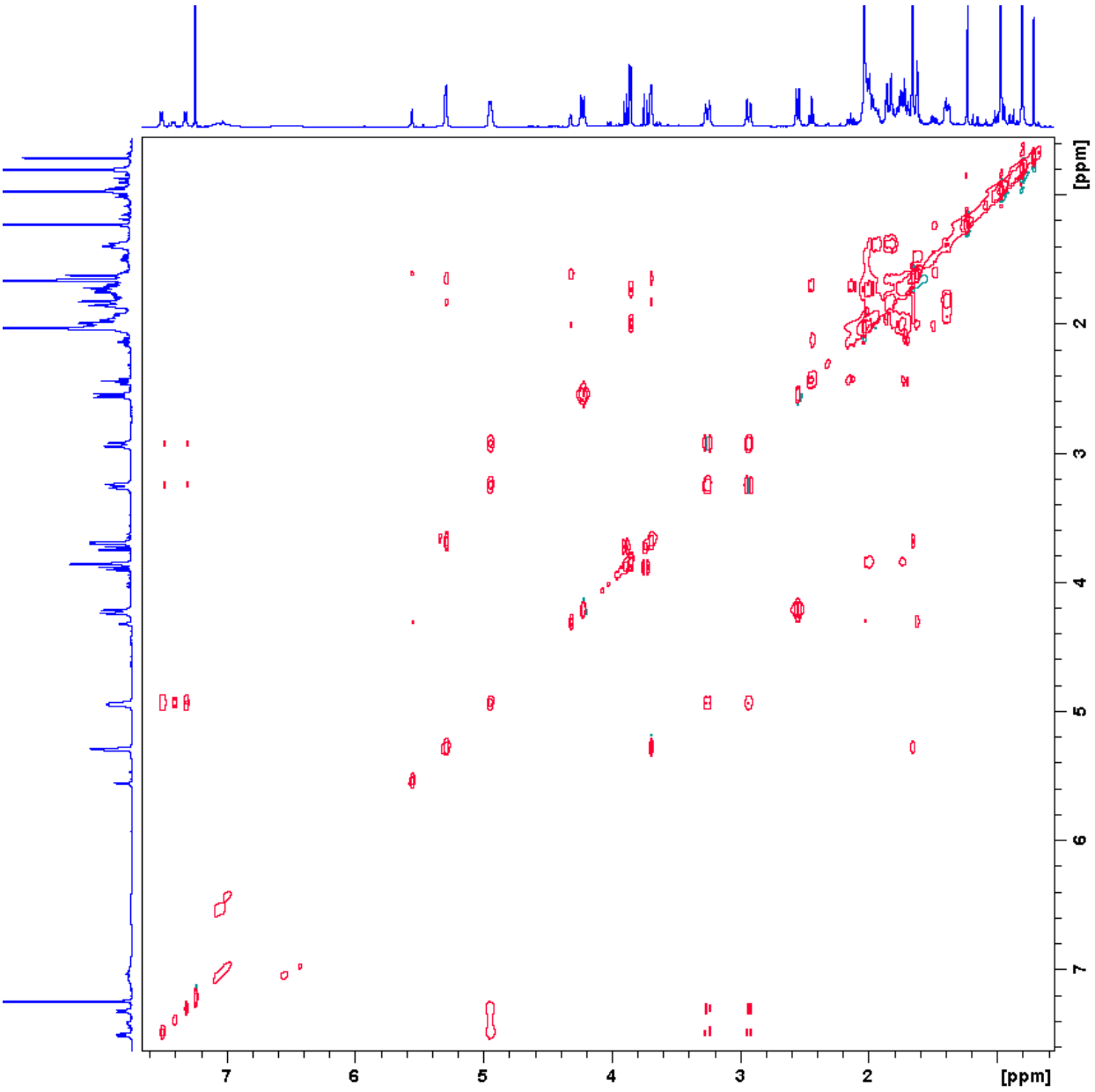

Fig. S2.6. TOCSY spectrum of 12, 13-N-acetylcystidyl-isotrichodiol (**1**) in $CDCl_3$.

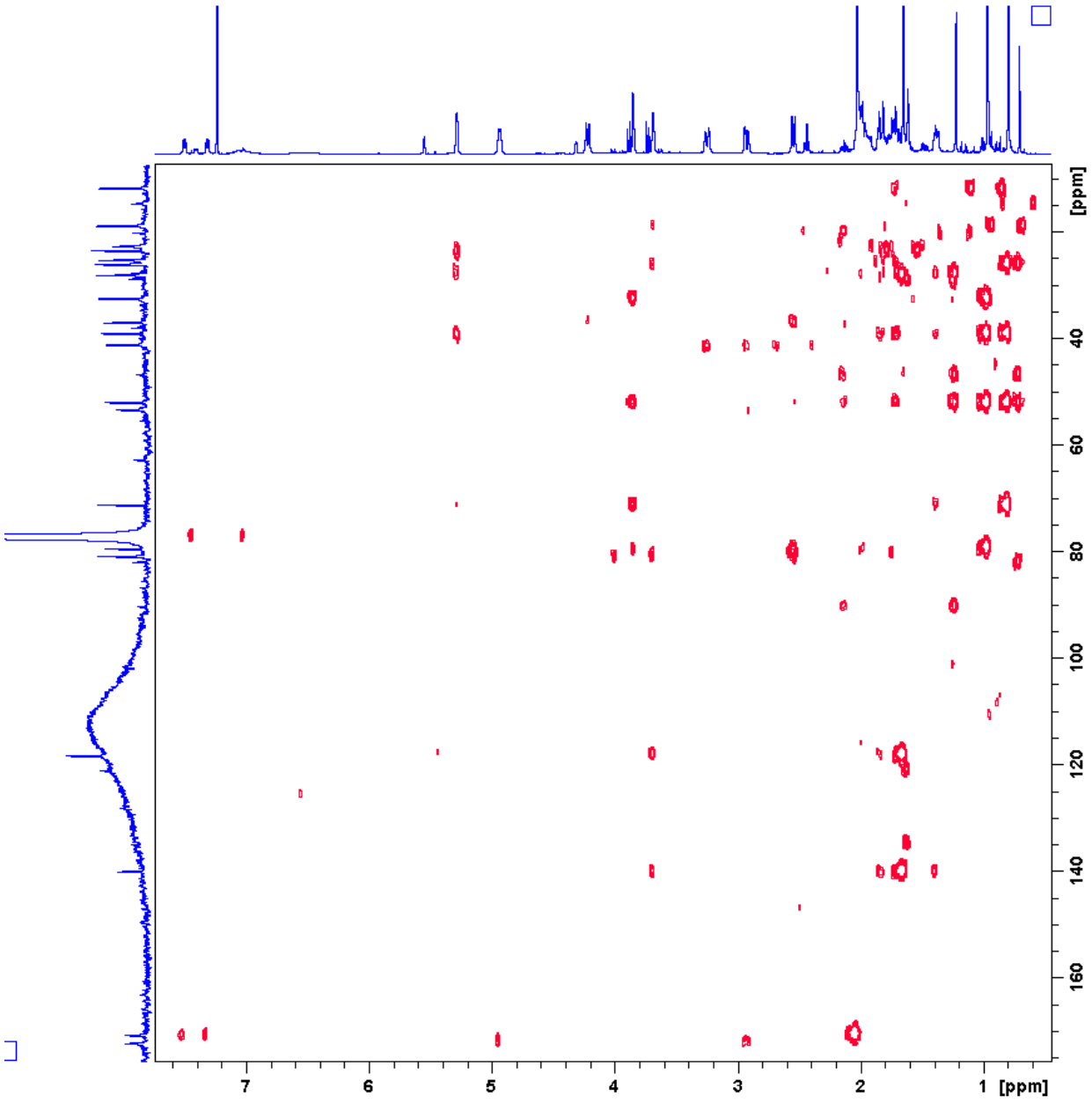

Fig. S2.7. HMBC spectrum of 12, 13-N-acetylcystidyl-isotrichodiol (**1**) in $CDCl_3$.

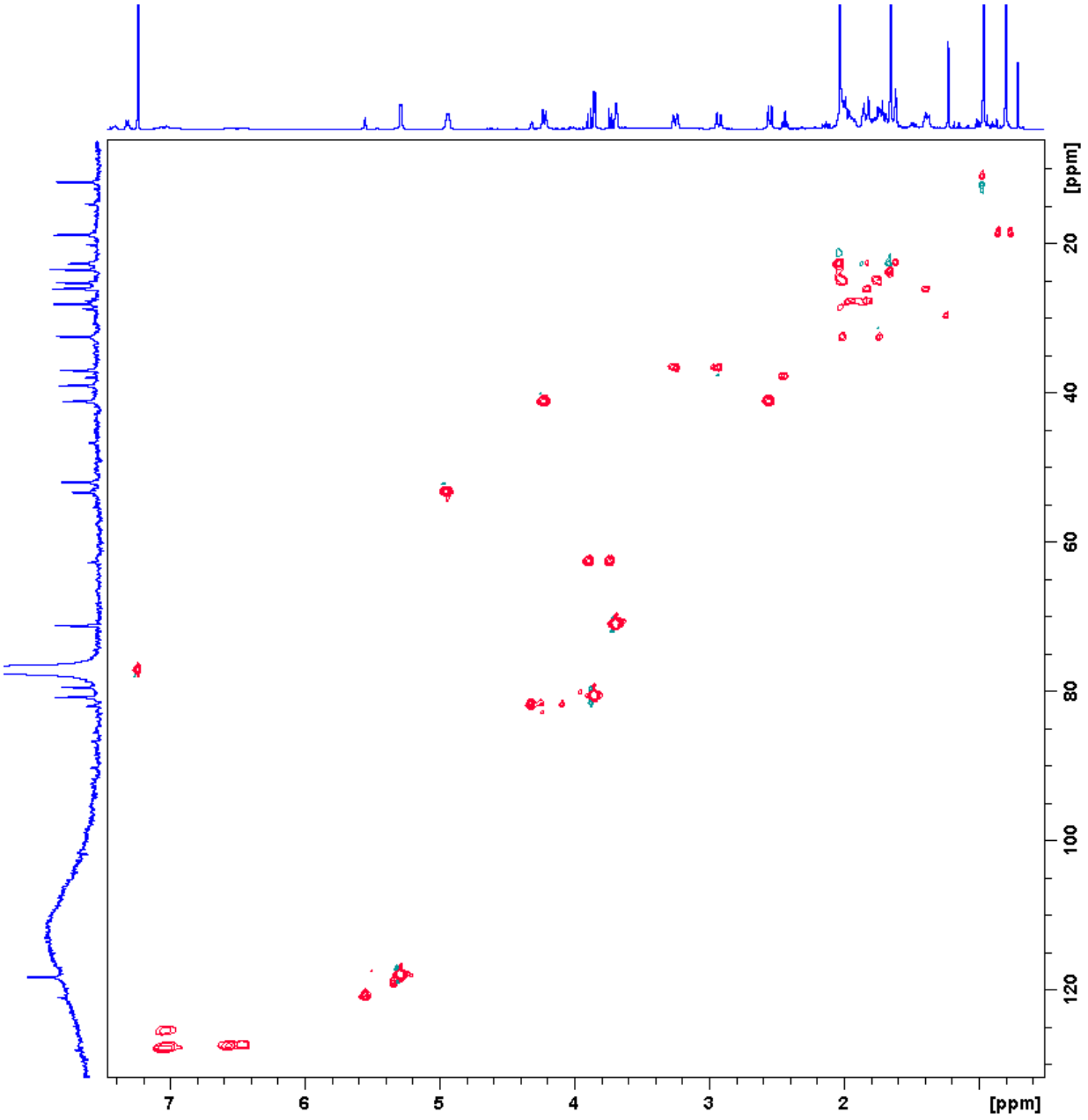

Fig. S2.8. ^{1}H – ^{13}C HSQC spectrum of 12, 13-N-acetylcystidyl-isotrichodiol (**1**) in $CDCl_3$.

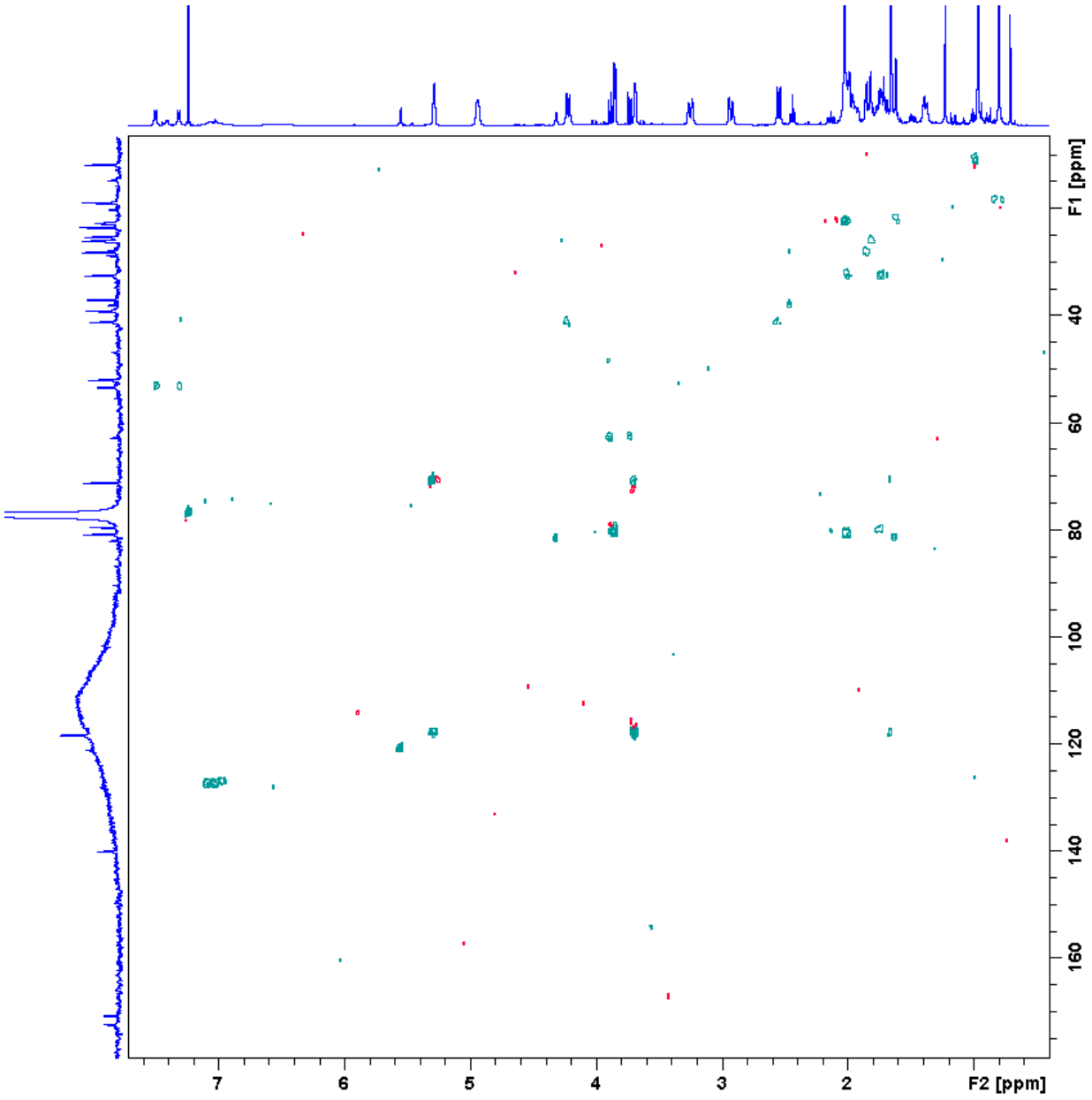

Fig. S2.9. ^{1}H – ^{13}C HSQC – TOCSY spectrum of 12, 13-N-acetylcystidyl-isotrichodiol (**1**) in $CDCl_3$.

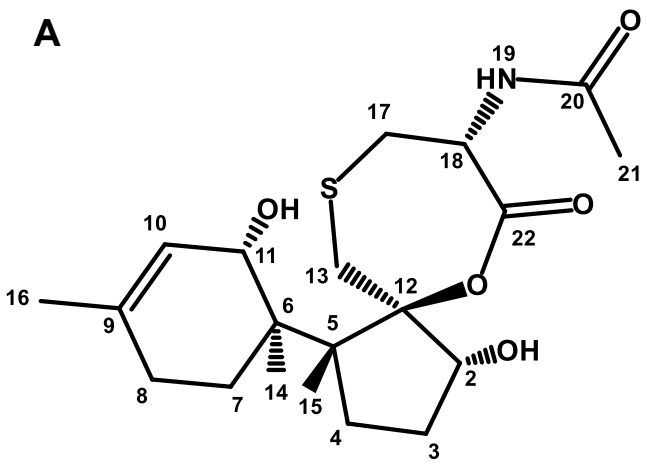

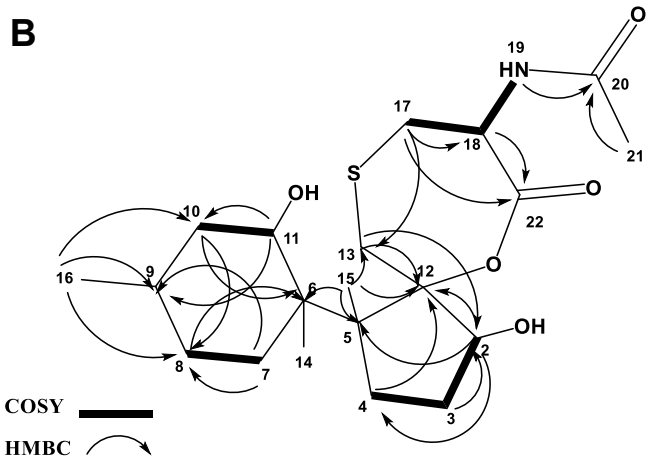

C

Position	δ_C, Type	δ_H, (J, Hz)	COSY	HMBC
2	80.7, CH	3.85, d (4.8)	H3b	C4, C5, C11, C12
3	25.2, CH2	1.75, m	H4b	C2
		2.02, m	H2, H4a	
4	32.4, CH2	1.73, m	H3b	C5, C6
		2.01, m	H4a	C12
5	51.9, C			
6	38.9, C			
7	26.06, CH2	1.38, m	H7b, H8a, H8b	C6, C8, C9, C11
		1.82, m	H7a, H8a, H8b	C9
8	28.07, CH2	1.83, m	H7a, H7b, H8b	C6
		1.97, m	H7a, H7b, H8a	
9	140.2, C			
10	118.2, CH	5.29, d (4.3)	H16, H11	C6, C8, C16
11	71.1, CH	3.69, d (4.1)	H7, H10, H16	C2, C7, C9, C10, C7
12	79.3, CO			
13	41.2, CH2	4.23, d (12.0)	H13b	C17
		2.55, d (12.0)	H13a	C2, C12, C17
14	18.8, CH3	0.80, s		C5, C6, C7, C11
15	11.7, CH3	0.97, s		C4, C5, C6, C12
16	22.6, CH3	1.65, s	C10	C8, C9, C10
17	37, CH2	2.93, dd (3.7, 14.5)	H17b, H18	C13, C18, C22
		3.25, dt (3.8, 14.4)	H17a, H18	C13
18	53.3, CH	4.94, m	H17a, H17b, H19	C22
19	NH	7.41, d (7.9)	H18	C20
20	170.9, CO			
21	23.5, CH3	2.03, s		C20
22	172.6, CO			

Fig. S2.10. 2D structure of 12, 13-N-acetylcystidyl-isotrichodiol (1) (**A**). Selected COSY and HMBC correlations used to elucidate it (**B**), and the corresponding ^{1}H (500 MHz) and ^{13}C (125 MHz) NMR data (**C**).

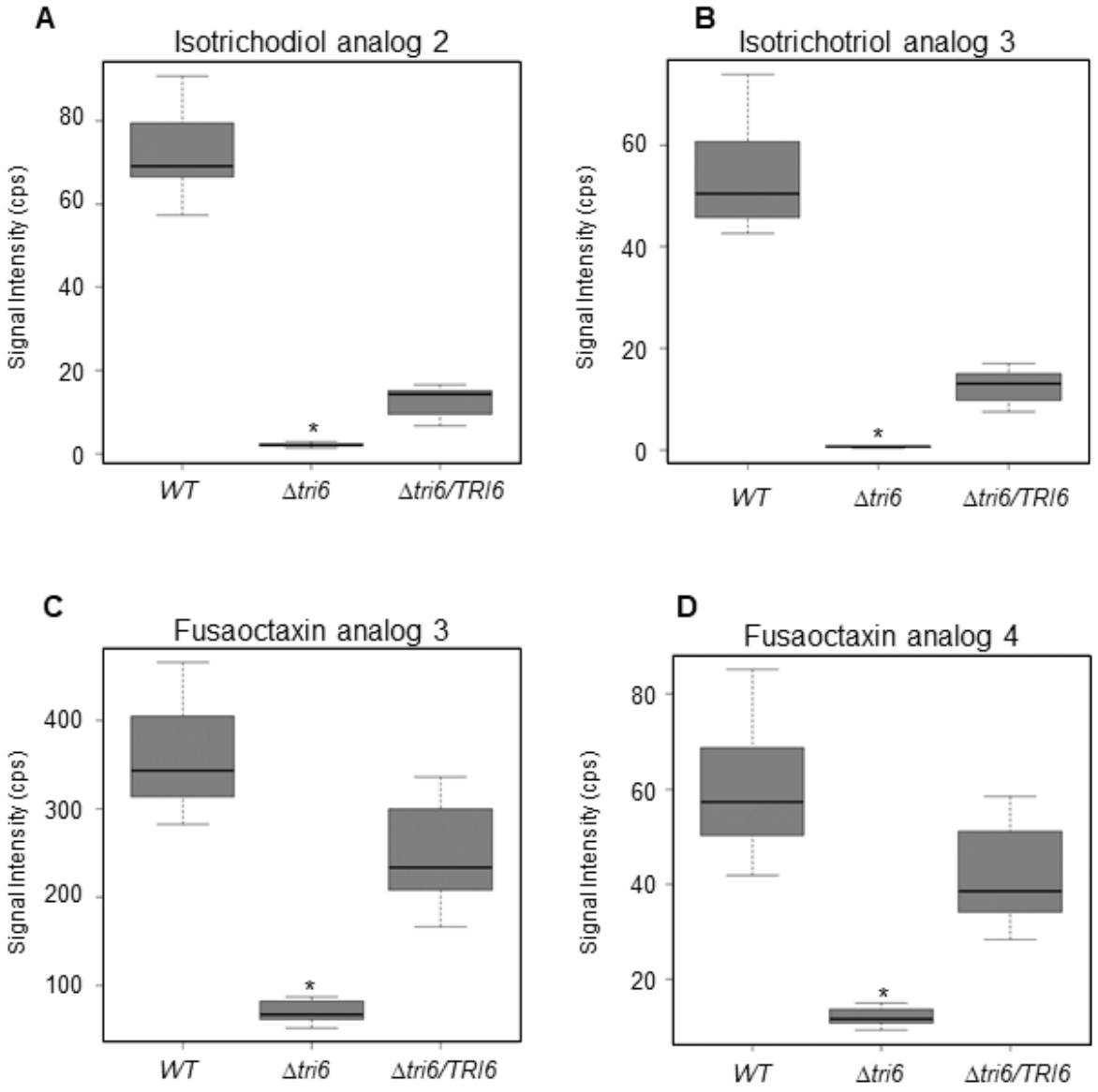

Fig. S2.11. *TRI6* regulates the production of isotrichodiol and fusaoctaxin analogs produced by *F. graminearum.* Wildtype, Δ*tri6,* and Δ*tri6/TRI6* strains were grown in the PN environment for 8 days. Quantities of uncharacterized metabolites produced from trichothecene (**A,B**) and fusaoctaxin A (**C,D**) SM gene clusters were measured. The amounts synthesized in the Δ*tri6* strain were significantly less than in either the wildtype or the Δ*tri6/TRI6* strains ($p \leq 0.05$). Box plots are representative of four biological and three technical replicates. Signal intensity was measured in counts per second (cps) and normalized to total ion current.

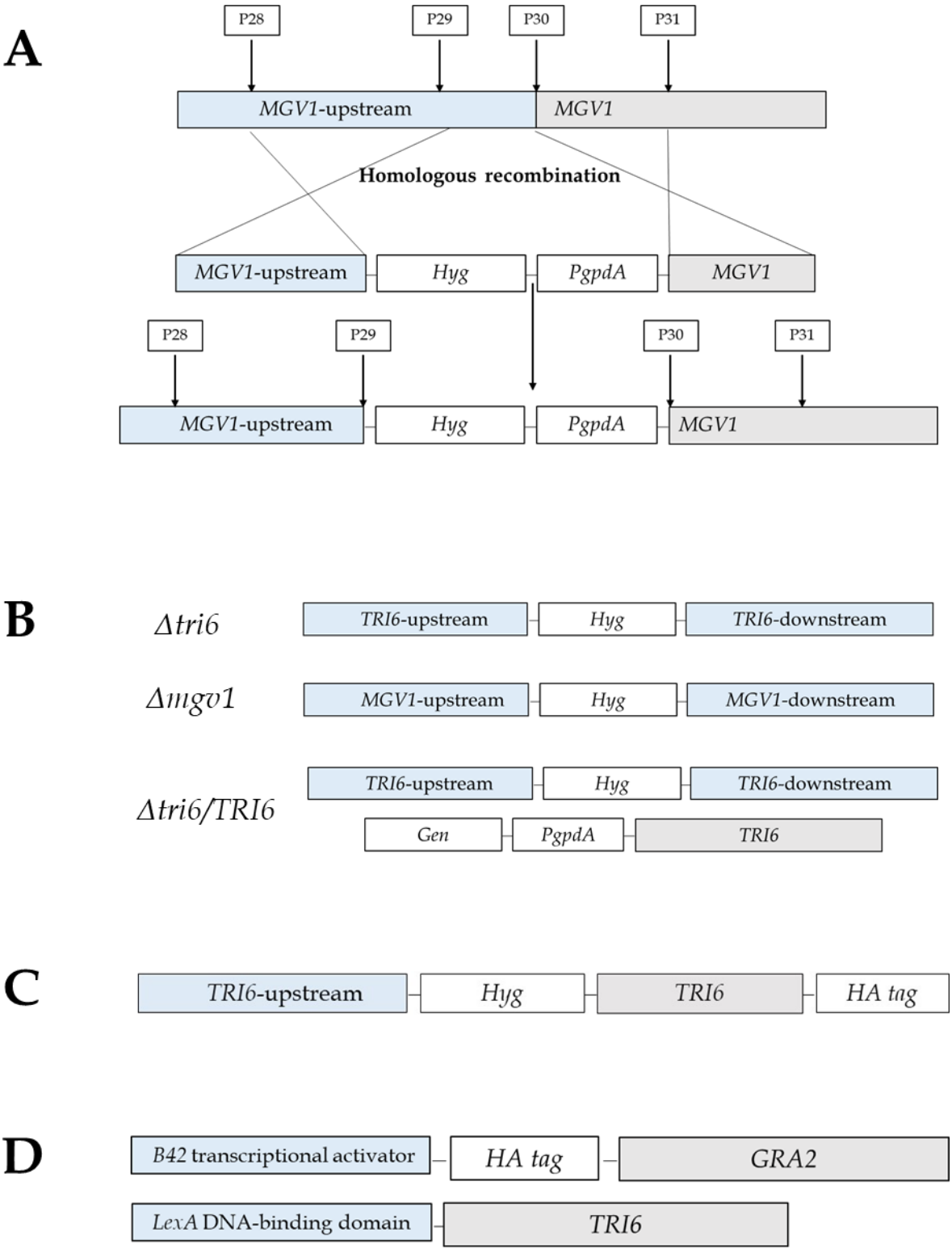

Figure S2.12 Schematic representation of the vectors and gene loci of the *F graminearum* mutant strains used in this thesis. **(A)** Fragment of the HU2E vector used for construction of the *F. graminearum* strain constitutively expressing *MGV1* (courtesy of D. Gonzalez-Pena). **(B)** Gene loci of the *Δtri6, Δmgv1, Δtri6/TRI6 F. graminearum* strains. **(C)** Gene locus of the *HA-TRI6* strain used for the ChIP-qPCR experiment (Chapter 2). **(D)** Schematics of the GRA2(AD) and TRI6(BD) vector used for the Y2H experiment (Chapter 2).

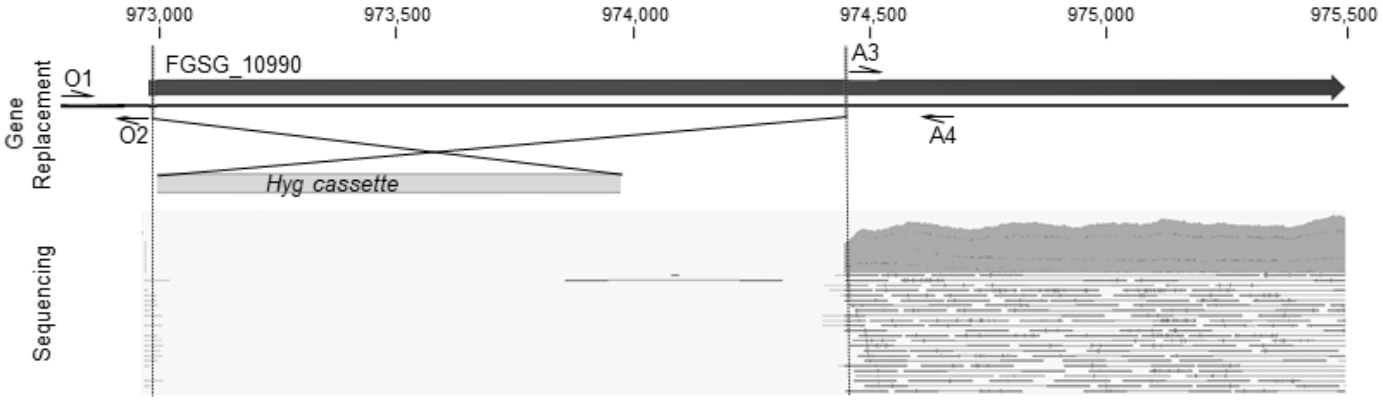

Fig. S2.13. The construction and verification of *NPS9 (*FGSG_10990*)* deletion mutant. The *NPS9* was replaced the marker hygromycin (*Hyg*) and the deletion was confirmed by sequencing. Regions upstream of the start codon and 1,463 base pairs into the gene were amplified using primer pairs O1/2 and A3/4 and used for homologous recombination of the hygromycin resistance gene. DNA sequencing confirmed deletion of the first 1,463bp of the 2,514bp sequence.

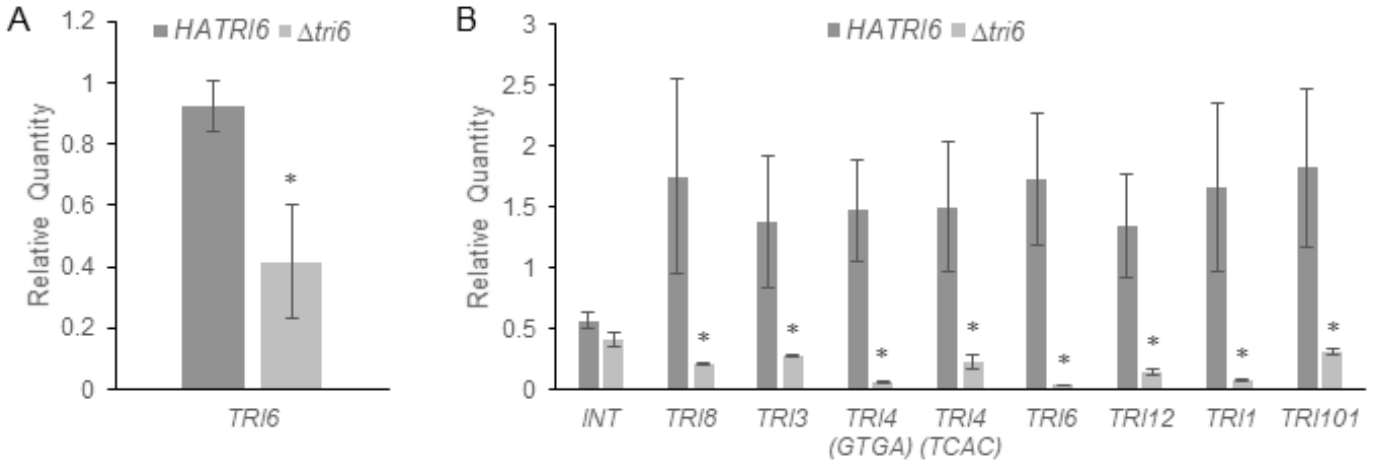

Fig. S2.14. TRI6 binds to the promoters of *TRI* genes in an environment-dependent manner. Binding in the *HA*-tagged *TRI6* strain was measured relative the Δ*tri6* strain by quantitative PCR (qPCR). (**A**). TRI6 binds its own promoter in the PN conditions. (**B**). TRI6 binds promoters of all *TRI* genes including *TRI6* in the NPN conditions, but not a region lacking a TRI6-binding motif (INT). qPCR reactions were performed in triplicates using Applied Biosystems PowerUp SYBR Green reaction mix and QuantStudio Real-Time PCR system. Relative expression was calculated using Pfaffl method with *TRI10* genomic sequence (FGSG_03538) and *EF1a* (FGSG_08811) as references. Bars represent a mean of two biological replicates with error bars representing standard deviation. Significance was determined by student's *t*-test at $p \leq 0.05$.

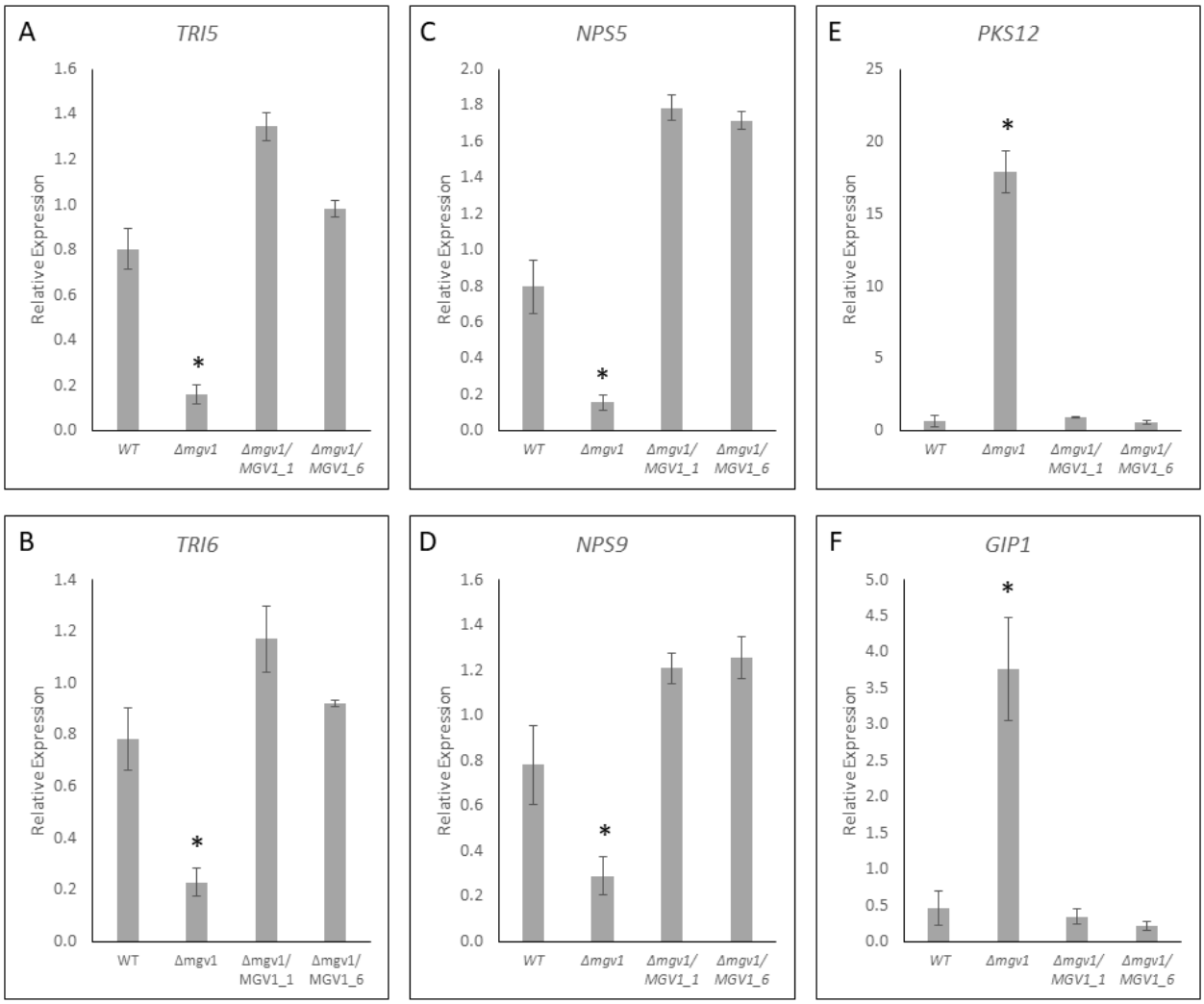

Fig. S3.1. *MGV1* affects expression of SMC genes. The wildtype (*WT*), the Δ*mgv1,* Δ*mgv1/MGV1_OX1,* and Δ*mgv1/MGV1_OX6* strains were grown in NPN conditions for 24 hours, total RNA was isolated and RT-qPCR was performed with six genes that are differentially expressed in the RNA-seq analysis. *TRI5, TRI6, NPS5,* and *NPS9* are positively regulated by *MGV1* (**A-D**), *PKS12* and *GIP1* are negatively regulated (**E,F**). The RT-qPCR reactions were performed in technical triplicates using Applied Biosystems PowerUp SYBR Green reaction mix and QuantStudio Real-Time PCR system. Relative expression was calculated using Pfaffl method with *EF1a (*FGSG_08811*)* and *β-tubulin (*FGSG_09530*)* as reference genes. Bars represent a mean of three biological replicates with error bars representing standard deviation. Significance was determined by Student's *t*-test at $p \leq 0.05$

Fig. S3.2. (pg. 157) *TRI6* regulates genes involved in amino acid biosynthesis in NPN conditions. Gene FGSG numbers are indicated next to the red arrows indicating the steps in the pathway they are associated with. Alternative colours are used to highlight genes involved in several steps of the pathway. Symbol "+" next to the gene name indicates positive regulation by *TRI6,* "-" indicates negative regulation. Gene were mapped to the pathways using the "KEGG Mapper" function of the Kyoto Encyclopedia of Genes and Genomes (Kanehisa *et al.,* 2002).

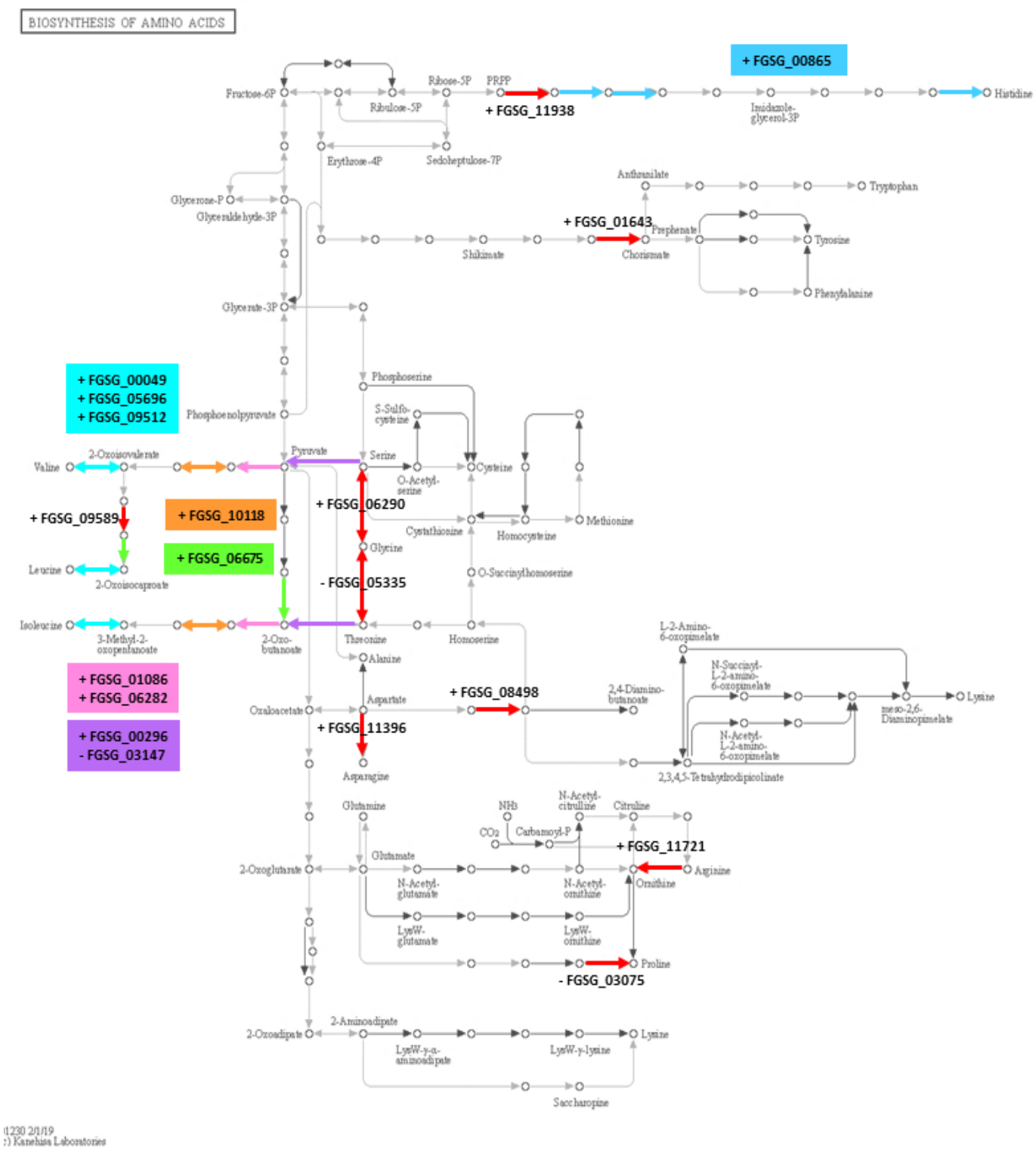

Fig. S3.3. (pg. 159) *TRI6* regulates genes involved in fatty acid biosynthesis in NPN conditions. Gene FGSG numbers are indicated next to the red arrows indicating the steps in the pathway they are associated with. Alternative colours are used to highlight genes involved in several steps of the pathway. Symbol "+" next to the gene name indicates positive regulation by *TRI6,* "-" indicates negative regulation. Gene were mapped to the pathways using the "KEGG Mapper" function of the Kyoto Encyclopedia of Genes and Genomes (Kanehisa *et al.,* 2002).

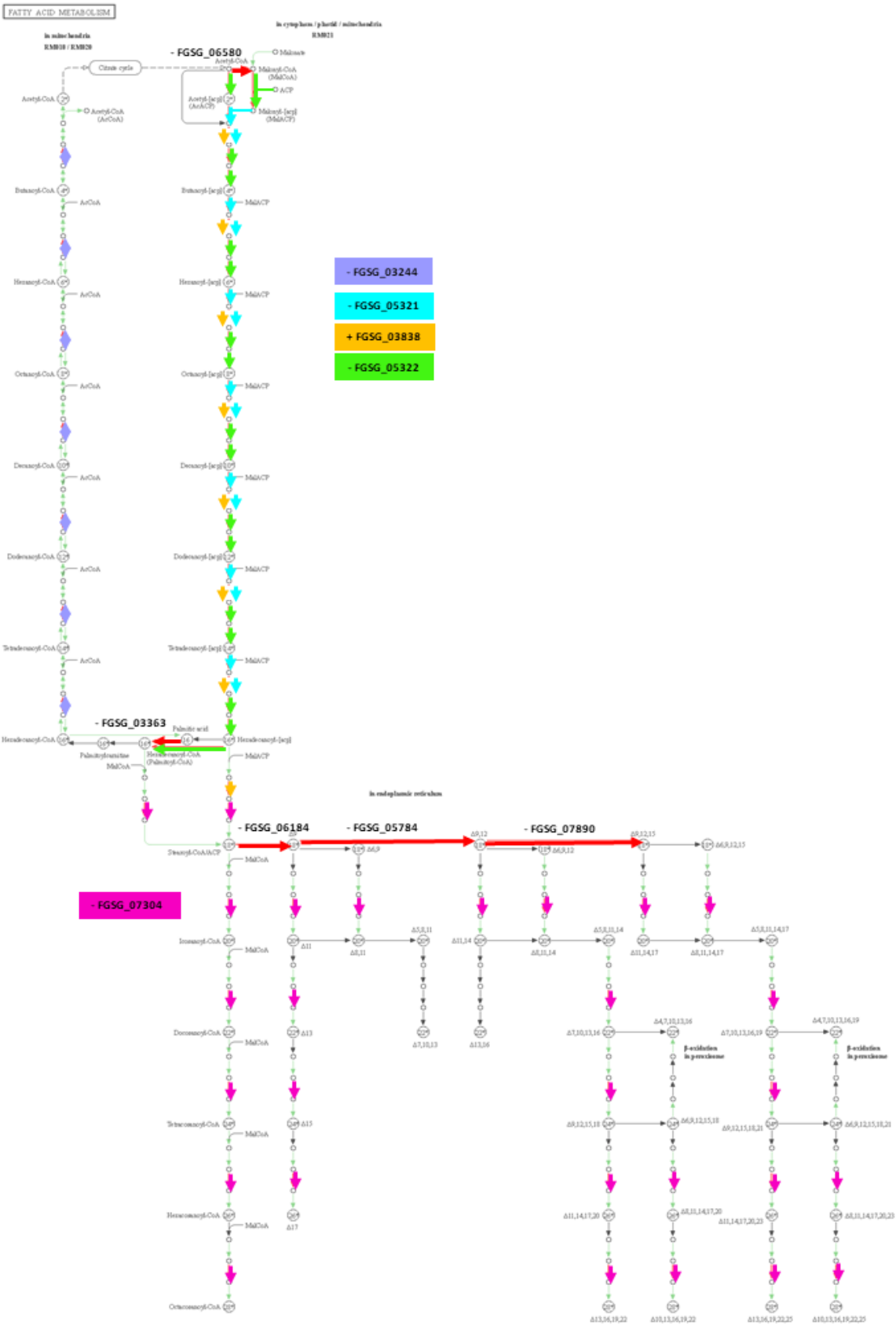
FATTY ACID METABOLISM
- FGSG_06580
- FGSG_03244
- FGSG_05321
+ FGSG_03838
- FGSG_05322
- FGSG_03363
- FGSG_06184
- FGSG_05784
- FGSG_07890
- FGSG_07304